Deposition of Diamond-like Carbon Films by Liquid Electrochemical Technique

Dissertation

Zur Erlangung des akademischen Grades
Doktor rerum naturalium

Vorgelegt der
Fakultät für Physik der
Universität Duisburg-Essen

von

Yangyang He

geboren am 09. Nov. 1982
in Liaoning

Tagder Einreichung: 15. Nov. 2011
Prüfungsvorsitzende: Prof. Dr. Jürgen König
Erster Gutachter: Prof. Dr. Volker Buck
Zweiter Gutachter: Prof. Dr. Xin Jiang
Prüfer: Prof. Dr. Gerhard Wurm
Tag der Disputation: 09.12.2011

for my mother

the one gave me not only life

Versicherung

Hiermit versichere ich, dass ich die vorliegende Arbeit selbstständig verfasst und keine anderen als die angegebenen Quellen und Hilfsmittel benutzt habe. Die Stellen der Arbeit, die dem Wortlaut oder Sinn nach anderen Werken entnommen wurden, habe ich in jedem einzelnen Fall unter Angabe der Quelle als Entlehnung kenntlich gemacht. Das Gleiche gilt auch für beigegebene Zeichnungen, Kartenskizzen und Darstellungen. Anfang und Ende von wörtlichen Textübernahmen habe ich durch Anführungszeichen bzw. Zitatformatierung, sinngemäße Textübernahmen durch direkten Verweis auf die Verfasserin oder den Verfasser gekennzeichnet.

Die Arbeit ist noch nicht an anderer Stelle als Prüfungsleistung vorgelegt worden.

Duisburg, den 15. Nov. 2011

Contents

Abstract

Diamond-like carbon (DLC) films are amorphous carbon films that can be produced with or without hydrogen, depending on the deposition techniques and conditions. Besides the conventional vapor deposition, DLC films can be deposited by liquid electrochemical technique that utilizes the electrolysis of organic solution. Liquid electrochemical deposition of DLC films has gained growing interest because of the simplicity of experimental setup, the scalability of the process, low process temperature and the possibility of deposition on substrates with complex shape.

Although some work has already been published, some important aspects are still missing. The aim of this dissertation is to investigate the influence of the experimental set-up and deposition parameters, as well as to evaluate possible technological applications of the process.

Diamantähnliche Kohlenstoffschichten (DLC) sind amorphe Kohlenstoffschichten, die abhängig von der Abscheidetechnik und den Abscheidebedingungen, sowohl mit als auch ohne Wasserstoff hergestellt werden können. Neben der konventionellen Gasphasenabscheidung können DLC Schichten auch mittels elektrochemischer Abscheidung aus der flüssigen Phase hergestellt werden. Unter der angelegten Spannung reagieren die organischen Moleküle und werden zu DLC-Schichten auf dem Substrat. Die elektrochemische Abscheidung von DLC Schichten gewinnt aufgrund der Einfachheit des experimentellen Aufbaus, der Skalierbarkeit des Prozesses, der niedrigen Prozesstemperatur und der Möglichkeit auch geometrisch komplexe Strukturen zu beschichten zunehmend an Interesse.

Obwohl bereits einige Arbeiten zu diesem Thema veröffentlicht wurden, fehlen noch entscheidende Aspekte. Das Ziel dieser Dissertation ist es daher, den Einfluss des experimentellen Aufbaus und der Abscheidebedingungen zu untersuchen und das technologische Potential des Verfahrens einzuschätzen.

1 Introduction

1.1 DLC Films and Liquid Electrochemical Deposition

Diamond-like carbon films (DLC) refer to a metastable form of amorphous carbon with significant sp^3 bonding, with or without hydrogen. DLC films have been successfully prepared by physical vapor deposition (PVD) and chemical vapor deposition (CVD). Deposition of DLC films by liquid electrochemical technique was first published in 1992. This method utilizes the electrolysis of organic solution. Under the applied potential, the organic molecules react and then turn into DLC films attached on the substrate. Liquid deposition of DLC films has received growing interest due to the simplicity of experimental setup, low deposition temperature and the possibility of complicated substrate deposition. However, some important aspects are missing after taking an overview of the publications. Here liquid electrochemical technique was applied to deposit DLC films, concentrating on the influence of the experimental facilities and deposition parameters, as well as the possible applications.

1.2 Objectives

The objective of this dissertation includes three aspects: investigating the experimental facilities; studying the effects of various parameters on the deposition of DLC films; attempting DLC films liquid deposition for application.

1.3 Organization of Dissertation

The first chapter is a general introduction of this dissertation. The background and literature review are presented in chapter 2. Chapter 3 consists of the characterizations of DLC films used in this work. Chapter 4 shows the experimental set-up, including deposition facilities and experimental procedure, as well as the introduction of several parameters in liquid deposition. Experimental facilities such as reactor and anode design in liquid electrochemical deposition are investigated in chapter 5. Chapter 6 discusses the influence of various deposition parameters including chemical, geometrical and electrical parameters. Chapter 7 displays three-dimensional substrates and high voltage deposition of DLC films by liquid electrochemical technique. Chapter 8 is named further attempts and outlook, including investigation of liquid plasma generation and some properties measurement of typical DLC films deposited. The whole work is summarized in Chapter 9.

2 Background and Literature Review

In this chapter, carbon and diamond-like carbon (DLC) films are introduced at first, including the hybridization of carbon, the structures, properties and applications of DLC films. Additionally, the deposition techniques of DLC films are presented, especially liquid electrochemical technique which is used in this dissertation.

2.1 Diamond-like Carbon (DLC) Films

2.1.1 Structure and Composition of DLC Films

Carbon forms a great variety of crystalline and disordered structures because it is able to exist in three hybridizations, sp^3, sp^2 and sp^1, as shown in Fig. 2.1 [J. Robertson 1986]. There are four valence electrons in a carbon atom. In the sp^3 configuration, as in diamond, all the valence electrons are each assigned to a tetrahedrally directed sp^3 orbital which makes a strong σ bond to an adjacent atom. In the sp^2 configuration, as in graphite, three valence electrons enter trigonally directed sp^2 orbitals which form σ bonds in a plane, and the fourth electron of the lies in a pπ orbital. In the sp^1 configuration, two valence electrons enter σ orbitals, each forming a σ bond directed along the ±x-axis, and the other two electrons enter pπ orbitals in the y and z directions [J. Robertson 2002].

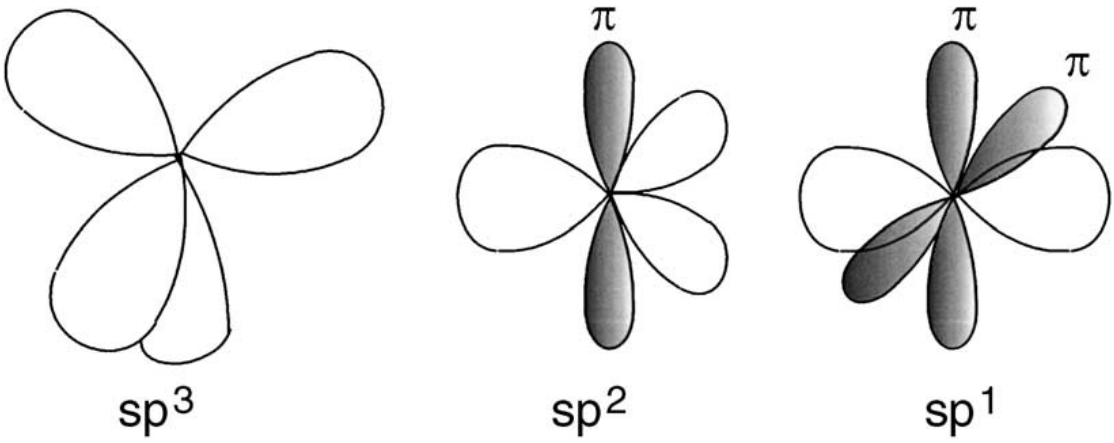

Fig. 2.1 The sp^3, sp^2 and sp^1 hybridized bondings of carbon.

The different forms of hybridizations lead to totally different configurations of carbon, such as diamond, graphite, fullerenes [H.W. Kroto 1985], nanotubes [S. Iijima 1991; T.W. Ebbesen 1997], diamond-like carbon [J. Robertson 1991], and so on.

The term of Diamond-like Carbon (DLC) has turned out for many years. However, DLC is not a certain kind of material because a wide range of structures are all covered by the same name. Composition of DLC can be explained by the ternary phase diagram in Fig. 2.2, given by Robertson [J. Robertson 1993]. The three corners correspond to diamond (sp^3), graphite (sp^2) and pure hydrogen, respectively. DLC consists not only of the amorphous carbon (a-C) but also of the hydrogenated alloys, a-C: H. This ternary phase diagram displays the compositions of the various forms of amorphous C-H alloys. However, not films corresponding to any point exist. In the right corner no film deposition is possible, because volatile hydrocarbon products are built. A description of the acronymes used is given in VDI 2840. Overall, Robertson [J. Robertson 2002] gave a description of DLC films: amorphous carbon with short and medium range order of sp^2 and sp^3 sites, with or without hydrogen depending on the deposition techniques.

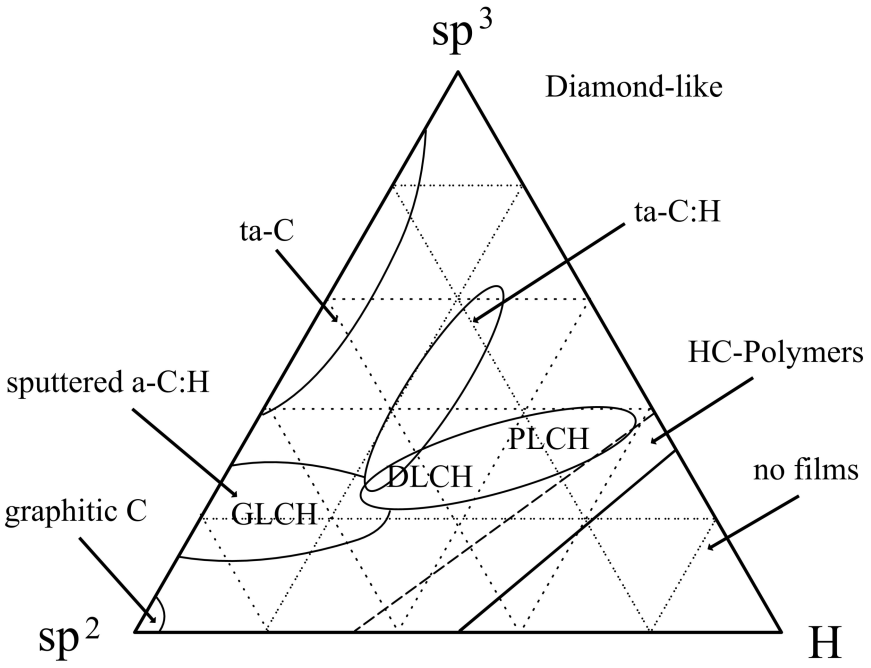

Fig. 2.2 Phase diagram showing composition of carbon-containing materials.

2.1.2 Properties and Applications of DLC Films

DLC films have some extreme properties, such as hardness, elastic modulus, high wear resistance and low friction coefficients, optical transparency and chemical inertness, high electrical resistivity and the field emission properties and the low dielectric constants, and etc [J. Robertson 2002].

The widest application of DLC films is using as protective coatings, exploiting the properties of high wear resistance and low friction coefficients. DLC films can be used as biomedical coatings because they have been found to satisfy both mechanical and biological requirements, such as coatings on artificial heart valves and artificial joints. DLC films can also be used as protective coatings in other fields, such as magnetic storage disks, optical windows and micro-electromechanical devices (MEMs) [C.J. McHargue 1991; A. Grill 1999; J. Robertson 2001; R. Hauert 2003; G. Dearnaley 2005].

Although DLC films own such outstanding properties and widespread applications, it does not mean one kind of DLC films is excellent on all the aspects mentioned above. DLC is a whole class of materials covered by the same name, however, of different structures and compositions. The performances of DLC films are significantly related to the film structures and compositions. This means that the properties of one certain DLC film might be totally different from those of another one. In general, the films are diamond-like if the sp^3 bonding is dominant, while the films are graphite-like with a predominant sp^2 bonding. The deposition method, hydrogen content and amount of doping determine the amount of sp^3 and sp^2 content in the film. Nevertheless, it is just the variety of structures and compositions introduce various properties and the correlated applications of DLC films.

2.2 Deposition Techniques of DLC Films

2.2.1 Vapor Deposition

Vapor deposition of DLC films are mainly classified into two groups: physical vapor deposition (PVD) and chemical vapor deposition (CVD). PVD is a variety of vacuum deposition to grow thin film by the condensation of a vaporized form of the material onto substrates. PVD involves purely physical processes rather than involving any chemical reaction. PVD techniques of DLC films include ion beam, mass selected ion beam, sputtering and ion assisted sputtering, cathodic arc and pulsed laser deposition. CVD includes chemical reactions during the deposition process of thin films. CVD techniques of DLC films include direct photo CVD and plasma enhanced CVD [J. Robertson 2002]. Some of the deposition methods are introduced below.

(1) Ion beam and Mass selected ion beam (MSIB) deposition

The first successful DLC films were prepared by Aisenberg and Chabot [S. Aisenberg 1971] in early 1970 by ion beam deposition (IBD). They quenched a beam of C^+ ions, generated by sputtered carbon electrodes, in the presence of Ar, to form an amorphous layer of microcrystallites. Ion beam deposition of DLC films is a physical process. In a typical ion beam deposition system, carbon ions are produced by the plasma sputtering of a graphite cathode or a hydrocarbon gas such as methane. The carbon ions or hydrocarbon ions are accelerated to form the ion beam in the high vacuum deposition chamber. The ion beam is extracted through a grid from the plasma source by a bias voltage. And then the DLC film is condensed from a beam containing medium energy (~100 eV) carbon or hydrocarbon ions. It is the impact of these ions on the growing film that induces the sp^3 bonding [J. Robertson 2002].

Mass selected ion beam deposition (MSIB) is a controlled deposition. The key difference from conventional ion beam deposition is that MSIB can control deposition species and energy, filter out of non-energetic species [J. Robertson 2002].

(2) Sputtering deposition

Sputter deposition is a kind of physical vapor deposition. The hypostasis is ejecting material from a solid target by bombardment using energetic particles, and then depositing onto a substrate [R. Behrisch 1981]. The most common form uses the dc or rf sputtering of a graphite electrode by an Ar plasma. The advantage of sputtering deposition is that the deposition conditions can be controlled by the plasma power and gas pressure. The disadvantage is not easy to get both high sp^3 content and high growth rate of the DLC films [J.J. Cuomo 1991; J. Schwan 1996]. Sputtering deposition of DLC films is the most common industrial process [N. Sawides 1986; J. Robertson 2002].

(3) Plasma enhanced chemical vapor deposition (PECVD)

Plasma-enhanced chemical vapor deposition (PECVD) is a process used to deposit DLC films from hydrocarbon gases onto a substrate. Chemical reactions are involved in the process, which occur after creation of plasmas from the reacting gases. The plasma is generally created by radio frequency (r.f.) or direct current (dc) discharge between two electrodes, the space between which is filled with the reacting hydrocarbon gases. PECVD utilizes plasma to enhance chemical reaction rates of the precursors. The hydrocarbon source materials which can be used for deposition by PECVD are methane, ethane, acetylene, benzene, ethylene, propane, isopropane, etc. Bias voltage and total pressure of the system are two important parameters of these PECVD methods [J. Robertson 2002]. PECVD can be classified into dc plasma, rf plasma, microwaves plasma, electron cyclotron resonance (ECR) and inductive coupled plasma (ICP) systems.

2.2 Liquid Electrochemical Deposition

Most materials which can be deposited from the vapor phase can also be deposited in liquid phase using electroplating techniques [L.I. Maissel 1970]. DLC films can be successfully deposited by various vapor techniques, and liquid phase deposition of DLC films is attempted. The first report of carbon films liquid phase deposition is based on the electrolysis of organic solution in 1992 [Y. Namba 1992]. Fig. 2.3 shows the schematic diagram of the liquid deposition system. A silicon wafer of low resistivity was used as substrate, the distance between the substrate and positive carbon electrode was set to 5 mm. The characterization of the film morphology, composition and crystal structure suggested that diamond phase carbon films were deposited on silicon substrates at the temperature lower than 50 ºC by electrolyzing ethanol solution.

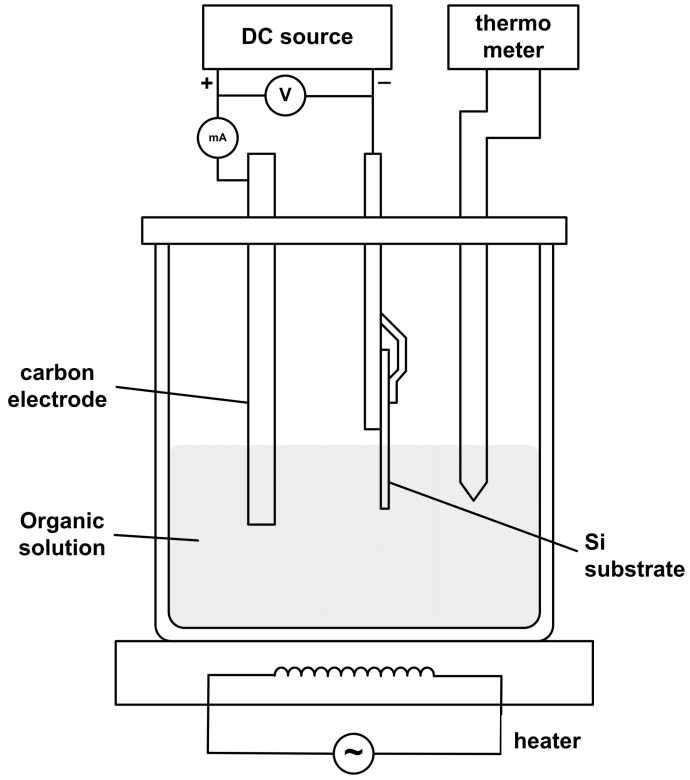

Fig. 2.3 Schematic diagram of the liquid phase deposition system reported by Namba [Y. Namba 1992].

The results from Namba confirmed that it is possible to deposit carbon phase films by liquid electrochemical technique. Since then liquid electrochemical deposition is considered to be a novel technique to grow carbon phase films. Up to now various kinds of carbon phase films have been deposited by liquid electrochemical technique under various deposition parameters [T. Suzuki 1995; H. Wang 1996; V.P. Novikov 1997; D. Guo 2000; Z. Sun 2000; W.L. He 2005].

Liquid electrochemical deposition of DLC films is mainly based on the electrolysis of organic solutions. Under the applied potential, the organic molecules react and turn into DLC films attached on the substrates. The liquid electrochemical technique is different from traditional electroplating because organic solvents without ions are used as electrolyte. Compared with vapor deposition techniques, liquid electrochemical deposition of DLC films owns some significant advantages, such as simplicity of the experimental setup without vacuum system, low process temperature, and the availability of large or complex substrate deposition [K. Cai 1999; M.C. Tosin 1999; D. Guo 2000; Z. Sun 2000; D. Guo 2001; H. Wang 2001; P.K. Lin 2003; R.S. Li 2009].

(1) Vacuum system is a necessary and complex part in all the vapor deposition system, however, liquid deposition of DLC films is carried out in atmospheric pressure without any vacuum facility. The deposition system of liquid technique is constitutionally an electrolytic cell and therefore owns the advantage of very simple experimental setup. In addition, without waiting for the appropriate vacuum liquid deposition can save a lot of time and make the deposition process easy to operate.

(2) Liquid deposition of DLC films is carried out at low temperature, less than 100 ºC. On the one hand, depositing films at low temperature can minimize the thermal stresses between films and substrates. On the other hand, low process temperature can greatly extend the selecting range of substrates. For example, some polymer materials which are not stable at high temperature can be selected as substrates in liquid phase deposition.

(3) The essence of liquid deposition of DLC films is quite similar to the process of electrolysis which can be applied on large or irregular areas depending on the size of the electrolytic cell. Thus, it is possible to deposit DLC films on large or complicated conductive substrate using liquid technique.

In this work, liquid electrochemical technique was applied to deposit DLC film at low temperature under atmospheric pressure. The influence of experimental facilities and several parameters on the liquid deposition of DLC films are investigated.

References

A. Grill. "Diamond-like carbon: state of the art" Diamond and Related Materials **8**(1999): 428-434.

C.J. McHargue. "Applications of diamond films and related materials". New York, Elsevier(1991).

D. Guo, K. Cai, L.T. Li, Y. Huang, Z.L. Gui, H.S. Zhu. "Electrodeposition of diamond-like amorphous carbon films on Si from N; N-dimethylformamide" Chemical Physics Letters **329**(2000): 346-350.

D. Guo, K. Cai, L.T. Li, Y. Huang, Z.L. Gui, H.S. Zhu. "Evaluation of diamond-like carbon films electrodeposited on an Al substrate from the liquid phase with pulse-modulated power" Carbon **39**(2001): 1395-1398.

D. Guo, K. Cai, L.T. Li, Y. Huang, Z.L. Gui, H.S. Zhu, . "Evaluation of diamond-like carbon films electrodeposited on an Al substrate from the liquid phase with pulse-modulated power" Carbon **39**(2000): 1395-1398.

G. Dearnaley, J.H. Arps. "Biomedical applications of diamond-like carbon (DLC) coatings: A review" Surface and Coatings Technology **200**(2005): 2518-2524.

H. Wang, M. Yoshimura. "Electrodeposition of diamond-like carbon films in organic solvents using a thin wire anode" Chemical Physics Letters **348**(2001): 7-10.

H. Wang, M.R. Shen, Z.Y. Ning, C. Ye, C.B. Cao, H.Y. Dang, H.S. Zhu. "Deposition of diamond-like carbon films by electrolysis of methanol solution" Applied Physics Letters **69**(1996): 1074-1076.

H.W. Kroto, J.R. Heath, S.C. O'Brien, R.F. Curl, R.E. Smalley. "C60 buckminsterfullerene" Nature (London) **318**(1985): 162-163.

J. Robertson. "Amorphous carbon" Advances in Physics **35**(1986): 317-374.

J. Robertson. "Hard amorphous (Diamond-Like) carbons" Solid State Chemistry **21**(1991): 199-333.

J. Robertson. "Deposition mechanisms for promoting sp^3 bonding in diamond-like carbon" Diamond and Related Materials **2**(1993): 984-989.

J. Robertson. "Ultrathin carbon coatings for magnetic storage technology" Thin Solid Films **383**(2001): 81-88.

J. Robertson. "Diamond-like amorphous carbon" Materials Science and Engineering R **37**(2002): 129-281.

J. Schwan, S. Ulrich, H. Roth, H. Ehrhardt, S.R.P. Silva, J. Robertson, R. Samlenski. "Tetrahedral amorphous carbon films prepared by magnetron sputtering and DC ion plating" Journal of Applied Physics **79**(1996): 1416-1422.

J.J. Cuomo, J.P. Doyle, J. Bruley, J.C. Liu. "Sputter deposition of dense diamond-like carbon films at low temperature" Applied Physics Letters **58**(1991): 466-468.

K. Cai, C.B. Cao, H.S. Zhu. "Deposition of diamond-like carbon films on aluminum in the liquid phase by an electrochemical method" Carbon **37**(1999): 1860-1862.

L.I. Maissel, R. Glang. "Handbook of thin film technology". New York, McGraw-Hill(1970).

M.C. Tosin, A.C. Peterlevitz, G.I. Surdutovich, V. Baranauskas. "Deposition of diamond and diamond-like carbon nuclei by electrolysis of alcohol solutions" Applied Surface Science **144-145**(1999): 260-264.

N. Sawides. "Optical constants and associated functions of metastable diamondlike amorphous carbon films in the energy range 0.5-7.3 eV" Journal of Applied Physics **59**(1986): 4133-4145.

P.K. Lin, M.R. Shen, W.W. Cao. "Temperature-dependence of carbon film growth by electrolysis of a methanol solution" Carbon **41**(2003): 594-598.

R. Behrisch. "Sputtering by particle bombardment". Berlin, Springer(1981).

R. Hauert. "A review of modified DLC coatings for biological applications" Diamond and Related Materials **12**(2003): 583-589.

R.S. Li, M. Zhou, X. J. Pan, Z.X. Zhang, B.A. Lu, T. Wang, E.Q. Xie. "Simultaneous deposition of diamondlike carbon films on both surfaces of aluminum substrate by electrochemical technique" Journal of Applied Physics **105**(2009): 066107-1-3.

S. Aisenberg, R.Chabot. "Ion-Deposition of thin films of Diamondlike Carbon" Journal of Applied Physics **42**(1971): 2953-2958.

S. Iijima. "Helical microtubules of graphitic carbon" Nature (London) **354**(1991): 56-58.

T. Suzuki, Y. Manita, T. Yamazaki, S. Wada, T. Noma. "Deposition of carbon films by electrolysis of a water-ethylene glycol solution" Journal of Materials Science **30**(1995): 2067-2069.

T.W. Ebbesen. "Carbon nanotubes: preparation and properties". Boca Raton, CRC Press(1997).

V.P. Novikov, V.P. Dymont. "Synthesis of diamondlike films by an electrochemical method at atmospheric pressure and low temperature" Applied Physics Letters **70**(1997): 200-202.

W.L. He, R. Yu, H. Wang, H. Yan. "Electrodeposition mechanism of hydrogen-free diamond-like carbon films from organic electrolytes" Carbon **43**(2005): 2000-2006.

Y. Namba. "Attempt to grow diamond phase carbon films from an organic solution" Journal of Vacuum Science Technology A **10**(1992): 3368-3370.

Z. Sun, Y. Sun, X. Wang. "Investigation of phases in the carbon films deposited by electrolysis of ethanol liquid phase using Raman scattering" Chemical Physics Letters **318**(2000): 471-475.

3 Characterizations of DLC Films

Characterizations of the DLC films used in this dissertation are introduced in this chapter. These measurements are classified into five groups according to the information provided, such as film morphology, chemical composition, microstructure, bond-structure and other film properties.

3.1 Morphology

In thin film technology, morphology has influence on the film properties and applications. The investigation of morphology is therefore necessary in our work. The aim of characterizing film performances is capable to understand the relationship between the deposition parameters and the films morphology. Microscopic methods such as atomic force microscopy and scanning electron microscopy are used in this work.

3.1.1 Atomic Force Microscopy (AFM)

Atomic force microscopy (AFM) is widely used to measure the surface morphology and roughness in thin film technology. It is over 1000 times better than the optical diffraction limit [M. Born 1997]. AFM owns the advantages of no sample pretreatment, working in air or liquid environments, detecting both conducing and dielectric materials, and providing three-dimensional (3D) images of the sample surface.

An AFM works by scanning a probe over the sample surface, building up a map of the height or topography of the surface as it goes along. Depending on the radius of curvature of the tip and the roughness of the surface, the resolutions of 0.1-10 nm are possible. Thus even single atoms can be shown. Fig. 3.1 shows the working principle of AFM. A tip is located at the end of a cantilever which will bend when it meets the deflection of surface stiffness or topography. The bending of the cantilever is detected with a laser light beam and converted into signals. The scanner is capable of sub-angstrom resolution in x-, y- and z- directions, while the z-axis is conventionally perpendicular to the sample. The 3D topographical image of the surface is therefore generated [P. Eaton 2010].

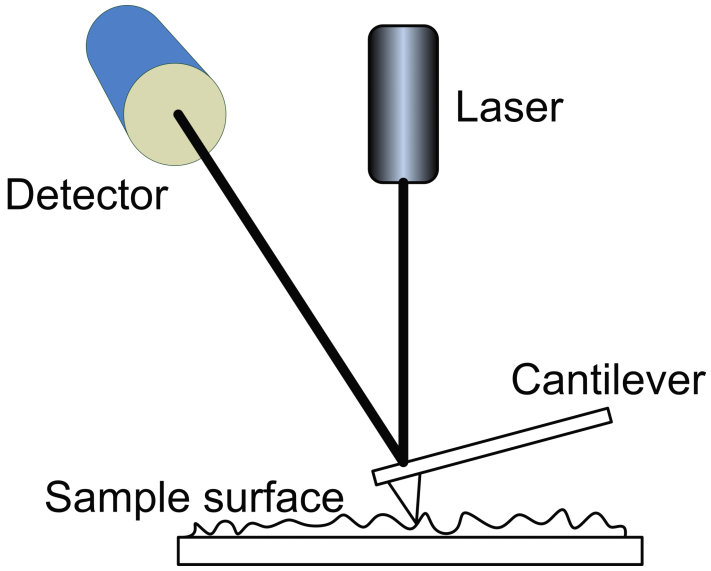

Fig. 3.1 Diagram of AFM working principle.

AFM can be operated under several modes, mainly contact mode and non-contact mode. Contact mode is the most common operating mode of AFM. Under the contact mode, the tip of the probe is always in direct contact with the surface by means of repulsive force. The force is kept constant during scanning process by maintaining a constant deflection. This contact mode is not suitable for soft materials because of the quite strong lateral forces which will course damage of the sample surface [Q. Zhang 1993; S. Karrasch 1993]. However, there are lately some reports of soft biological samples successfully imaged by contact mode [C. Le Grimellec 1998; M.F. Murphy 2006].

In the non-contact mode, the tip of the cantilever does not contact with the sample surface. The cantilever is externally oscillated through an external periodic force slightly above its resonance frequency. When the tip gets closer to the surface, the oscillation gets damped due to the attractive forces, e.g. van-der-Waals forces, and the amplitude as well as the frequency of the oscillation decrease. This makes the tip oscillating in a small distance to the surface. Measuring the tip-to-sample distance at each (x,y) data point allows the scanning software to construct a topographic image of the sample surface. Non-contact mode AFM does not suffer from tip or sample degradation effects and this makes non-contact AFM preferable for measuring soft samples [P. Eaton 2010].

The AFM measurement was carried out with the help of AFM Veeco Dimension 3100. The 3D images and roughness of the films were measured using the tapping mode. The dimension of the scanned area depends on the applied scanner and is 5 μm × 5 μm in this work. Fig. 3.2 shows an AFM image of DLC films deposited by liquid

electrochemical technique. The electrolyte, applied potential and the deposition time were analytically pure 2-propanol, 1000 V (frequency 10 kHz, duty cycle 50%) and 2 h, respectively. The anode material, substrate and anode-substrate distance were graphite, silicon wafer ($13\times12\times0.5mm^3$) and 6 mm, respectively. The AFM results were analyzed with the help of software WSxM 3.1. The RMS (Root Mean Square) roughness of this DLC film is 54.7 nm.

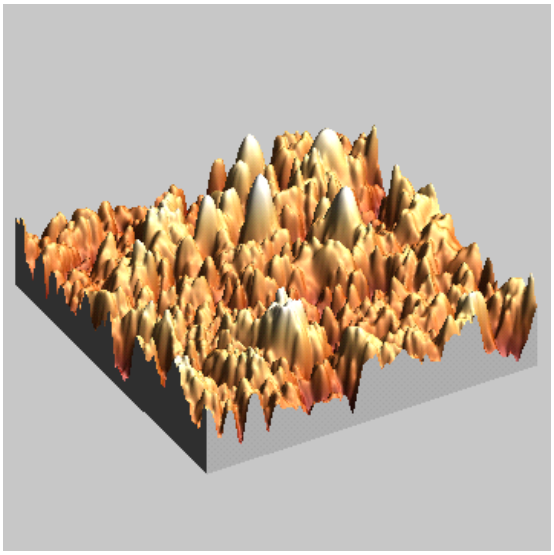

Fig. 3.2 An AFM image of DLC films deposited by liquid electrochemical technique.

3.1.2 Scanning Electron Microscopy (SEM)

The film morphology can be measured with the help of scanning electron microscope (SEM). The signal is generated at the specimen surface or within the specimen by scanning it with a fine electron probe. The interaction between primary electrons (PE) and surface layers of the specimen is shown in Fig. 3.3, this zone in which such interaction occurs and different signals are produced is called "interaction volume" or "electron-diffusion cloud". The primary electrons interact in various ways with the surface layers of the specimen. Secondary electrons (SE), back scattered electrons (BSE), and absorbed electrons are produced, flowing off as specimen current. In addition, X-rays, Auger electrons, and cathodoluminescence are produced. Transmission electrons may exist depending on the energy of primary electrons and the thickness of specimen. SE and BSE are two parts of signals that contribute to the formation of SEM images [B. Jaehne 1999].

Secondary electrons are produced in the entire interaction volume, however, they can only escape from surface layers with the escape energy of ≤ 50 eV. There are several

sources of SE. Approximately half of all SE are produced very near to the point of impact of PE. SE is also produced at a distance in the range of 0.1 to some mm to the point of impact because back scattered electrons diffuse in the specimen material. Back scattered electrons reacting with the wall of the specimen chamber are the third source of SE. The SE signal, comprising all essential information on topography, produces electron-micrographs of high resolution.

The electrons escaping from the surface of specimen and having energy of ≥ 50 eV are referred to back scattered electrons (BSE). BSE are produced in the entire interaction volume at a larger distance to the point of impact of PE, as shown in Fig. 3.3. The higher the PE energy and the smaller the atomic number of the specimen material, the more extends the area of production of BSE and the lower the achievable resolution. A material contrast can be made visible due to the dependence on the atomic number of the sample material which is apart from the topography contrast [B. Jaehne 1999].

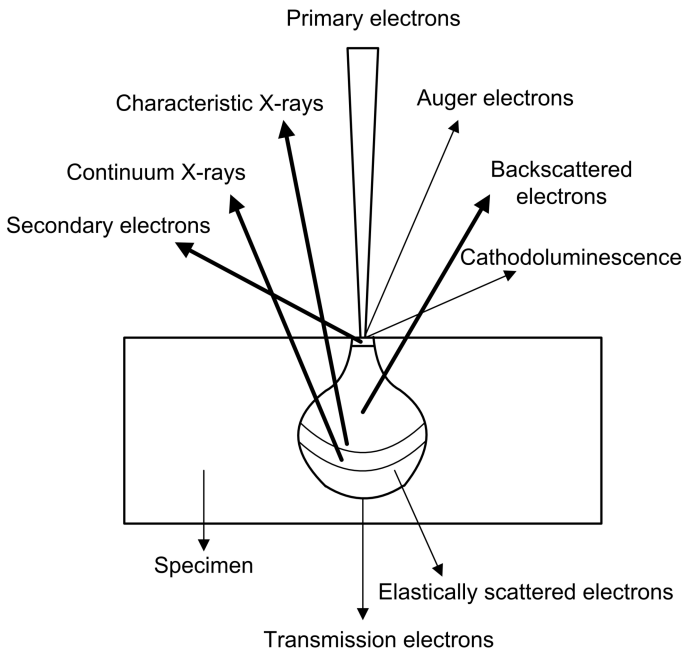

Fig. 3.3 Interaction between primary electrons and surface layers of the specimen.

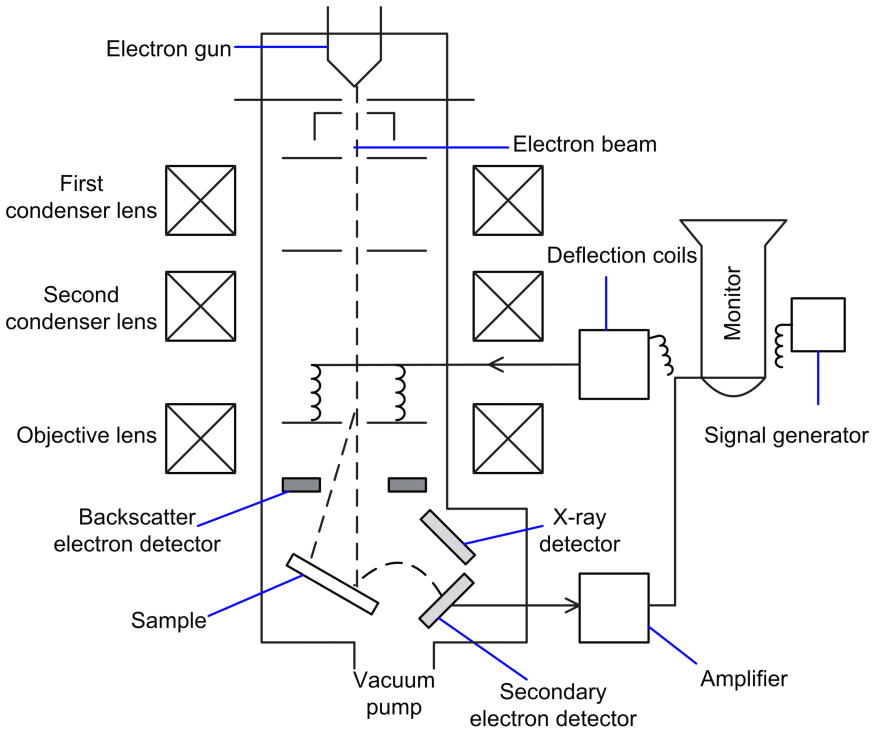

Fig. 3.4 Diagram of scanning electron microscope (SEM).

SEM mainly consists of signal-producing system, signal-processing system and detectors. Fig. 3.4 illustrates the basic design of a scanning electron microscope. The signal-producing system is the part to generate a probe of the smallest diameter and maximum brightness when hitting the surface of the specimen. It consists of an electron gun, lens system and the specimen chamber. Pumps are required to reduce the pressure to a certain vacuum. The electron beam produced in the electron gun from a sharp tungsten tip with a radius of less than 100 nm, is accelerated through apertures of micron-scale holes in a metal film and electronic lenses both of which control the diameter of the beam, deflector coils which raster the beam over the sample, and the objective lens which focus the beam on the specimen. Detectors connect the signal-producing system and the signal-processing system in SEM. They can convert the signals produced which are in the form of electrons into electrical signals. Nevertheless, each kind of signals, such as SE, BSE and X-rays, requires a specific detector. The signal-processing system is capable to amplify and modulate electrical signals into video signals. The microscopy of the specimen is therefore presented [M. Dufek 2008].

The morphology of the films deposited in this work was measured with the help of ESEM Quanta 400 FEG. The high voltage is continuous from 0.2 to 30 kV and the magnification ranges from 7 to 1 000 000.

Fig. 3.5 compares SEM images of the films deposited on Si substrates using glass reactor with PTFE-coating inside (a) and quartz reactor (b), respectively. The applied potential, the electrolyte and the deposition time were 900 V (frequency 4.2 kHz, duty cycle 50%), acetone/deionized water solution in the volume ratio of 2:1 and 5 h, respectively. The deposition temperature was kept at 60 ºC by water cooling to the wall of the reactor. The anode material, substrate and anode-substrate distance were graphite, silicon wafer ($13\times12\times0.5mm^3$) and 6 mm, respectively. The film deposited using glass reactor with PTFE-coating inside was relative rough, while the film deposited using quartz reactor was relative smooth. It is evident that the surface morphology can be clearly presented by SEM images. So SEM images of the films were taken to investigate effects of liquid deposition parameters on the film morphology.

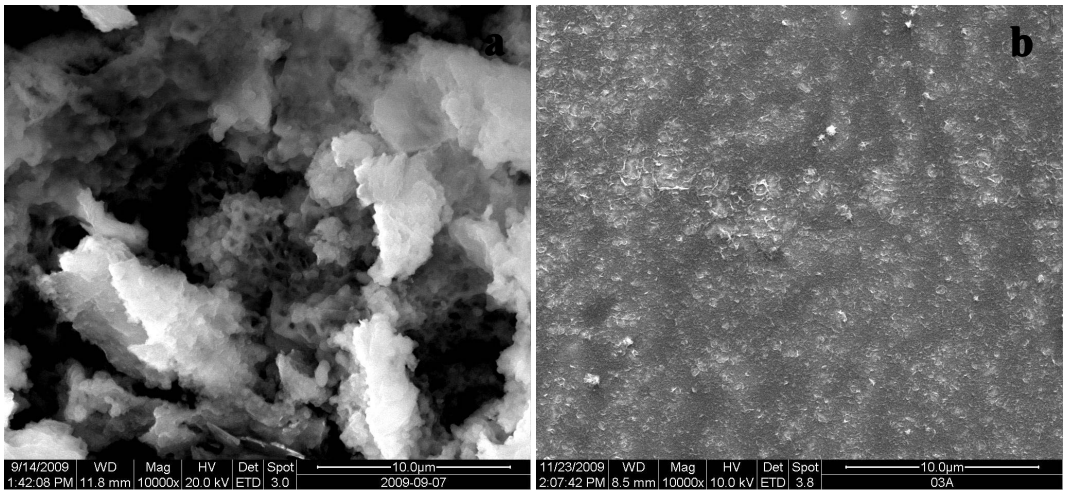

Fig. 3.5 Comparison of SEM images of DLC films deposited by liquid electrochemical technique.

3.2 Chemical Composition

3.2.1 Energy Dispersive X-ray Spectroscopy (EDX)

According to the interaction between primary electrons and surface layers of the specimen, characteristic X-rays can be excited, as shown in Fig. 3.3. Because the atom of every element releases X-rays with unique amounts of energy, the element can be identified. The characteristic X-rays can be collected by specific detectors, and then the Energy Dispersive X-ray Spectroscopy (EDX) is displayed [M. Dufek 2008].

EDX is introduced for the elemental and composition analysis of the DLC films deposited. In this work, EDX measurement was carried out with the SEM facility ESEM Quanta 400 FEG. Fig. 3.6 shows the EDX spectrum of a doped DLC film deposited by liquid electrochemical technique. The film was deposited on Si substrate using anode made of stainless steel. The applied potential, the deposition time and the electrolyte were 900 V (frequency 10 kHz, duty cycle 50%), 5 h and acetone/deionized water solution in the volume ratio of 2:1, respectively. The deposition temperature was kept at 60 ºC by water cooling to the wall of quartz reactor. The analysis of the EDX spectrum is as following: the silicon peak is obviously due to the Si substrate, the presence of C peak is due to the DLC film, other elements such as Fe, Mn, Ni, Cr, Sn and S are all doping elements in this film. The attached quantitative analysis of EDX spectrum can show the ratio of every element by weight and by atom.

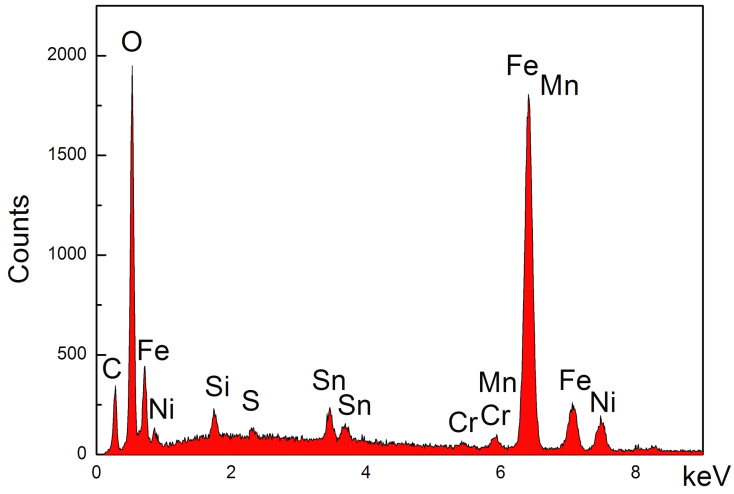

Fig. 3.6 An EDX spectrum of a doped DLC film deposited by liquid electrochemical technique.

3.2.2 Atomic Absorption Spectroscopy (AAS)

Atomic Absorption Spectroscopy (AAS) is able to determine a particular element in solution and give the corresponding concentration, especially metals in water solution. The principle of AAS is that concrete wavelength of light can be absorbed by particular free atoms and provide the absorption spectroscopy. Compared with the calibration spectra, elements contained in the solution can be determined. The amount of light absorbed depends on the amount of the element, the concentration of the element can be measured [J.W. Robinson 1975; E. Metcalfe 1987].

The deionized water used to make electrolyte for DLC films liquid phase deposition was measured by AAS because we needed to confirm the purity of the electrolyte, Ca contained or not. In this work, the AAS measurement was carried out by Shimadzu AA-6200 atomic absorption flame emission spectrophotometer.

3.3 Microstructure

3.3.1 X-ray Diffraction (XRD)

X-ray diffraction occurs when the conditions of certain constructive interference are fulfilled. X-ray diffraction behaves like "reflection" from the planes of atoms within the crystal and that only at specific orientations of the crystal with respect to the source and detector. These specific directions appear as spots on the diffraction pattern called reflections. However, it is different from the reflection of light from a mirror, X-ray diffraction requires that the angle of incidence equals the angle of reflection and is possible for all angles. Laue photograph and Bragg low are two expressions of X-ray diffraction [L. Smart 1996].

Fig. 3. 7 shows Bragg reflection from a set of crystal planes with a spacing d ABC and DFH are two X-ray beams, the difference in path length between these two beams is equal to (DF+FH)–(AB+BC). Because BE and BG are both at right angles to the beams, AB and DE have the same length, so do BC and GH. The difference in path length is therefore changed to EF+FG=$2d\sin\theta$. This must be equal to an integral number, n, of wavelengths. If the wavelength of the X-ray is λ, then comes the function $n\lambda=2d\sin\theta$ which is called Bragg equation. Here d is the spacing between diffracting planes, θ is the incident angle at which reflection form these planes are observed, n is any integer, and λ is the wavelength of the beam.

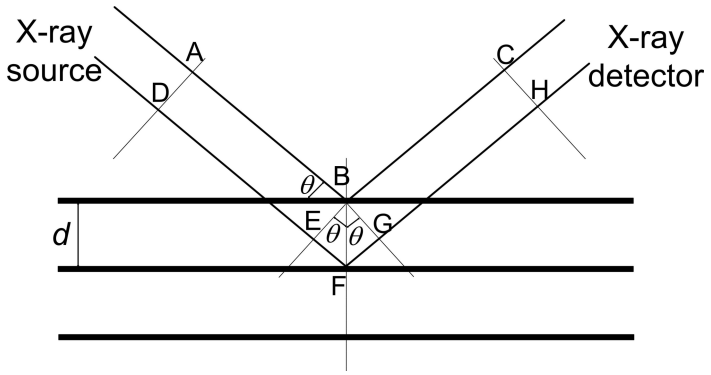

Fig. 3.7 Bragg condition for the reflection of X-rays.

The resulting diffraction pattern of a crystal, comparing both the positions (by means of θ) and intensities of the diffraction effect, is a fundamental physical property of the substance. Analysis of the positions of the diffraction effect leads immediately to a knowledge of the size, shape and orientation of the unit cell.

The crystalline structure of the films was routinely investigated by X-ray Diffraction (XRD) with a Phillips PANalytical X'Pert PRO using CuKα1 and Kα2 radiations in this work. Fig. 3.8 shows the XRD of a typical DLC film deposited using glass reactor. It could be concluded that calcium carbonate existed as a kind of impurities in the films because of the assigned $CaCO_3$ crystal orientations.

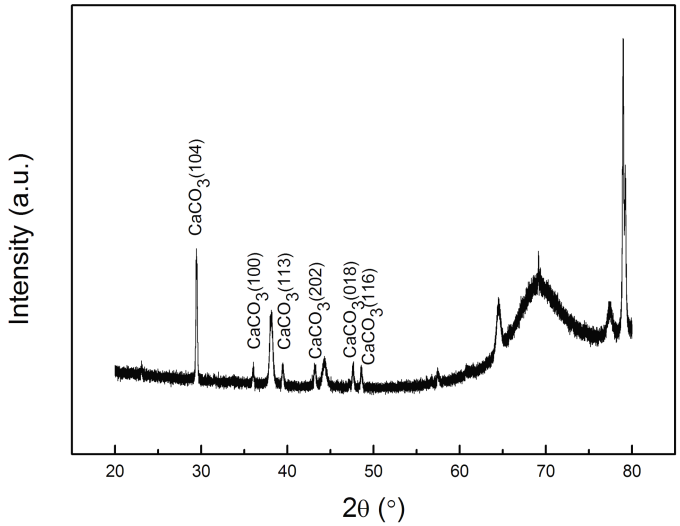

Fig. 3.8 The X-ray diffraction (XRD) patterns of a typical DLC film deposited using glass reactor which contained calcium carbonate (JCPDS: 5-586).

3.4 Bond-structure

3.4.1 Raman Spectroscopy (Raman)

Raman is a main diagnostic used throughout this work, and it is therefore described in more detail in this section.

(1) Raman Scattering

Raman scattering is a kind of inelastic scattering. There are two types of Raman scattering, Stokes scattering and anti-Stokes scattering. When the light is scattered from an atom or molecule, the atom or molecule may absorb energy, the emitted photons will have less energy and shift to a lower frequency. When the light is

scattered from an atom or molecule, the atom or molecule may lose energy, the emitted photons will have more energy and shift to a higher frequency [D.C. Harris 1989]. Fig. 3.9 gives a schematic diagram of visual light scattering.

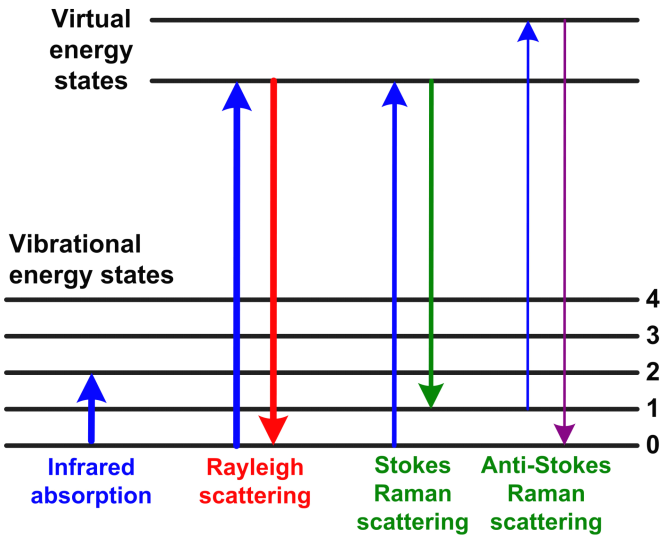

Fig. 3.9 Different types of visual light scattering: Rayleigh scattering, Stokes Raman scattering and anti-Stokes Raman scattering.

(2) Raman Spectroscopy and Carbon Materials

Raman spectroscopy is based on the Raman effect which is in fact solids inelastic scattering on optical phonons. Since internal vibrational pattern is specific to the chemical bonds and symmetry of molecules, Raman spectroscopy therefore provides information about the structure and composition of the materials to be identified.

As an application of Raman spectroscopy, it is widely used in the non-destructive characterization of carbon based materials, including diamond, graphite, fullerenes, nanotubes and diamond-like carbon (DLC). As shown in Fig. 3.10, diamond has a single Raman active mode at 1332 cm^{-1}. Single crystal graphite has a single Raman active mode at 1580 cm^{-1} labelled “G” for “graphite”. Disordered graphite has a second mode at around 1350 cm^{-1} labelled “D” for “disordered”. Raman spectra of most disordered carbons remain dominated by these two G and D modes of graphite, even when the carbons do not have particular graphitic ordering [A.C. Ferrari 2000]. It is therefore possible that Raman can be used to derive the structural information of DLCs and the corresponding sp^3 fraction.

Fig. 3.11 shows the eigenvectors of the Raman G and D modes in graphite and amorphous carbons. Ferrari *et al* [A.C. Ferrari 2000] found out that the G mode is actually the stretching vibration of any sp^2 sites, whether in C=C chains or in aromatic

rings. Thus the G-Peak does not only indicate “graphite” in the specimen. Contrary to that the D-Peak is the breathing mode of sp^2 carbon aligned in rings and not in chains.

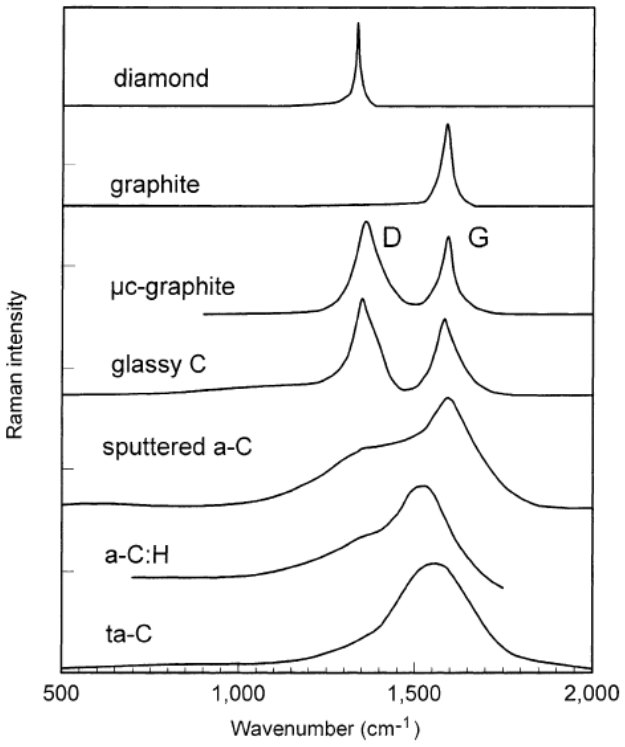

Fig. 3.10 Comparison of typical Raman spectra of carbons.

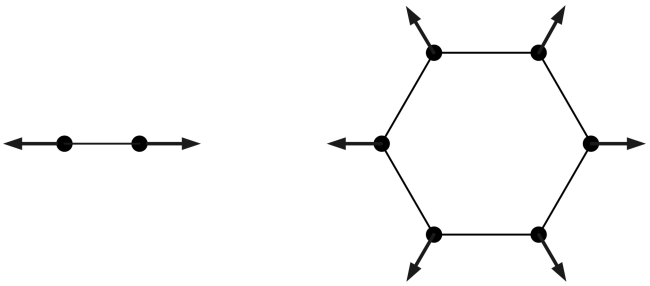

Fig. 3.11 Eigenvectors of the Raman G and D modes in graphite and amorphous carbons.

Robertson *et al* [J. Robertson 2002] have done a great work on diamond-like amorphous carbon. Fig. 3.12 shows the relationship between non-crystalline carbon film structure and the appearance of Raman spectroscopy. There are various factors which can shift the G and D peaks in either direction and also change their relative

intensities and FWHM (full width at half maximum). The structural information of non-crystalline carbon films can be of course obtained from the visible Raman spectroscopy.

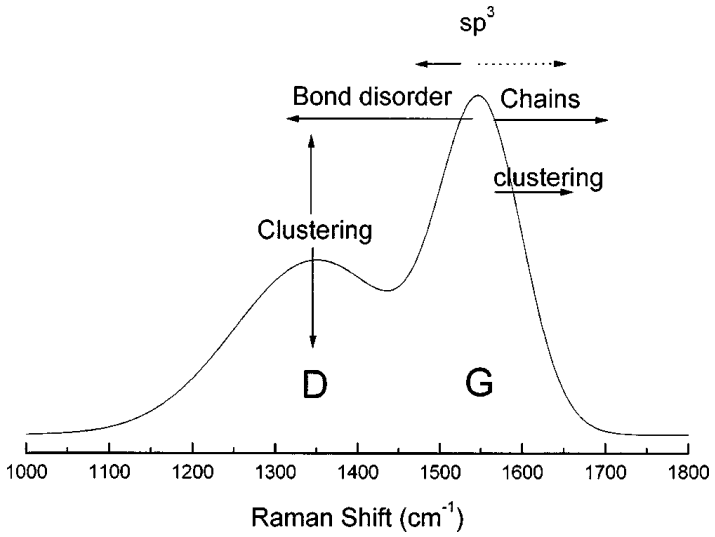

Fig. 3.12 Schematic of the factors affecting the position and heights of the Raman G and D peaks of non-crystalline carbons.

All Raman spectra of amorphous carbon films can be described by the three-stage model according to the degree of disorder [A.C. Ferrari 2000; A.C. Ferrari 2001], as shown in Fig. 3.13. First of all, the Raman spectra were fitted with a skew Lorentzian line shape for the G peak and a Lorentzian for the D peak. With the increase of disorder, amorphous carbon is divided into three stages, perfect graphite to nano-crystalline graphite, nano-crystalline graphite to sp^2 a-C, sp^2 a-C to sp^3 a-C, respectively. D peak comes out because of the increase of disorder. Structural arrangements of the carbon atoms in amorphous carbon materials can be gained from the analysis of Raman spectroscopy, such as G position and I(D)/I(G). However, it is necessary to pay attention to both G position and I(D)/I(G) to know which stage the carbon film belongs to. Because different carbon structures with the same I(D)/I(G) may have different G positions. For instance, one can not confirm which stage the carbon film belongs to only with the known I(D)/I(G) is 1, the G position is the other necessary parameter to make certain the structure of amorphous carbon film by this three stage model.

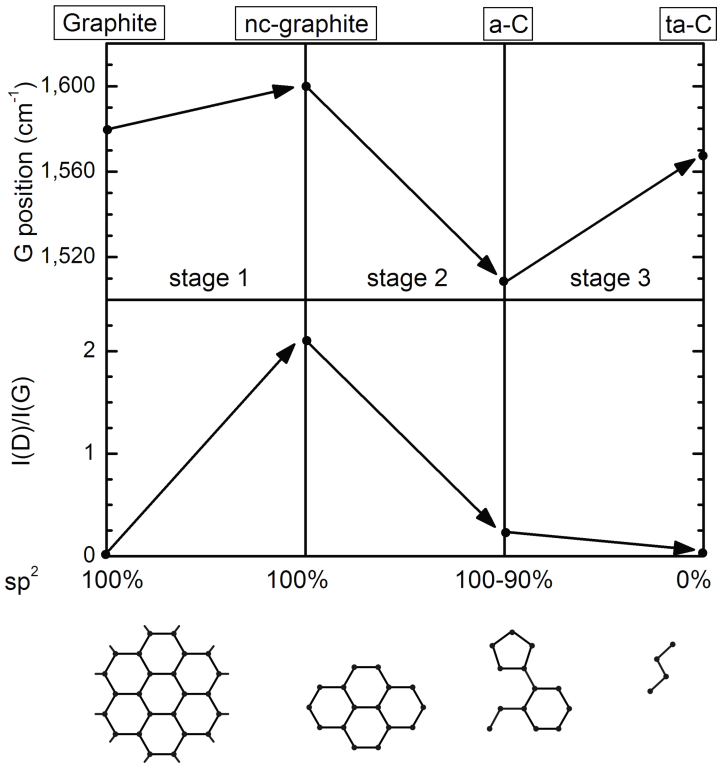

Fig. 3.13 Schematic variation of the Raman G peak wavenumber, and I(D)/I(G) ratio with the degree of disorder, showing three stages of amorphisation of carbon.

Additionally, the structure information of amorphous carbons can be gained from the shift of G-position with excitation wavelength of Raman spectroscopy, as shown in Fig. 3.14. The slope of these several line sections are different corresponding to different structures. The multi-wavelength excitation therefore gives structural information of the carbon films. Also other characters of Raman spectroscopy such as full width at half maximum of G peak (FWHMG), G-Peak dispersion and so on can be used to analysis the structure of carbon films. In conclusion, structural information of carbon films can be acquired with respect of Raman analysis.

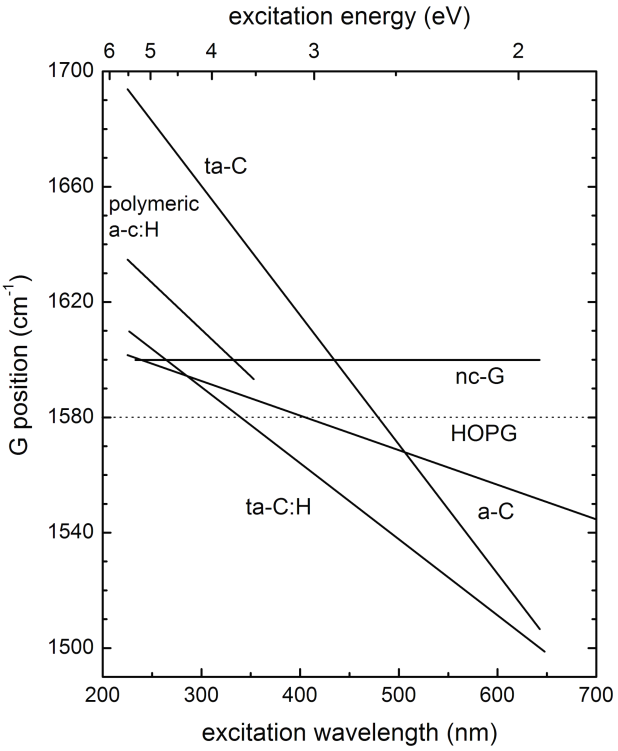

Fig. 3.14 Schematic variation of the Raman G peak wavenumber with the excitation wavelength of Raman spectroscopy.

(3) Raman Spectroscopy of DLC films deposited by liquid electrochemical technique

The films deposited by liquid electrochemical technique in this work were measured by Raman spectroscopy. The Raman measurement was carried out by using the micro-Raman system of Jobin Yvon with laser source wavelength of 632.817 nm and 514.532 nm.

Fig. 3.15 shows a typical example of Raman analysis. The Raman spectrum were Lorenz fitted on a linear background with the help of Origin 7.0 and more information can be calculated, including the centre position of D peak and G peak, the relative intensity I(D)/I(G) and FWHMG. The structural information of the DLC films are acquired, the relationship between film structure and film deposition are therefore investigated.

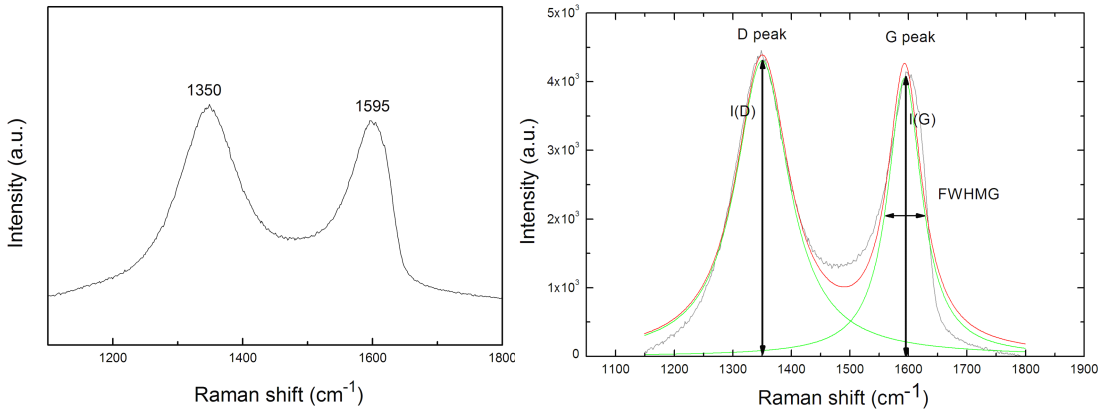

Fig. 3.15 A typical Raman spectrum of the DLC films deposited by liquid electrochemical technique and the corresponding peak deconvolution.

3.4.2 Fourier Transform Infrared Spectroscopy (FTIR)

Infrared spectroscopy (IR spectroscopy) is a widely used non-destructive method in the analysis of amorphous carbon films bonding configuration, especially sensitive to the C-H bonds in amorphous carbon films diagnostic [W. Beyer 1982]. The common laboratory instrument using this IR absorption technique is the Fourier Transform Infrared Spectroscopy (FTIR) in which a data-processing technique called Fourier transform is included [H. Guenzler 1996].

When infrared light interacts with the material, molecules can absorb specific frequencies which match the frequencies of the bonds or groups that vibrate, and this is the principle of IR characterization to determine the structure of materials. For example, the "C=C" has absorption in the range of 1600-1680 cm^{-1}, the "C≡C" has absorption in the range of 2100-2250 cm^{-1} [P. Couderc 1987; J. Ristein 1998].

In this work, FTIR of the DLC films were measured with a Bruker IFS 55 Equinox FTIR. The IR spectra were measured in the range of 1000-4000 cm^{-1} [Analytische Messtechnik GmbH 1995].

In terms of hydrogenated carbon films, the FTIR spectra consist of C-H stretching modes around 2800-3100 cm^{-1} and the C-H bending modes in 1300-1500 cm^{-1} [J. Ristein 1998].

Fig. 3.16 shows an example of peak deconvolution of the C-H stretching vibration band. The applied potential, the electrolyte and the deposition time were 1000 V (frequency 4.2 kHz, duty cycle 50%), analytically pure 2-propanol and 2 h, respectively. The deposition temperature was kept at 60 ºC by water cooling to the wall of the reactor. The anode material, substrate and anode-substrate distance were graphite, silicon wafer ($13\times12\times0.5mm^3$) and 6 mm, respectively. The FTIR spectra

were Gauss fitted with the help of Origin 7.0 in order to carry out the quantitative analysis of amorphous carbon films. The spectrum was fitted into five peaks and the fitting constraints are listed in Table 3.1.

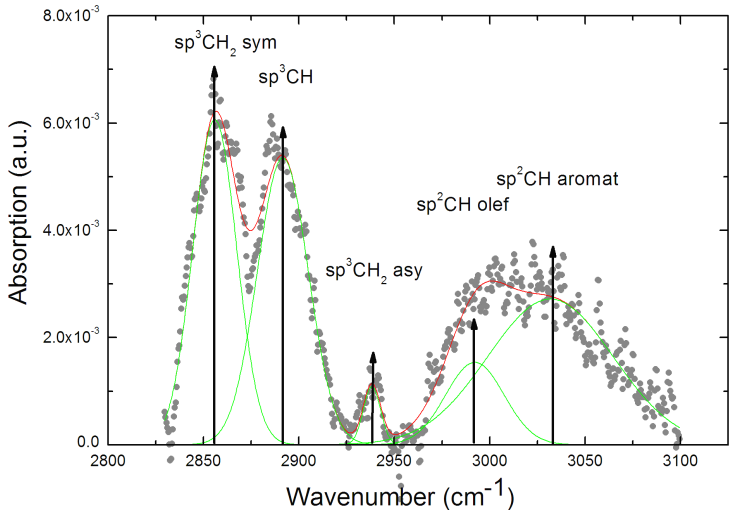

Fig. 3.16 An example of peak deconvolution of the C-H stretching vibration band.

Table 3.1 Survey of frequency and symmetry of C-H stretching vibrations in this work.

No	Peak Position (cm^{-1})	C-H Stretching Modes
1	3020-3061	sp^2CH aromat
2	2973-2998	sp^2CH olef
3	2938-2945	sp^3CH_2 asy
4	2891-2904	sp^3CH
5	2855-2881	sp^3CH_2 sym

The hydrogen content can be calculated with the fitting results of IR spectroscopy [P. Couderc 1987].

$$[H] = \frac{A}{(1.68E + 05)\rho + 0.916A}$$

Where A is the total absorption band of the stretching frequencies of the C-H bonds [cm^{-2}], ρ is the density of the amorphous carbon films measured [g/cm^3].

A quantitative determination of the concentration of CH_x configurations has to be done carefully, because the relation of each CH configuration to the total IR absorption is different. Thus, a calibration factor B_i was used to describe the different absorption strengths of the CH vibration modes.

The integral over the absorption band $A_i = \int \alpha_i(\tilde{\nu}) d\tilde{\nu}$ which belongs to a certain CH configuration, is given by:

$$A_i = \int \alpha_i(\tilde{\nu}) d\tilde{\nu} = \sigma_i \cdot \tilde{\nu}_i \cdot N_i$$

where

α_i = differential absorption coefficient of the vibrational mode i [cm^{-1}],

$\int \alpha_i(\tilde{\nu}) d\tilde{\nu}$ = integrated partial absorption coefficient of the vibrational mode i (from our fit) [cm^{-2}],

N_i = density of the infrared active CH_x bond [cm^{-3}],

σ_i = infrared cross section of a infrared active CH_x bond [cm^2],

$\tilde{\nu}_i$ = wave number of a vibrational mode i [cm^{-1}].

The defined infrared cross section is given:

$$\sigma_i = \frac{\ln(10)}{\tilde{\nu}_i \cdot N_{Avo} \cdot f_i} B_i$$

where

B_i = calibration factor which stands for the ratio of a CH_x vibrational mode to the integrated absorption [cm^{-2}/mol^{-1}],

N_{Avo} = Avogadro constant [mol^{-1}],

f_i = number of hydrogen atoms in a CH configuration: one (CH), two (CH_2), or three (CH_3).

The density N_i of infrared active CH_x bonds is:

$$N_i = \frac{\int \alpha_i(\tilde{\nu}) d\tilde{\nu}}{\ln(10) \cdot B_i} N_{Avo} \cdot f_i.$$

With N_i [cm^{-3}], the sp^3/sp^2 ratio can be calculated by the sum of the area of sp^3 and sp^2 vibration modes as the formula below [J. Ristein 1998].

$$\frac{sp^3}{sp^2} = \frac{\sum N_i(CH_x sp^3)}{\sum N_i(CH_x sp^2)}$$

However, FTIR spectroscopy is only sensitive to the bonded hydrogen in the film. On the one hand, the hydrogen content calculated from FTIR is only the bonded hydrogen content without considering any free hydrogen in the films. On the other hand, the sp^3/sp^2 ratio calculated from FTIR is only the sp^3/sp^2 ratio of the hydrogen-bonded carbon without considering the ones not bonded with hydrogen in the films, e.g. C-C bonds.

3.5 Film Properties

3.5.1 Film Thickness and Growth Rate

Film thickness is one of the most important parameters of thin film characterization. On the one hand, many properties of thin films are dependent on the film thickness. On the other hand, some other parameters such as film growth rate and mass density of the film can be derived from thickness measurement.

In this work, the Dektak 6M Stylus Surface Profilometer and cross sectional scanning electron microscopy (SEM) were used to measure film thickness.

(1) Thickness of the DLC films deposited on Si substrates was measured by Dektak 6M stylus profiler. The Dektak 6M is a semi-manual instrument which gives profile data of a sample detecting the vertical detection of a stylus in contact with the sample which is moved horizontally across the sample surface. Film thickness is the vertical difference between the surfaces of the film and substrate. And then the film growth rate could be easily calculated with film thickness and deposition time.

(2) Because the Dektak 6M was designed with silicon electronics in mind, the samples should be planar, approximately flat and level. However, the stainless steel substrates were easily bended during cutting process and not viable to be measured by the stylus profiler. Then the cross sections of the films deposited on stainless steel substrates were taken to measure the film thickness. The ESEM Quanta 400 FEG was

used to investigate the cross sections of the films deposited on the stainless steel substrates.

Figure 3.17 shows the cross section image of a DLC film deposited on stainless steel substrate. The film was deposited based on the electrolysis of analytically pure isopropyl alcohol using graphite anode. The applied potential and the deposition time were 1000 V (frequency 10 kHz, duty cycle 50%) and 2 h, respectively. The deposition temperature was kept at 60 ºC by water cooling to the wall of quartz reactor. The film thickness taken from the cross section picture was estimated to be 1.96 μm, and then the calculated growth rate was 0.65 μm/h.

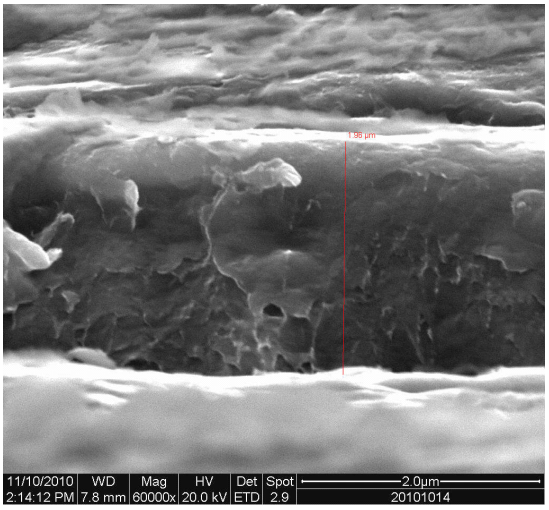

Fig. 3.17 A cross section SEM image of a DLC film deposited on stainless steel substrate by liquid electrochemical technique.

3.5.2 Mechanical Properties

One of the most important applications of DLC films is as protective coatings. The mechanical properties of DLC films are therefore significant. The main mechanical properties, such as friction coefficient and nanohardness are measured here.

The friction coefficient was measured by a Wazau TRM 1000 tribometer using the disc-on-disc test. Nanohardness was measured by Fischer according to the standard of ISO 14577 in the fem Research Institute Precious Metals & Metals Chemistry.

Rrferences

A.C. Ferrari, J. Robertson. "Interpretation of Raman spectra of disordered and amorphous carbon" Physical Review B **61**(2000): 14095-14107.

A.C. Ferrari, J. Robertson. "Resonant Raman spectroscopy of disordered, amorphous, and diamondlike carbon" Physics Review B **64**(2001): 075414-075426.

Analytische Messtechnik GmbH. "User manual FTIR spectrometer IFS 28/IFS 55 Equinox® ". Ettlingen, Analytische Messtechnik GmbH(1995).

B. Jaehne, H. Haussecker, P. Geissler. "Handbook of Computer Vision and Applications Volume 1 Sensors and Imaging". San Diego, London, Boston, New York, Sydney, Tokyo, Toronto, Academic Press(1999).

C. Le Grimellec, E. Lesniewska, M.-C. Giocondi, E. Finot, V. Vie, J.-P. Goudonnet. "Imaging of the surface of living cells by low-force contact-mode atomic force microscopy" Biophysical Journal **75**(1998): 695-703.

D.C. Harris, M.D. Bertolucci. "Symmetry and spectroscopy: an introduction to vibrational and electronic spectroscopy". New York, Dover Publications(1989).

E. Metcalfe. "Atomic absorption and emission spectroscopy". Chichester, Wiley(1987).

H. Guenzler, H.M. Heise. "IR-Spektroskopie". Weinheim, VCH Verlagsge- sellschaft GmbH(1996).

J. Ristein, R. T. Stief, L. Ley. "A comparative analysis of a-C:H by infrared spectroscopy and mass selected thermal effusion" Journal of Applied Physics **84**(1998): 3836-3847.

J. Robertson. "Diamond-like amorphous carbon" Materials Science and Engineering R **37**(2002): 129-281.

J.W. Robinson. "Atomic Absorption Spectroscopy". New York, Marcel Dekker, INC.(1975).

L. Smart, E. Moore. "Solid state chemistry an introduction". UK, Department of Chemistry, The Open University(1996).

M. Born, E. Wolf. "Principles of optics". London, Cambridge University Press(1997).

M. Dufek (2008). The Quanta FEG User Operation Manual, FEI Company.

M.F. Murphy, M.J. Lalor, F.C.R. Manning, F. Lilley, S.R. Crosby, C. Randball, D.R. Burton, . "Comparative study of the conditions required to image live human epithelial and fibroblast cells using atomic force microscopy" Microscopy Research and Technique **69**(2006): 757-765.

P. Couderc, Y. Catherine. "Structure and physical properties of plasma-grown amorphous hydrogenated carbon films" Thin Solid Films **146**(1987): 93-107.

P. Eaton, P. West. "Atomic force microscopy". Oxford, Oxford University Press(2010).

Q. Zhang, D. Inniss, K. Kjoller, V.B. Elings. "Fractured polymer/silica fiber surface studied by tapping mode atomic force microscopy" Surface Science **290**(1993): 688-692.

S. Karrasch, M. Dolder, F. Schabert, J. Ramsden, A. Engel. "Covalent binding of biological samples to solid supports for scanning probe microscopy in buffer solution" Biophysical Journal **65**(1993): 2437-2446.

W. Beyer, H. Wagner. "Determination of the hydrogen diffusions coefficient in hydrogenated amorphous silicon from hydrogen effusion experiments" Journal of Applied Physics **53**(1982): 8745-8750.

4 Experimental Setup

The experimental setup used for liquid electrochemical deposition of DLC films is presented in this chapter. At first, the main components of the deposition system are described. In addition, the experimental procedures including substrate pretreatment and films deposition are introduced. Finally, there are introductions to several major deposition parameters.

4.1 Deposition Facility

DLC films were successfully deposited by liquid electrochemical technique. Compared with vapor depositions of DLC films, the most outstanding difference of liquid electrochemical technique is the simplicity of the experimental setup without any vacuum system. The deposition equipment used in this work was self designed. It was composed of a reactor, a power supply and a data acquisition system which can measure the real time voltage and current during deposition. The Optical Emission Spectroscopy (OES) for liquid plasma detection was also included in the deposition system. The spectra in this work were obtained by a Jobin Yvon HR 460 spectrometer which was coupled to the process chamber via a glass fiber. The schematic diagram of the construction of the electrochemical deposition system is displayed in Fig. 4.1.

The liquid deposition system was similar to an electrolytic cell. A club-shaped electrode (made of graphite or metal) in diameter of 6 mm with a cone-shaped tip was used as the anode electrode, and a substrate was mounted on the cathode electrode. The distance between the two electrodes could be continuously changed from 0 to 12 mm. The sample holder inside the reactor was made of chemically stable materials polytetrafluoroethylene (PTFE) in order to get rid of unwanted impurities. The deposition process leads to sufficient heating of the organic solution that makes a cooling system necessary. Water-cooling to the wall of the reactor (made of glass or quartz) was used to control the deposition temperature.

The power supply used in this work was Magpuls QP-1000/10/20 BP. The applied potential, duty cycle and frequency could be changed from 0 to 1000 V, 0 to 100% and 0.05 to 33 kHz, respectively.

The data acquisition system included a voltage probe, a current probe, an oscillograph and a computer. Testec High Voltage Probe TT-HVP 15HF was used to measure the voltage during deposition process, while P6022 Current Probe was used to measure the current at the same time. The real time voltage and current were simultaneously recorded by the TDS 2012 two-channel digital storage oscilloscope. The dependence of voltage and current on time was recorded by the computer.

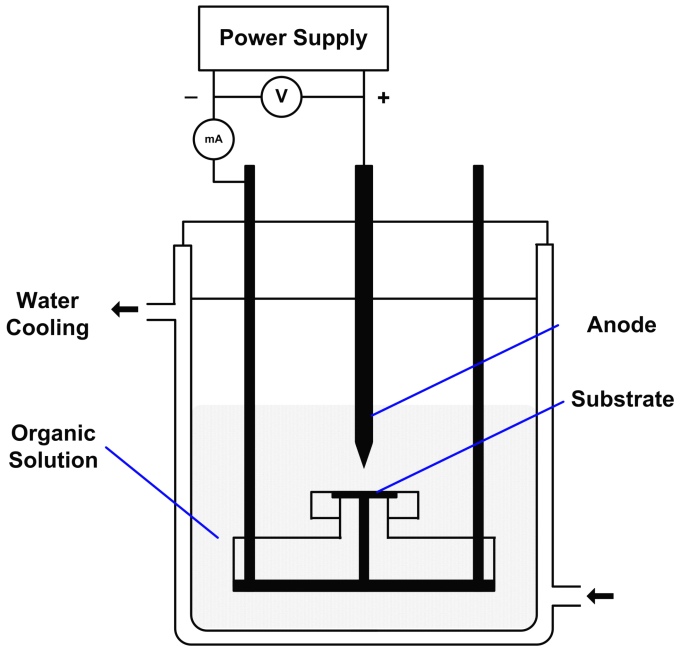

Fig. 4.1 Schematic diagram of the liquid electrochemical deposition system used in this work.

4.2 Deposition Procedure

The liquid electrochemical deposition of DLC films was carried out in four steps as following.

4.2.1 Substrate Pretreatment

Si and stainless steel wafers were used as substrate in this work. As well known, pretreatment of the substrates is a critical point in the deposition of thin films. Different sample pretreatments before deposition can therefore lead to totally different performance of the films. For example, roughness of the substrate surface has a strong influence on quality and adhesion of the films. To attain comparable and good quality results, all the same kind of substrates had been treated in the same way before deposition. The standard substrate pretreatment procedure for each kind of substrates is described below.

(1) Si substrates

N(p)-type (100) oriented single side polished silicon wafers of resistivity 5-10 Ω·cm with the thickness of 525±20 μm were carefully cut into pieces of 13 mm × 12 mm as substrates. Prior to the deposition, the substrates were polished by 0.1 μm diamond paste and ultrasonically cleaned in 2-propanol and deionized water for 10 min, respectively, and then dried with pure nitrogen.

(2) Stainless steel substrates

The stainless steel substrates in the dimension of 13 mm × 12 mm × 0.5 mm were electrochemical polished in the workshop in campus Essen. The cleaning process of stainless steel substrates were the same as that of Si substrates.

4.2.2 Preparation before Deposition

The substrate was mounted on the negative electrode after weighing by a balance. And then the organic solution of certain composition was filled into the reactor. The electrodes were connected with the power supply and also the data acquisition system which was used to measure the voltage and current during deposition process.

4.2.3 Deposition of DLC Films

The deposition started as soon as the potential was applied. The dependence of voltage and current on time was recorded during deposition process. The deposition temperature was controlled in the range of 60-70 ºC by water-cooling to the wall of the reactor. The deposition time was a variable parameter according to the requirement of the deposition. The power supply was turned off when deposition time came to the time planned. The cooling water was switched off when the temperature decreased to room temperature.

4.2.4 Process after Deposition

The substrate was taken out of the reactor after deposition, and then it was dried by pure nitrogen and the weight was measured. The samples were stored for characterization.

4.3 Deposition Parameters

Deposition of DLC films using liquid electrochemical technique is quite sensitive to the deposition parameters, such as carbon source, additive, applied potential, anode-substrate distance and temperature and so on.

4.3.1 Carbon Source

4.3.1.1 To Confirm Organic Solution is the Carbon Source of DLC Films Deposited by Liquid Electrochemical Technique

Growth of carbon films using electrochemical technique was first attempted by Namba [Y. Namba 1992]. Since then liquid electrochemical technique has been applied to deposit DLC films. Different kinds of organic solutions were used as electrolyte, either pure organic chemicals or mixed ones. For instance, DLC films were deposited from methanol [H. Wang 1996] and analytically pure N, N dimethylformamide (DMF) [D. Guo 2000], respectively. Carbon films were deposited from water-ethylene-glycol solution [T. Suzuki 1995], and DLC films were deposited using a solution of acetylene in liquid ammonia [V.P. Novikov 1997]. All the researchers implied that organic chemicals play the role of carbon source in DLC films liquid electrochemical deposition. However, anode electrodes made of graphite are widely used. Besides organic solutions, the graphite anode also contains carbon in the deposition system and could possibly provide carbon in the liquid deposition process. It is therefore not believable to say that organic solutions play the role of carbon source without any proof. But deposition of DLC films using non-carbon electrode is rare to see. In this section, anode made of Pt which can avoid carbon from the graphite anode was introduced into the liquid deposition system, in order to investigate whether organic solutions are carbon source of DLC films.

(1) Experimental details

A quartz reactor with water cooling was used here. The distance between Pt anode and Si substrate was set to 6 mm. The applied potential, electrolyte and the deposition time were 1000 V (frequency 10 kHz, duty cycle 50%), analytically pure 2-propanol and 2 h, respectively. Microstructure of the films deposited was investigated using a micro-Raman system Jobin Yvon with a laser source wavelength of 514.532 nm.

(2) Results

Raman is a widely used non-destructive way to obtain the detailed bonding structure of DLC materials [J. Robertson 2002]. Fig. 4.2 shows Raman spectroscopy of the DLC films deposited using Pt anode. Raman analysis confirmed that typical DLC

films were deposited. It is evident that typical DLC films could be deposited by liquid electrochemical technique using Pt electrode. Since the analytically pure 2-propanol was the only component containing carbon element, it must be the carbon source of the DLC films deposited.

(3) Conclusions

DLC films were deposited by electrochemical technique using non-carbon anode electrode such as Pt. Organic solution was the only component containing carbon element in the deposition system. Organic solutions are therefore proved to be the carbon source of DLC films deposited by liquid electrochemical technique.

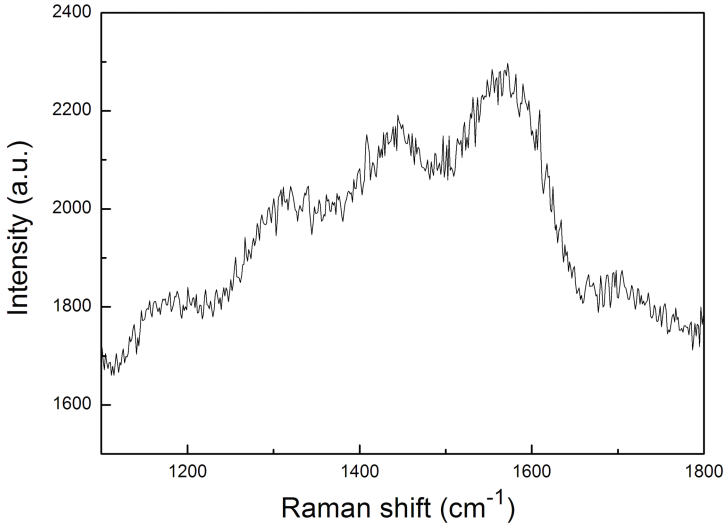

Fig. 4.2 Raman spectroscopy of the DLC films deposited by liquid electrochemical technique using Pt anode.

4.3.1.2 Introduction of Carbon Source

Organic solution indicates to liquid chemical compound whose molecules contain carbon, and it has already been proved to be the carbon source in DLC films liquid electrochemical deposition.

The idea that the deposition of DLC films and the film properties could be affected by the organic chemicals was suggested by the published articles [H.S. Zhu 2003; W.L. He 2005]. Thus carbon source is considered to be an important parameter in the deposition of DLC films deposited by liquid electrochemical technique.

4.3.2 Additive

The electrolysis of analytically pure organic chemicals has been widely used to prepare DLC films [H. Wang 1996; R.S. Li 2009]. Nevertheless, some researchers tend to put additives into pure organic chemicals in order to avoid the disadvantages of pure chemicals and get ideal DLC films [T. Suzuki 1995; V.P. Novikov 1997].

Additive is another kind of chemical besides the carbon source and is added into the electrolyte in liquid electrochemical technique. The additive plays the role of activator in the electrochemical reaction. Because the additive could directly change the composition and dielectric constant of solution, and it is possible to affect the deposition of DLC films in liquid electrochemical method.

4.3.3 Anode-Substrate Distance

As the name implies, “Anode-Substrate Distance” is vertical distance between anode and substrate. In our deposition system, the distance between anode and substrate is designed adjustable, continuously various from 0 to 12 mm.

4.3.4 Applied Potential

Applied potential is exported from the power supply and applied on the anode and cathode. Applied potential is an important parameter in the traditional electrochemical reactions. So does in the deposition process of DLC films by liquid electrochemical technique, which is essentially a process of electrolysis. Both the decomposition of organic chemicals and the growth of DLC films require energy which could only be provided by the power supply. High applied potential means that more energy is inputted into the deposition process. However, it does not mean that high applied potential could definitely get DLC films formation or appropriate film growth rate. The effects of various applied potential on the deposition of DLC films using liquid electrochemical technique should be investigated.

4.3.5 Deposition Temperature

The electrolysis process could lead to sufficient heating of the electrolyte. On the one hand, high temperature advances the mobility of the organic molecules. And this leads more particles to the substrate and it is propitious to films deposition. On the other hand, the electrolyte will be acutely boiled if the temperature is over the boiling point

of the used organic chemicals. The composition of the mixed solution will be changed due to the evaporation of organic chemicals. Thus the deposition system should be controlled under the boiling point of the organic solution but as high as possible. In this work, the deposition temperature was controlled according to the boiling points of different organic chemicals by water-cooling to the wall of the reactor. For example, the boiling point of analytically pure methanol is 64.5 ºC in standard atmosphere. It is better to control the temperature below 60 ºC when methanol is used as electrolyte.

References

D. Guo, K. Cai, L.T. Li, Y. Huang, Z.L. Gui, H.S. Zhu, . "Evaluation of diamond-like carbon films electrodeposited on an Al substrate from the liquid phase with pulse-modulated power" Carbon **39**(2000): 1395-1398.

H. Wang, M.R. Shen, Z.Y. Ning, C. Ye, C.B. Cao, H.Y. Dang, H.S. Zhu. "Deposition of diamond-like carbon films by electrolysis of methanol solution" Applied Physics Letters **69**(1996): 1074-1076.

H.S. Zhu, J.T. Jiu, Q. Fu, H. Wang, C.B. Cao. "Aroused problems in the deposition of diamond-like carbon films by using the liquid phase electrodeposition technique" Journal of Materials Science **38**(2003): 141-145.

J. Robertson. "Diamond-like amorphous carbon" Materials Science and Engineering R **37**(2002): 129-281.

R.S. Li, M. Zhou, X. J. Pan, Z.X. Zhang, B.A. Lu, T. Wang, E.Q. Xie. "Simultaneous deposition of diamondlike carbon films on both surfaces of aluminum substrate by electrochemical technique" Journal of Applied Physics **105**(2009): 066107-1-3.

T. Suzuki, Y. Manita, T. Yamazaki, S. Wada, T. Noma. "Deposition of carbon films by electrolysis of a water-ethylene glycol solution" Journal of Materials Science **30**(1995): 2067-2069.

V.P. Novikov, V.P. Dymont. "Synthesis of diamondlike films by an electrochemical method at atmospheric pressure and low temperature" Applied Physics Letters **70**(1997): 200-202.

W.L. He, R. Yu, H. Wang, H. Yan. "Electrodeposition mechanism of hydrogen-free diamond-like carbon films from organic electrolytes" Carbon **43**(2005): 2000-2006.

Y. Namba. "Attempt to grow diamond phase carbon films from an organic solution" Journal of Vacuum Science Technology A **10**(1992): 3368-3370.

5 Effects of Experimental Facilities on Deposition of DLC Films by Liquid Electrochemical Technique

Diamond-like carbon (DLC) films have attracted interesting attention in recent years due to their excellent physical and chemical properties, such as high hardness, low friction coefficient, wear-resistance and chemical inertness [Y. Lifshitz 1999; J. Robertson 2002]. DLC films can be prepared by physical vapor deposition (PVD) and chemical vapor deposition (CVD) at low pressure and temperature (< 200 ºC) [J.J. Cuomo 1991; M. Zarrabian 1997]. Because most of the thin film materials can be synthesized in liquid phases based on electroplating techniques [L.I. Maissel 1970], growth of diamond phase carbon films was first attempted using liquid electrochemical technique by Namba [Y. Namba 1992] in 1992. Since then liquid phase deposition has received growing interest, DLC films were deposited from various organic solutions [H. Wang 1996; V.P. Novikov 1997; D. Guo 2000]. In addition, several kinds of materials have been attempted as substrates, including silicon, stainless steel and aluminum [Y. Namba 1992; H. Wang 1996; Z. Sun 2000; J.Y. Du 2007; R.S. Li 2009]. All the articles implied that carbon films could be deposited on different substrates by liquid electrochemical technique. However, further research work about experimental facility in detail is rare to see. The aim of this chapter is to correlate the effects of reactor and anode design on the deposition of carbon films using liquid electrochemical technique.

5.1 Reactor Design

5.1.1 Experimental Details

A graphite anode was used as the anode electrode and Si wafer was mounted on the negative electrode. The distance between anode and substrate was fixed at 6 mm. The applied potential, the electrolyte and the deposition time were 900 V (frequency 4.2 kHz, duty cycle 50%), acetone/deionized water solution in the volume ratio of 2:1 and 5 h, respectively. Glass reactor, glass reactor with PTFE-coating inside, glass reactor with quartz-coating inside and quartz reactor were used in our deposition system, respectively. The effects of reactor design in DLC films liquid phase deposition are investigated.

The surface morphology of the films was measured by scanning electron microscopy (SEM) ESEM Quanta 400 FEG, and Energy Dispersive X-ray Spectroscopy (EDX) was used to measure the composition of the films at the same time. The microstructure of the carbon films deposited was investigated using the micro-Raman

system of Jobin Yvon with a laser source wavelength of 632.8 nm. Also the X-ray diffraction (XRD) technique with Phillips PANalytical X'Pert PRO was used to measure the phase structure of the films.

5.1.2 Results

5.1.2.1 Glass Reactor

Carbon films were deposited by electrolysis of acetone/deionized water solution using glass reactor at first. All the films deposited appeared grey in color. Fig. 5.1 shows typical SEM images and the corresponding EDX spectra of the films deposited on Si substrates using glass reactor. Some crystals of several micrometers were observed on the surface of a smooth film which made the films very non-uniform, as shown in Fig. 5.1a and Fig. 5.1c. The EDX spectra of the areas demonstrated by boxes in Fig. 5.1a and Fig. 5.1c identify the chemical composition of the crystals, which are shown in Fig. 5.1b and Fig. 5.1d. The sharp silicon peaks are obviously due to the Si substrates, while the presence of sharp calcium (Ca) peaks confirm that the crystals contained nearly 10 at.% of calcium. However, Ca is considered to be a kind of impurity in non-doped carbon films. It is necessary to make the structure of crystals clear because there is too much impurity of Ca in the films deposited and maybe the combination between Ca and other compositions will affect the structure and property of the carbon films. SEM, Raman and XRD were used to measure both morphology and structure of the crystals. The results are discussed as following.

SEM images of the crystals in Fig. 5.1a and Fig. 5.1c with high magnification are shown in Fig. 5.2a and Fig. 5.2b, respectively. Fig. 5.2c and Fig. 5.2d show typical calcite rhombohedral crystals and vaterite spherulites crystals which are two main shapes of $CaCO_3$ [R.J. Nemanich 1988]. The crystals deposited on the films have quite similar morphology with $CaCO_3$ crystals by comparison. It is possible that Ca^{2+} ions could easily react with the carbide and oxide which are existent in the experimental organic solution to form $CaCO_3$. Therefore, other measurements such as Raman and XRD were carried out to determine the structure of the crystals.

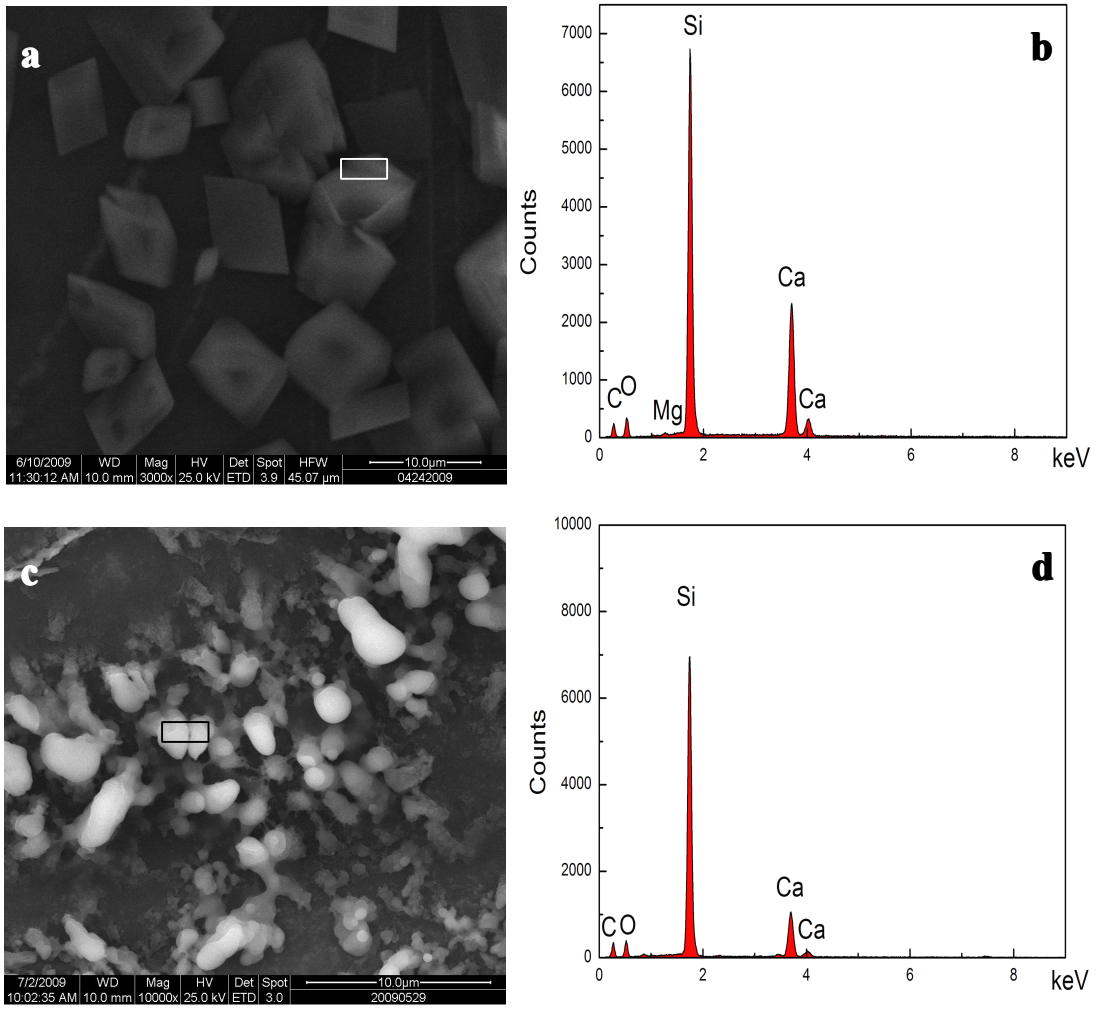

Fig. 5.1 Two typical SEM images (a and c) of the films deposited on Si substrates using glass reactor and the corresponding EDX spectra (b and d) of the areas demonstrated by boxes.

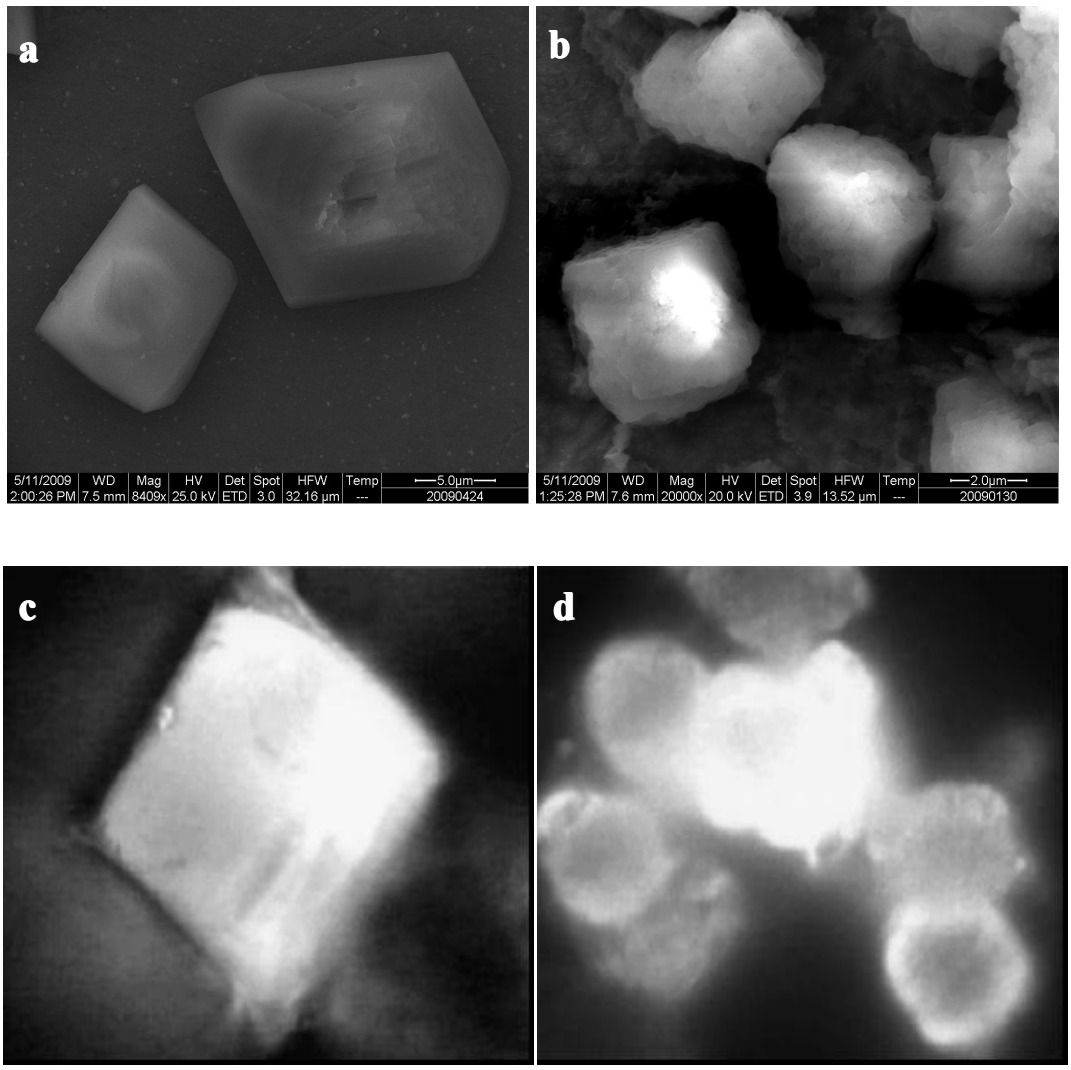

Fig. 5.2 Fig. 5.2a and Fig. 5.2b are high magnification of the crystals shown in Fig. 5.1a and Fig. 5.1c. Fig. 5.2c and Fig. 5.2d are typical SEM images of calcite are from reference [S. Martinez-Ramirez 2003].

Raman spectroscopy is the most important tools for characterizing diamond and DLC materials. Fig. 5.3 is the Raman spectrum of the area demonstrated by the box in Fig. 5.1a. Two broad peaks around 1332 cm^{-1} and 1595 cm^{-1} appear in the Raman spectrum, respectively. These two peaks are related to D peak at 1355 cm^{-1} and G peak at 1580 cm^{-1}, indicating that some sp^2 amorphous carbon phases exist in the film [R.J. Nemanich 1988; D.S. Knight 1989; W.A. Yarbrough 1990]. Also there is another sharp peak at 1085 cm^{-1} which does not belong to any carbon phase. This peak is assigned to calcite or aragonite (two crystallized forms of calcium carbonate $CaCO_3$) crystals [C. Gabrielli 2000], and the line width of the peak is 7.73 cm^{-1} which indicates that the quality of the calcium carbonate crystals is quite good. The formation of $CaCO_3$ is possible with the existence of calcium (Ca), carbon (C) and

oxygen (O) in the liquid electrochemical deposition process. Within the three crystallized forms of calcium carbonate polymorphs, calcite is the most thermodynamically stable at ambient pressure and temperature. So the formation of calcite is favored and it is consistent with the result of Raman. However, it is not necessary to determine which kind of calcium carbonate was deposited on our carbon films.

The XRD pattern of the typical film deposited using glass reactor is displayed in Fig. 5.4. It is evident from the intensity of the peaks that the crystals are highly crystalline in nature. The peak positions correspond closely to the standard pattern of calcium carbonate (JCPDS: 5-586). It could be concluded by the analysis of XRD spectrum that $CaCO_3$ is included in the typical carbon films deposited using glass reactor by electrochemical technique.

According to the results of not only SEM and EDX, but also Raman and XRD, the conclusion is that the crystals are $CaCO_3$.

However, $CaCO_3$ is obviously not what we need in the deposition of DLC films by electrochemical technique. The impurity of Ca must be deleted in order to avoid the formation of calcium carbonate.

To find the source of Ca is the first step to avoid doping during the deposition process. Considering the deposition system of liquid electrochemical technique, the electrolyte solution used in this experiment and the glass reactor were the two possible sources of Ca. At first, the composition of the electrolyte was measured by atomic absorption emission spectrophotometer (AAS) AA-6200. However, the electrolyte was not the source of Ca because the electrolyte was composed of analytically pure acetone (99.8%) which contained Ca less than 0.000005 wt.% and deionized water with the proportion of Ca below the determination limit of AAS. After getting rid of the effect of electrolyte, the glass reactor could have the highest possibility to provide Ca. Normally calcium oxide (CaO) is added to common glass in order to avoid the glass soluble which is made by the addition of sodium carbonate (Na_2CO_3) [B.H.W.S. de Jong 1989]. Maybe the calcium in the form of atom or ion could come out from the glass and go into the electrolyte solution under the special condition during electrochemical deposition, such as organic solution, high electric field and so on.

The glass type used in our work is "G20®" made by Schott GmbH Mainz which contains 1.1% of CaO by weight. Let it be supposed that glass reactor is the source of Ca; then the following parallel experiments with the same parameters were carried out using glass reactor with coatings inside which could avoid the direct contact between glass reactor and electrolyte solution in order to exam whether glass reactor is the source of Ca.

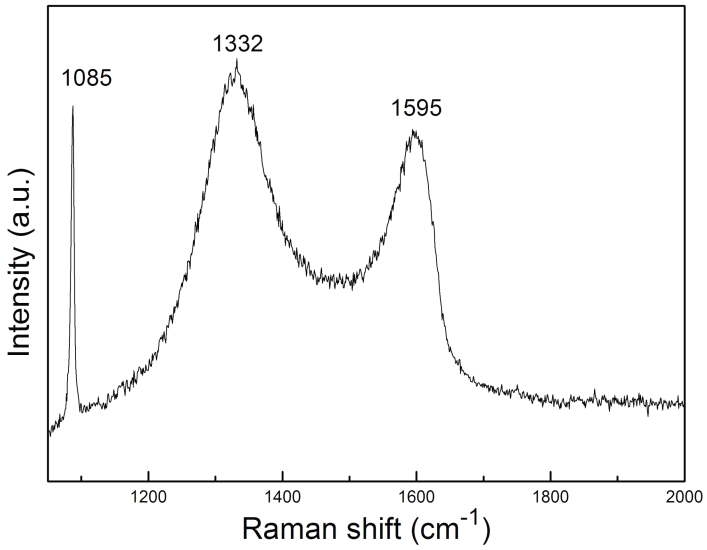

Fig. 5.3 The Raman spectrum of the area demonstrated by the box in Fig. 5.1a.

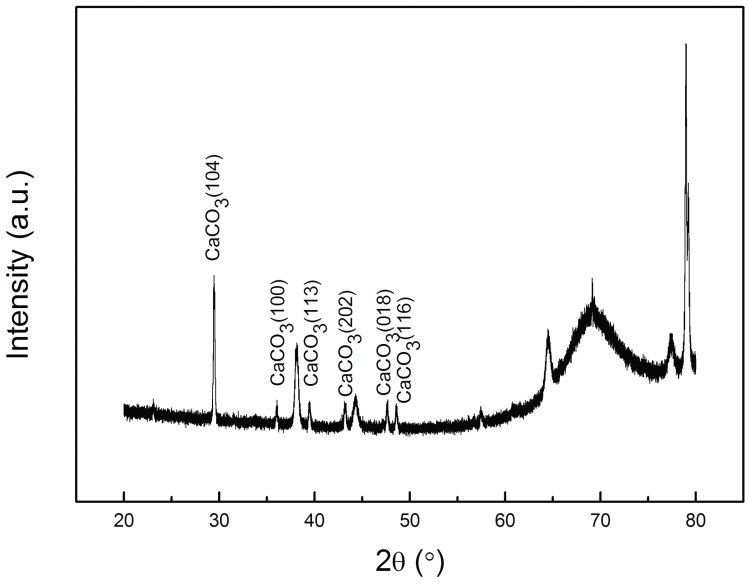

Fig. 5.4 The X-ray diffraction (XRD) patterns of the typical film (Fig. 5.1a) deposited using glass reactor.

5.1.2.2 Glass Reactor with PTFE-coating Inside

Polytetrafluoroethylene (PTFE) was attempted to be the first coating material deposited inside glass reactor because of the applied temperature and its excellent resistance to organic chemicals isolation. The Teflon-suspension from Dupont was deposited with an airbrush on the inside wall of the glass reactor which was already heated to 100 ºC. The reactor was annealed at 280 ºC for 2 h at first and then 320 ºC for 30 min in an oven, and cooled down to room temperature [S. Seisel 2009].

The typical SEM image (a) and the corresponding EDX spectrum (b) of the films deposited on Si substrates using glass reactor with PTFE-coating inside are shown in Fig. 5.5. The morphology of the film is very rough without any crystals on the surface, which is totally different from the film deposited using glass reactor shown in Fig. 5.1a. There is no Ca in the film because of the absence of Ca peak in the EDX spectrum, as shown in Fig. 5.5b. It is confirmed that glass reactor is the source of Ca and using a coating inside the reactor which can avoid the direct contact between electrolyte solution and glass is an effective solution to get rid of Ca coming from glass.

Although the PTFE-coating could successfully avoid the impurity of Ca coming from the glass reactor, the new impurities such as Sn, Cl and S which came from the PTFE-coating bring new problems. Maybe these new impurities could affect the morphology of the films deposited and make the films rough.

Even though some work during the preparation of PTFE-coating could be done to avoid the introduction of the non-metallic impurities mentioned above, the low hardness of PTFE- coating is another disadvantage impossible to conquer up to now.

PTFE has one of the lowest coefficients of friction against any solid and the coating was really easy to get broken by rubbing. As a result the glass reactor could have partially direct contact with the electrolyte again and then the impurity of Ca will go into the films again. From this point, PTFE is not an ideal coating material for a long term of application in our experiment.

On the one hand, PTFE-coating could introduce new impurities which could affect the morphology of the films deposited; on the other hand, PTFE-coating is not hard enough to protect electrolyte from contiguity with the glass reactor. Therefore, some other kinds of coatings which could overcome the disadvantages of PTFE-coating should be carried out in the following parallel electrochemical deposition.

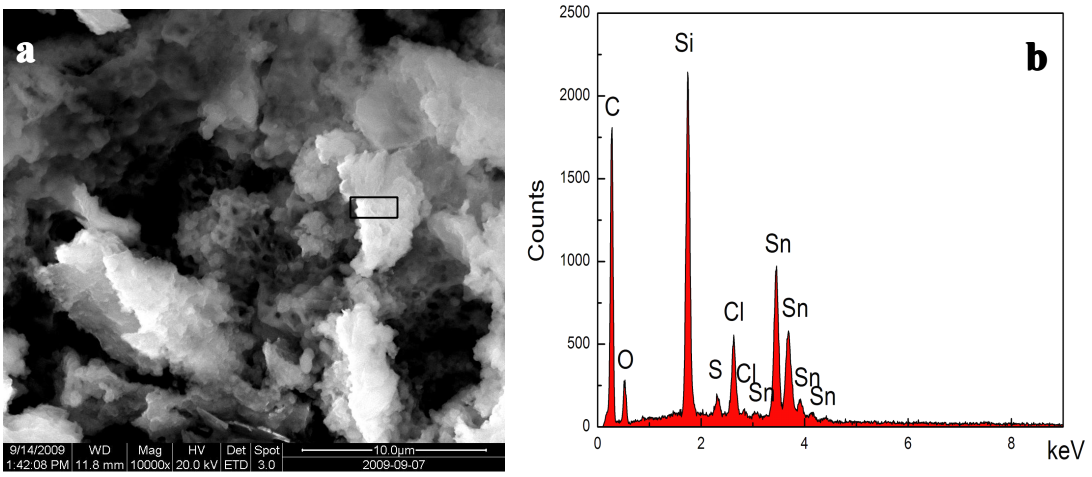

Fig. 5.5 A typical SEM image (a) of the films deposited on Si substrates using glass reactor with PTFE-coating inside and the corresponding EDX spectrum (b) of the area demonstrated by a box in Fig. 5.5a.

5.1.2.3 Glass Reactor with Quartz-coating Inside

Quartz was chosen as the second coating material in order to avoid the disadvantages of both glass reactor and glass reactor with PTFE-coating inside. Quartz coating was deposited inside of the glass reactor [M. Jerman] and carbon films were deposited under the same experimental parameters.

Typical SEM image (a) and the corresponding EDX spectrum (b) of the films deposited using glass reactor with quartz coating inside are displayed in Fig. 5.6. Compared with the morphology of the carbon films deposited using both glass reactor and glass reactor with PTFE-coating inside, the film deposited using glass reactor with quartz-coating inside is continuous and smooth without any obvious crystals and rough areas. The corresponding EDX spectrum of the area demonstrated by a box shows that there is no non-metallic impurities as caused by PTFE-coating but still a little bit of Ca (< 1 at. %) left. The left Ca might be from the glass reactor was partially uncovered by quartz-coating which could result in some direct contact between the electrolyte solution and glass reactor.

At least, quartz appeared to be an ideal coating material in our deposition system. However, more work should be done to avoid all the Ca, such as symmetrical quartz-coating with enough thickness should be prepared on the inside wall of glass reactor or reactor made of quartz should be introduced to our liquid electrochemical deposition system.

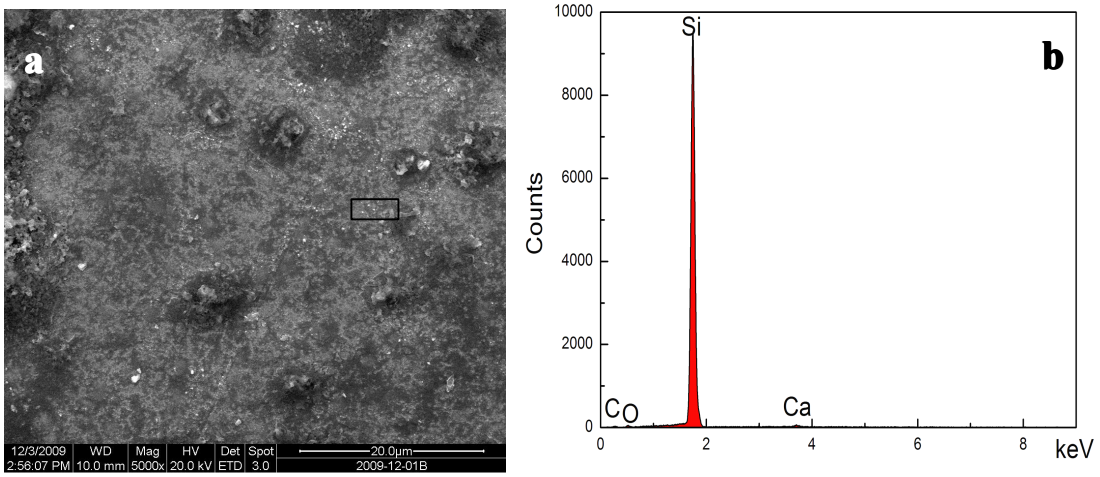

Fig. 5.6 A typical SEM image (a) of the films deposited on Si substrates using glass reactor with quartz-coating inside and the corresponding EDX spectrum (b) of the area demonstrated by a box in Fig. 5.6a.

5.1.2.4 Quartz Reactor

The reactor made of quartz was used in the following deposition because quartz-coating reactor had done a good job. All the films deposited using quartz reactor by liquid electrochemical technique appeared grey in color. A typical SEM image (a) coupled with the corresponding EDX spectrum (b) of the films deposited on Si substrates using quartz reactor is shown in Fig. 5.7. The film owns continuous and smooth surface without any crystals and rough areas. And there is no peak of Ca any more in the EDX spectrum. It is concluded that the quartz reactor could successfully avoid any impurities from other reactors.

Fig. 5.8 is the Raman spectrum of the area demonstrated by the box in Fig. 5.7a. Raman spectroscopy analysis confirmed that typical DLC film was deposited using quartz reactor by liquid electrochemical technique. The absence of $CaCO_3$ peak at 1085 cm^{-1} confirms no Ca is in the film and it is consistent with the result of EDX. DLC films without any impurity were deposited using quartz reactor by liquid electrochemical technique.

Compared with the Raman spectrum in Fig.5.3, the position of the D peak is shifted to higher values as shown. The D peak is attributed to the breathing modes of sp^2 atoms in rings [A.C. Ferrari 2000; T. Kumagai 2010]. The shift of the D peak must be attributed to modification of the local surrounding of the sp^2-rings, the exact origin is still discussed [A. Cuesta 1994].

Quartz is the perfect material to make reactors in the deposition of DLC films by liquid electrochemical technique.

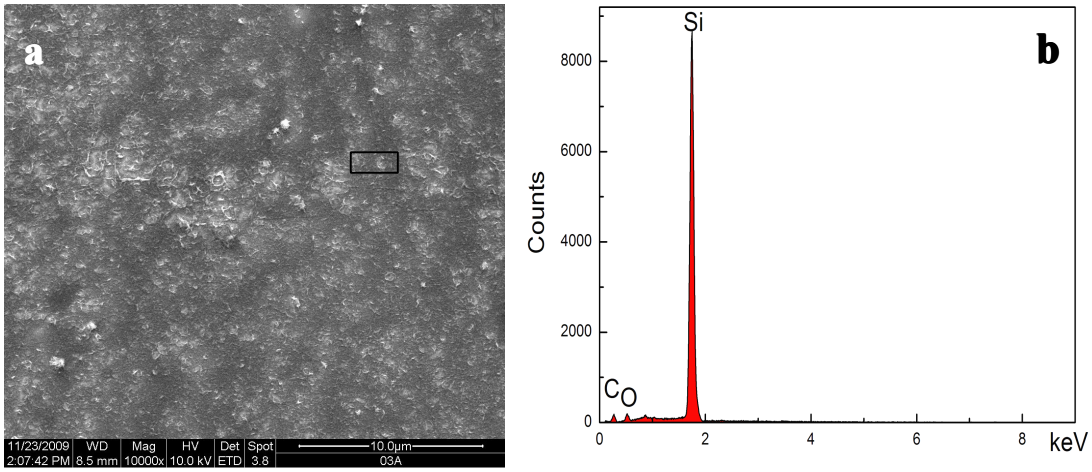

Fig. 5.7 A typical SEM image (a) of the films deposited on Si substrates using quartz reactor, and the corresponding EDX spectrum (b) of the area demonstrated by a box in Fig. 5.7a.

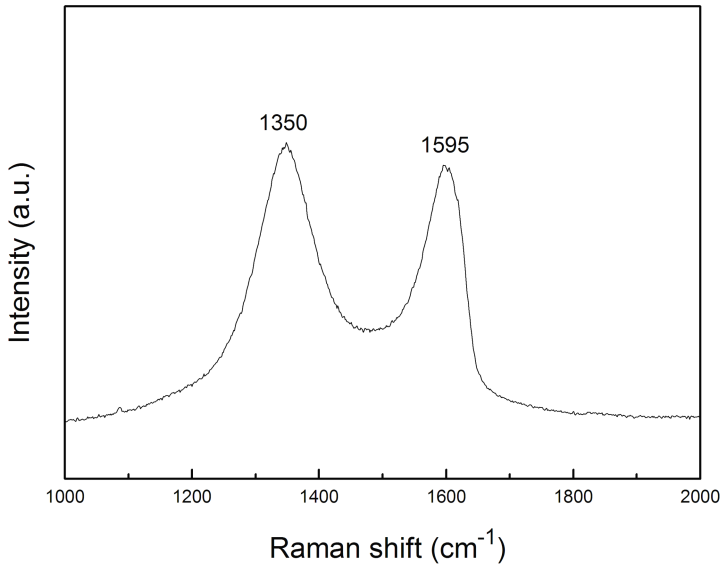

Fig. 5.8 Raman spectrum of the area demonstrated by a box in Fig. 5.7a.

5.2 Anode Design

Anode is a necessary part of the experimental facilities in liquid electrochemical deposition system. On the one hand, anode made of graphite was widely used by many researchers to deposit DLC films [T. Suzuki 1995; H. Wang 1996; V.P. Novikov

1997; D. Guo 2000]. On the other hand, platinum (Pt) wire was introduced as anode by Sun [Z. Sun 2000] and Du [J.Y. Du 2007]. It is evident that DLC films could be deposited using anodes made of either graphite or Pt. However, comparison of different anode materials on liquid electrochemical deposition of DLC films has never been investigated.

In this section, anodes made of graphite, Pt, Copper (Cu) and stainless steel were introduced into liquid electrochemical deposition system, respectively. Not only the deposition process, but also the morphology and microstructure of the films deposited were investigated. The aim of this study is to discuss the effects of different anode materials on the deposition of DLC films using liquid electrochemical technique.

5.2.1 Experimental Details

A quartz reactor with water cooling was used in our deposition system based on the investigation of reactor design. The anodes were made of graphite, Pt, Cu and stainless steel, respectively. The anodes made of graphite, Cu and stainless steel were all rods in diameter of 6 mm with a cone-shaped tip, while the anode made of Pt was a wire in diameter of 1 mm. The deposition parameters and characterization were the same as in the above section.

5.2.2 Results

5.2.2.1 Films Deposition

The film thickness was firstly measured and then the growth rate was calculated. Fig. 5.9 shows the growth rate of the films deposited using four different anodes. The highest growth rate was obtained by using stainless steel, and the second is using graphite. The growth rate of film deposited using Cu anode is much lower than the first two, but a little bit higher than the growth rate achieved by using Pt anode. It is obvious that anode materials have influence on the growth rate of the films deposited by liquid electrochemical technique.

The growth rate from graphite anode is significantly higher than those from Pt or Cu anodes, however, it can not be concluded that most of the coatings comes from the graphite anode because no films growth from a graphite anode in water is observed.

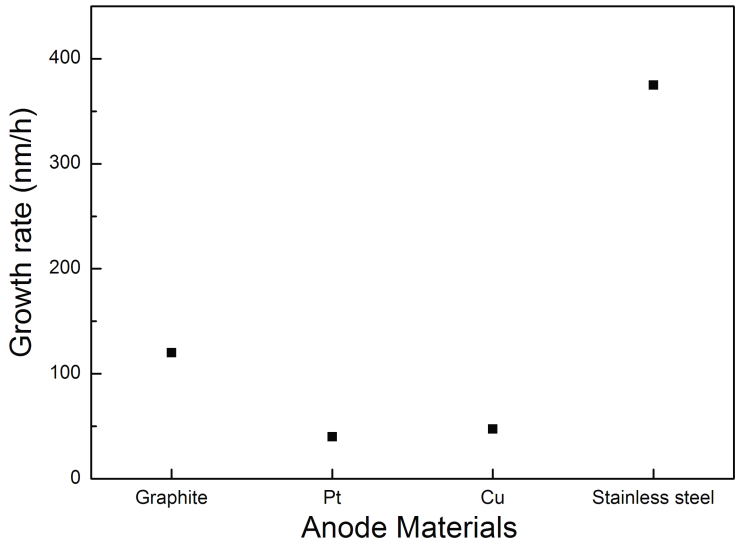

Fig. 5.9 Growth rate of the films deposited using different anodes.

5.2.2.2 Morphology of DLC Films

Deposits were observed on the substrates after experiments. The films deposited using graphite and Pt as anodes appeared grey in color. The film deposited using Cu was brown, and the film deposited using stainless steel had the color of ferruginous.

Typical SEM images of the films deposited are shown in Fig. 5.10. Compared with the others, the film deposited using graphite anode is continuous and the most smooth of all. As can be seen in Fig. 5.10b, the film deposited using Pt anode has many grains of different shapes and sizes. There are many grains in the size of 300 nm attached on the film surface when Cu anode was used. Fig. 5.10d shows the film deposited using stainless steel anode, it is very rough with grains in the size of 75 μm on the surface.

In conclusion, anode materials have great influence on the surface morphology of the films deposited by liquid electrochemical technique because the films have different surface appearance. Graphite anode is appropriate to get smooth film, however, the other three anodes can make the films very rough.

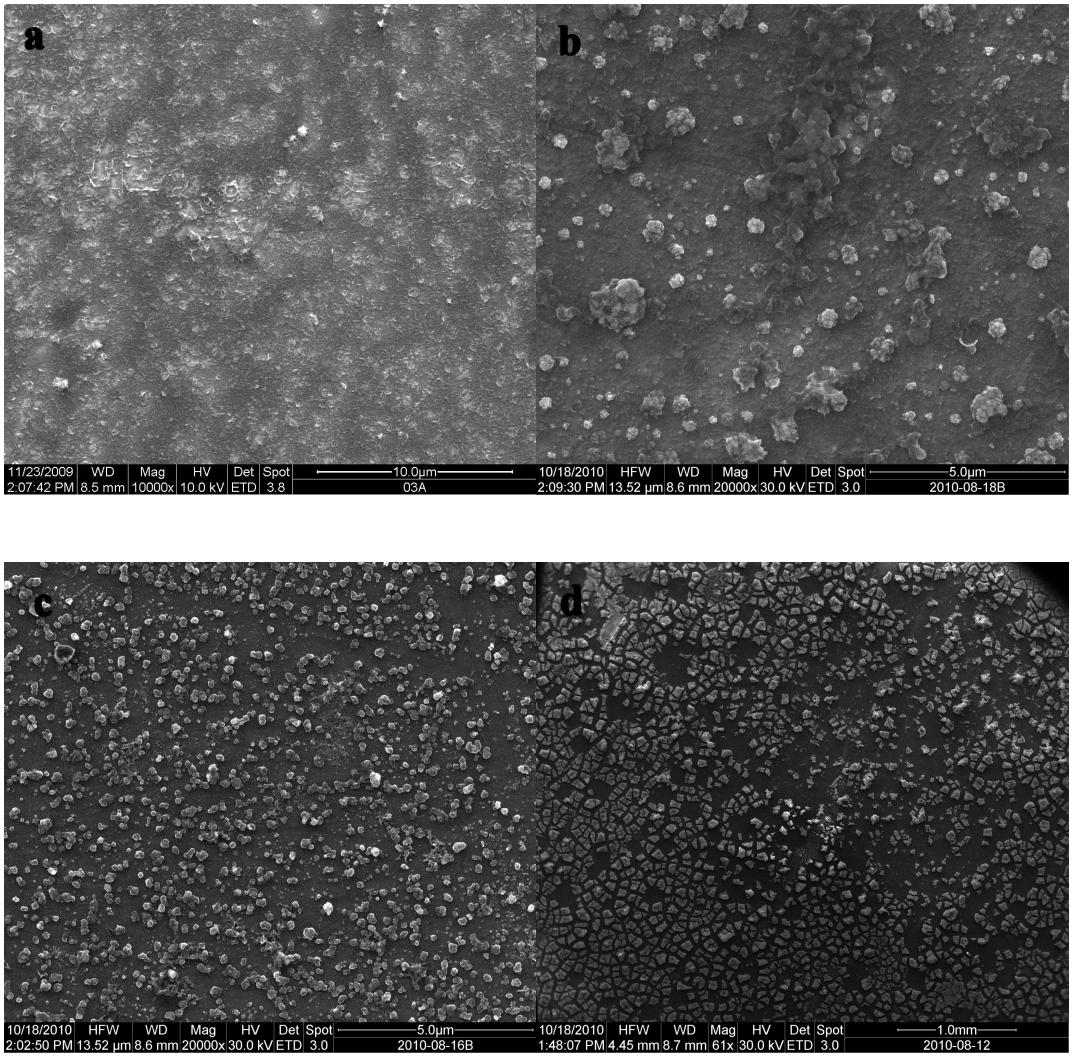

Fig. 5.10 Typical SEM images of the DLC films deposited using different anodes (a: graphite, b: Pt, c: Cu, d: stainless steel).

5.2.2.3 Chemical Composition and Bond-structure of DLC Films

EDX spectroscopy is a credible way to characterize the composition of thin films. The films deposited using anodes made of graphite, Pt, Cu and stainless steel were measured by EDX. The results are displayed in Fig. 5.11.

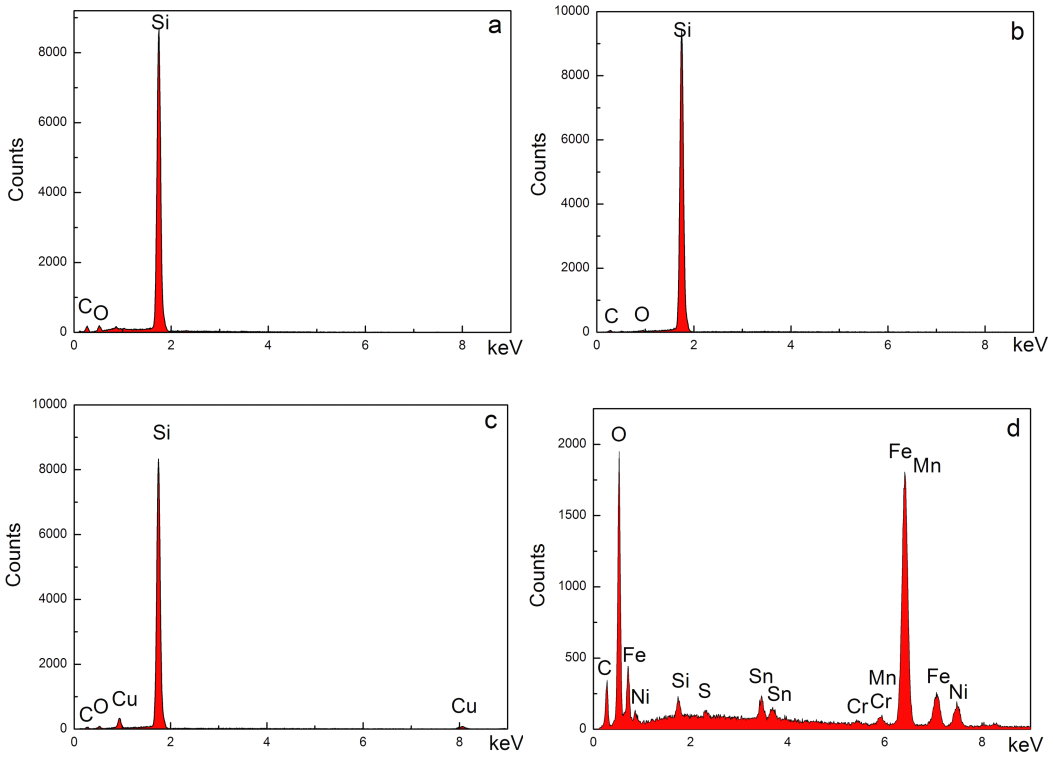

Fig. 5.11 Corresponding EDX spectra of the DLC films deposited using different anodes (a: graphite, b: Pt, c: Cu, d: stainless steel).

Carbon films without any other impurity were deposited using anodes made of graphite and Pt, respectively. Peaks of C, O and Si appear in Fig. 5.11a and Fig. 5.11b. The C and O peak belong to the carbon films deposited, the Si peak is obviously due to the silicon substrate. The absence of other elements indicates that the films deposited mainly consist of carbon.

Doped carbon films were deposited using anodes made of Cu and stainless steel, respectively. There are not only C, O and Si peaks, but also Cu peak in Fig. 5.11c. The presence of Cu peak confirms that Cu is contained in the carbon film deposited using Cu anode. Using stainless steel anode could bring many other impurities into the films, such as Fe, Mn, Sn, Ni, Cr and so on which come from stainless steel, as shown in Fig. 5.11d.

Graphite and Pt show good stability against the acetone/deionized water solution during the process of DLC films liquid phase deposition. However, the Cu and stainless steel anodes were eroded by the solution and therefore cause unwanted impurities in the carbon films deposited. This corrosion will of course affect the composition of the DLC films deposited by liquid electrochemical technique. So the corrosion stability of material should be considered as a selection rule of anode for DLC films liquid electrochemical deposition.

Raman spectroscopy was used to characterize the films deposited. Fig. 5.12 shows Raman measurement of the films deposited using four kinds of anodes.

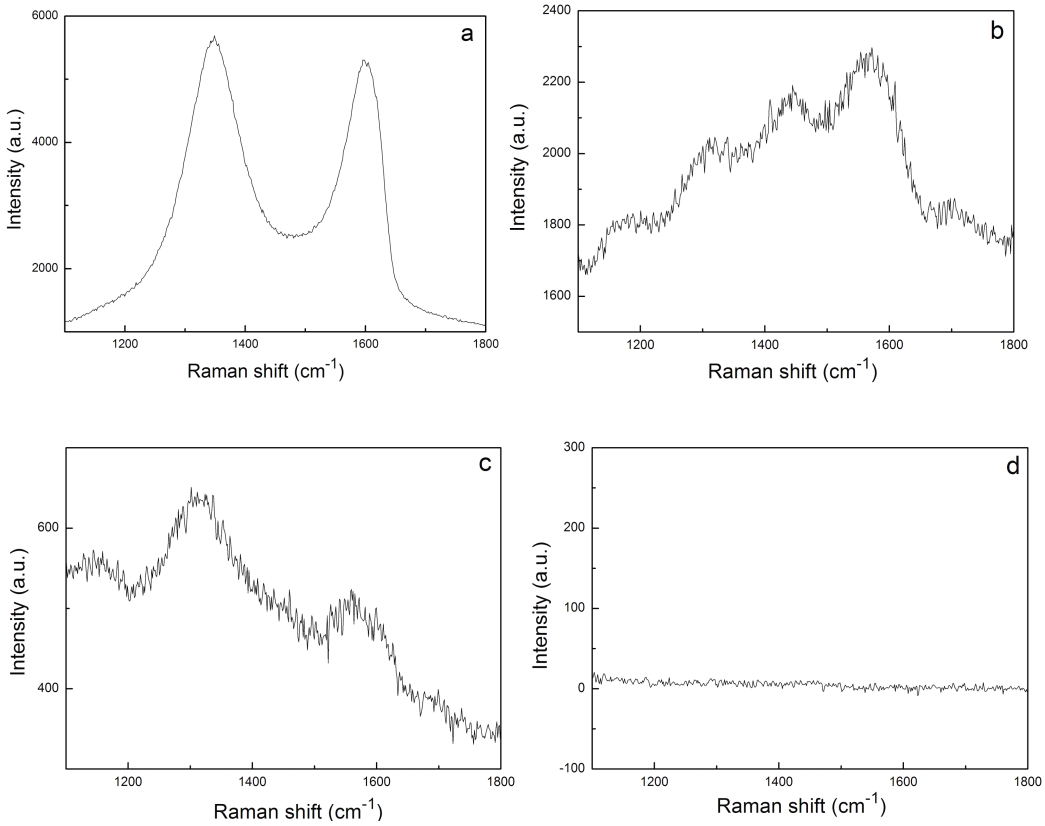

Fig. 5.12 Raman spectra of the films deposited using different anodes (a: graphite, b: Pt, c: Cu, d: stainless steel).

Fig. 5.12a is the Raman spectrum of the films deposited using graphite as anode. It is a typical Raman spectroscopy of DLC films. Two broad peaks around 1353 cm^{-1} (D peak) and 1588 cm^{-1} (G peak) appear in the Raman spectrum, indicating that some sp^2 amorphous carbon phases exist in the film. Fig. 5.12b is from the films deposited using Pt as anode. The peaks at 1572 cm^{-1} and 1340 cm^{-1} are related to D peak and G peak, respectively. The weak peaks around 1295 cm^{-1}, 1450 cm^{-1} are from the -CH_2- various stretch vibration mode. This result indicates that some alkyl structures -CH_2- existed in the film, and the film is hydrogenated diamond-like carbon [Z. Sun 2000]. Fig. 5.12c shows a Raman spectrum of the films deposited using the anode made of Cu. There are two broad peaks at 1320 cm^{-1} (D peak) and 1560 cm^{-1}(G peak), respectively. However, the slope of this Raman spectrum is negative and totally different from all the other Raman spectra. Fig. 5.12d is a Raman spectrum of the films deposited using stainless steel anode. No carbon signal can be observed here. Although carbon was found in the EDX spectrum, it is not enough to form carbon

phase films. It seems that the deposits on the substrate are because of the corrosion of the stainless steel anode.

Based on the comparison of the Raman spectra from four kinds of anodes, anode materials have influence on the microstructure of the films deposited by liquid electrochemical technique.

5.3 Discussions

One of the very important effects in thin film deposition is the so called “hidden parameters” i.e. parameters usually not known or documented. It turns out that the reactor and anode design are such “hidden parameters”. It is the first time that they are considered since liquid deposition of DLC films was carried out from 1992.

The materials of reactors have great influence over the deposition of DLC films using liquid electrochemical technique. Ca and other non-metallic impurities such as Sn, Cl and S were found in the films when some unsuitable materials were used to make reactors. Quartz-reactor is the most ideal one because it will not introduce any other impurities which could affect both morphology and structure of the films deposited.

The anode materials also have influence on the DLC films liquid phase deposition. Graphite and Pt appear good chemical stability, Cu and stainless steel anodes were eroded during the deposition process. The corrosion of anodes will bring impurities into the films and therefore affect the film morphology, composition and microstructure.

However, to find impurities in the films means that it is possible to deposit doped-DLC films by liquid electrochemical technique. It is well known that the properties of DLC films could be changed or improved by doping. Thus, doped-DLC films deposited by liquid electrochemical technique which own special properties would be worked out in the future.

5.4 Conclusions

The effects of experimental facilities in the liquid electrochemical deposition of DLC films were investigated, including reactor and anode design.

It appears clearly that the materials of reactors have significant influence on the composition, morphology and microstructure of films deposited by liquid electrochemical technique. Glass reactor, glass reactor with PTFE-coating inside and glass reactor with quartz-coating inside could introduce Ca or non-metallic impurities into the DLC films prepared by liquid electrochemical deposition. Using quartz reactor could successfully avoid the impurities from other reactors.

The anode materials have influence on the deposition of DLC films by liquid electrochemical technique, including films performance, composition and microstructure. DLC films without impurity were deposited using anodes made of graphite or Pt. Anodes made of Cu or stainless steel will bring impurities into the deposits.

Because the following work in this dissertation concentrates on the deposition of undoped-DLC films, the quartz reactor and anode graphite should be used to avoid impurity from the experimental facility.

References

A. Cuesta, P. Dhamelincourt, J. Laureyns, A. Martinez-Alonso, J.M.D. Tascon. "Raman microprobe studies on carbon materials" Carbon **32**(1994): 1523-1532.

A.C. Ferrari, J. Robertson. "Interpretation of Raman spectra of disordered and amorphous carbon" Physical Review B **61**(2000): 14095-14107.

C. Gabrielli, R. Jaouhari, S. Joinet and G. Maurin. "In situ Raman spectroscopy applied to electrochemical scaling. Determination of the structure of vaterite" Journal of Raman Spectroscopy **31**(2000): 497-501.

D. Guo, K. Cai, L.T. Li, Y. Huang, Z.L. Gui, H.S. Zhu, . "Evaluation of diamond-like carbon films electrodeposited on an Al substrate from the liquid phase with pulse-modulated power" Carbon **39**(2000): 1395-1398.

D.S. Knight, W.B. White. "Characterization of diamond films by Raman spectroscopy" Materials Research Society **4**(1989): 385-393.

H. Wang, M.R. Shen, Z.Y. Ning, C. Ye, C.B. Cao, H.Y. Dang, H.S. Zhu. "Deposition of diamond-like carbon films by electrolysis of methanol solution" Applied Physics Letters **69**(1996): 1074-1076.

J. Robertson. "Diamond-like amorphous carbon" Materials Science and Engineering R **37**(2002): 129-281.

J.J. Cuomo, J.P. Doyle, J. Bruley, J.C. Liu. "Sputter deposition of dense diamond-like carbon films at low temperature" Applied Physics Letters **58**(1991): 466-468.

J.Y. Du, G.F. Zhang, G.Q. Li, X.D. Hou. "Diamond-like-carbon film prepared on stainless steel substrates by liquid phase electrochemical deposition" Electrochen Istry **13**(2007): 58-62.

L.I. Maissel, R. Glang. "Handbook of thin film technology". New York, McGraw-Hill(1970).

M. Jerman, N. Woehrl, D. Mergel Optical properties and intrinsic stress of SiO_2-films prepared by anodic arc evaporation. Duisburg, University Duisburg Essen.

M. Zarrabian, N. Fourches-Coulon, G. Turban, C. Marhic, M. Lancin. "Observation of nanocrystalline diamond in diamondlike carbon films deposited at room temperature in electron cyclotron resonance plasma" Applied Physics Letters **70**(1997): 2535-2537.

R.J. Nemanich, J.T. Glass, G. Lucovsky, R.E. Shroder. "Raman scattering characterization of carbon bonding in diamond and diamondlike thin films" Journal of Vacuum Science & Technology A: Vacuum, Surfaces, and Films **6**(1988): 1783-1787.

R.S. Li, M. Zhou, X. J. Pan, Z.X. Zhang, B.A. Lu, T. Wang, E.Q. Xie. "Simultaneous deposition of diamondlike carbon films on both surfaces of aluminum substrate by electrochemical technique" Journal of Applied Physics **105**(2009): 066107-1-3.

S. Martinez-Ramirez, S. Sanchez-Cortes, J.V. Garcia-Ramos, C. Domingo, C. Fortes, M.T. Blanco-Varela. "Micro-Raman spectroscopy applied to depth profiles of carbonates formed in lime mortar" Cement and Concrete Research **33**(2003): 2063-2068.

S. Seisel (2009). Bochum, Ruhr University Bochum.

T. Kumagai, J. Choi, S. Izumi, T. Kato. "Structures and phonon properties of nanoscale fractional graphitic structures in amorphous carbon determined by molecular simulations" Journal of Applied Physics **107**(2010): 104307-104307-6.

T. Suzuki, Y. Manita, T. Yamazaki, S. Wada, T. Noma. "Deposition of carbon films by electrolysis of a water-ethylene glycol solution" Journal of Materials Science **30**(1995): 2067-2069.

V.P. Novikov, V.P. Dymont. "Synthesis of diamondlike films by an electrochemical method at

atmospheric pressure and low temperature" Applied Physics Letters **70**(1997): 200-202.

W.A. Yarbrough, R. Messier. "Current issues and problems in the chemical vapor deposition of diamond" Science **247**(1990): 688-696.

Y. Lifshitz. "Diamond-like carbon-present status " Diamond and Related Materials **8**(1999): 1659-1676.

Y. Namba. "Attempt to grow diamond phase carbon films from an organic solution" Journal of Vacuum Science Technology A **10**(1992): 3368-3370.

Z. Sun, Y. Sun, X. Wang. "Investigation of phases in the carbon films deposited by electrolysis of ethanol liquid phase using Raman scattering" Chemical Physics Letters **318**(2000): 471-475.

6 Effects of Various Parameters on Deposition of DLC Films by Liquid Electrochemical Technique

Deposition of DLC films using liquid electrochemical technique has attracted great interest in recent years. The publications suggested that microstructure and properties of the carbon films deposited could be strongly affected by the preparation conditions, such as electrolyte, substrate material, applied potential, temperature and power source [J.T. Jiu 2002; H.S. Zhu 2003]. Although a lot of work has been attempted, liquid phase deposition of DLC films is still a complicated chemical and physical reaction process with many unclear questions. It is therefore necessary to investigate the effects of various parameters on the deposition of DLC films, including the formation, morphology and microstructure of DLC films. The deposition parameters are classified into three parts: chemical parameters, geometrical parameters and electrical parameters. Section 6.1 talks about the chemical parameters, mainly about the electrolyte, including analytically pure organic chemicals and mixed organic solutions. Section 6.2 discusses the effects of anode-substrate distance which obviously belongs to geometrical parameters in the deposition system. Electrical parameters are mainly the applied potential, the effects of applied potential on deposition of DLC films are discussed in section 6.3.

6.1 Chemical Parameter

The electrolyte is a critical chemical parameter in electrochemical reaction. The electrolytes used for liquid electrochemical deposition of DLC films are organic chemicals. Many kinds of organic chemicals have been selected as electrolyte to deposit DLC films by liquid electrochemical technique, including pure organic chemicals and mixed solutions. The first example is that Namba [Y. Namba 1992] attempted to deposit carbon phase films in alcohol solution. Wang *et al.* [H. Wang 1996] and Novikov *et al.* [V.P. Novikov 1997] reported that DLC films could be obtained in methanol or in a solution of acetylene in liquid ammonia, respectively. And DLC films were deposited from the electrolysis of ethylene glycol [T. Suzuki 1995], dimethylformamide [D. Guo 2000] and acetonitrile [K. Cai 2000].

On the one hand, carbon films could be deposited by electrolysis of various organic solutions and the organic chemicals have been proved to be the carbon source of DLC films deposited in liquid electrochemical deposition in chapter 4. On the other hand, the publications suggested that the film formation and microstructure were strongly affected by the organic chemicals used. It is essential to investigate the relationship between the electrolyte and DLC films deposition in this liquid electrochemical

method. Here the effects of the chemical parameter are discussed in two parts: pure organic chemicals and mixed organic solutions.

6.1.1 Pure Organic Chemicals

Organic chemicals indicate the liquid chemical compounds whose molecules contain the element carbon. In this section, six kinds of analytically pure organic chemicals were selected as electrolyte to carry out DLC liquid electrochemical deposition, including methanol (CH_3OH), ethanol (CH_3CH_2OH), acetone (CH_3COCH_3), 2-propanol ($(CH_3)_2CHOH$), ethylene glycol ($C_2H_4(OH)_2$) and glycerol ($C_3H_5(OH)_3$). The basic principles of selecting organic chemicals: nontoxic and easily found in the chemistry laboratory.

The experimental setup and deposition procedure were described in chapter 4. In order to compare the effects of different electrolytes, all the deposition processes were carried out under the same experimental parameters. The anode material, substrate and anode-substrate distance were graphite, silicon wafer and 6 mm, respectively. The applied potential and the deposition time were 1000 V (frequency 10 kHz, duty cycle 50%) and 2 h, respectively.

The film thickness was measured by Dektak 6M Stylus Profiler after deposition. The surface morphology of the films deposited was measured by scanning electron microscopy (SEM) Quanta 400 FEG and atomic force microscopy (AFM) Veeco Dimension 3100. The microstructure of the DLC films was investigated using a micro-Raman system Jobin Yvon with a laser source wavelength of 514.532 nm and a Bruker IFS 55 Equinox FTIR in a spectral range from 1000 cm^{-1} to 4000 cm^{-1} using a reflection mode.

6.1.1.1 Films Deposition

Films were observed on the Si substrates using methanol, ethanol, acetone and 2-propanol, respectively, as electrolyte. All the films appear gray in color and do not dissolve in organic chemicals, such as ethanol and acetone. However, no obvious deposition was found after the electrochemical reaction of ethylene glycol or glycerol.

Growth rate is an important characterization in thin film technology. The film growth rates here vary with different organic chemicals. The film thickness was firstly measured after deposition and then it was calculated into film growth rate with the help of deposition time, the results are displayed in Fig. 6.1.

The highest growth rate is obtained by electrolysis of 2-propanol, the one using acetone as electrolyte owns the second place, the third one is from ethanol and the

growth rate using methanol is the lowest of all. The difference of film growth rate confirms that the electrolyte has influence on the film formation rate in liquid electrochemical deposition process under the same experimental parameters.

The results of films thickness measurement confirmed that no film was deposited from analytically pure ethylene glycol or glycerol under the same deposition parameters. Not all the organic chemicals are appropriate for film formation by liquid electrochemical technique, such as ethylene glycol and glycerol. The reason of no film deposition will be discussed with the comparison of the electrolyte physical constants and the description of the DLC film formation process, in section 6.1.3, as well as the different film growth rate obtained by the other four pure organic chemicals.

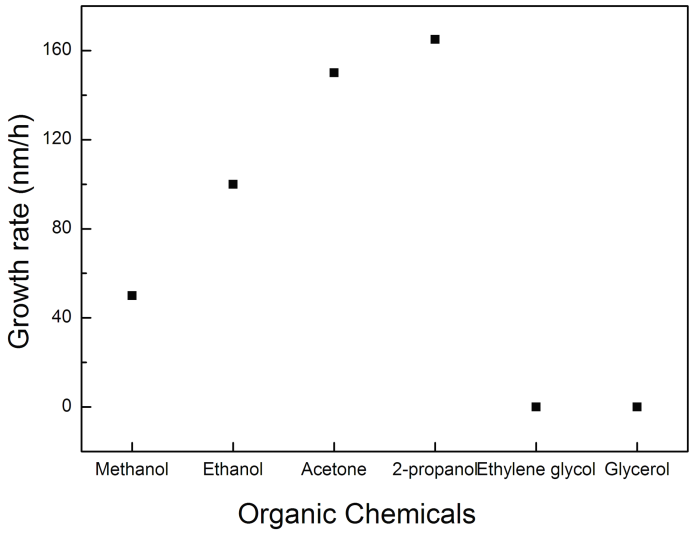

Fig. 6.1 Growth rate of the films deposited using several analytically pure organic chemicals as electrolyte.

6.1.1.2 Bond-structure and Chemical Composition of DLC Films

Raman is a widely used non-destructive way to obtain the detailed bonding structure information of the DLC materials [J. Robertson 1991; A.C. Ferrari 2000; J. Robertson 2002]. Diamond has a single Raman active peak at 1332 cm^{-1}. Single crystal graphite has a single Raman active peak at 1580 cm^{-1} called “G” peak for “graphite”. Disordered graphite has a second peak at around 1350 cm^{-1} called “D” peak for “disordered”. Raman spectra of most disordered carbons remain dominated by these two D and G peaks of graphite, even when the carbons do not have particular graphitic ordering [J. Robertson 2002]. Raman spectroscopy is therefore used for carbon films detection and the bonding structure characterization.

Fig. 6.2 shows Raman characterizations of the samples deposited using six kinds of analytically pure organic chemicals as electrolyte by liquid electrochemical technique. The appearance of two broad peaks around 1350 cm^{-1} (D peak) and 1580 cm^{-1} (G peak) suggests that DLC films were successfully deposited by the electrolysis of methanol, ethanol, acetone and 2-propanol, respectively. Thus, these four organic chemicals can play the part of carbon source to prepare DLC films by liquid electrochemical technique under our experimental parameters.

However, there is no obvious carbon peak in the Raman spectra of the samples using ethylene glycol or glycerol as electrolyte. It is confirmed that no carbon phase films were deposited from ethylene glycol or glycerol under the same experimental parameters. Nevertheless, the spectra are presented here for comparison, as shown in Fig. 6.2 e and Fig. 6.2 f. The lack of carbon information in the Raman spectra is corresponding to the results of film thickness measurement, in which no film could be found. As a conclusion, ethylene glycol and glycerol are not appropriate carbon source for DLC films formation by liquid electrochemical deposition.

All the DLC films deposited from pure methanol, ethanol, acetone and 2-propanol, respectively, have D peak around 1350 cm^{-1} and G peak around 1580 cm^{-1}, indicating that some sp^2 amorphous carbon phases exist in the films [R.J. Nemanich 1988; D.S. Knight 1989; W.A. Yarbrough 1990]. The bonding structure of DLC films deposited should be investigated in more detail. Thus the region from 1150 cm^{-1} to 1800 cm^{-1} in all the Raman spectra were further Lorenz fitted on a linear background to analyze the influence of electrolyte on the DLC films structure. The correlation between Raman fitting results and the organic chemicals is displayed in Fig. 6.3.

The I(D)/I(G) intensity ratio and the G peak position obtained from Raman measurements are correlated with the sp^3/sp^2 ratio. The I(D)/I(G) ratio of the films deposited by electrolysis of analytically pure chemicals, are approximately in the range of 0.92-1.12. As can be seen, the lowest I(D)/I(G) ratio was obtained at the DLC films deposited from acetone. And it is supposed to have the highest sp^3 content because a lower intensity ration can be interpreted as corresponding to higher sp^3 content [G. Irmer 2005]. Also the DLC films deposited from ethanol and 2-propanol both have low sp^3 content. The I(D)/I(G) ratio from methanol is the highest one, and the lowest sp^3 content is suggested.

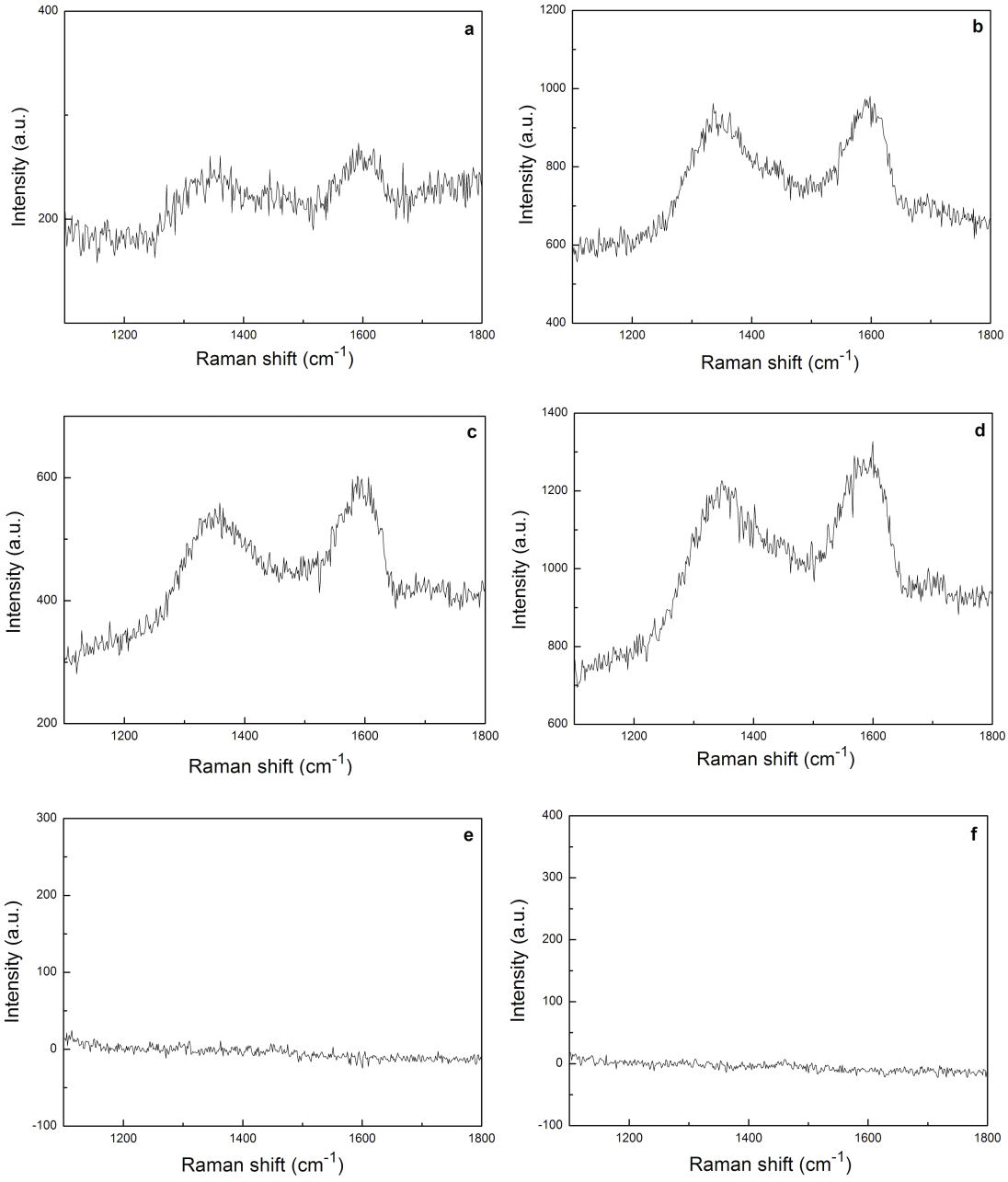

Fig. 6.2 Raman spectra of the films deposited using six kinds of analytically pure organic chemicals as electrolyte under the same deposition parameters (a: methanol, b: ethanol, c: acetone, d: 2-propanol, e: ethylene glycol, f: glycerol).

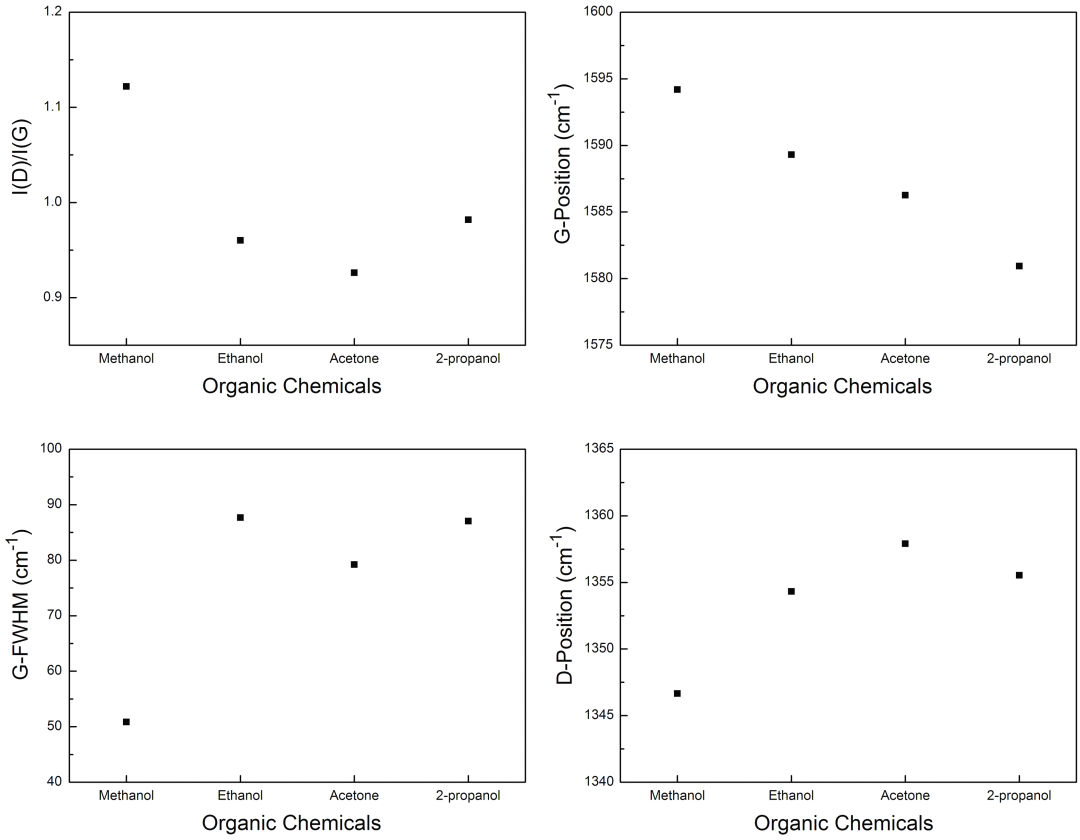

Fig. 6.3 Correlation between Raman fitting information and the DLC films deposited using various analytically pure organic chemicals as electrolyte.

To give a quantitative analysis of the sp^3 content in the DLC films, the parameters determined from Raman measurements of a:C-H films for λ=514 nm excitations can be introduced as a reference. Fig. 6.4a shows the correlation between G position and sp^3 content, I(D)/I(G) ratio and sp^3 content, respectively, from A.C. Ferrari [A.C. Ferrari 2000], the experimental data are exponential fitted and presented in Fig. 6.4b. The G peak position and I(D)/I(G) ratio of the DLC films deposited by different chemicals are placed on the "G peak position-sp^3 content" and "I(D)/I(G) ratio- sp^3 content" curves. The corresponding sp^3 content in each DLC film deposited from analytically pure chemical can be known. As shown in Fig. 6.4b, all the sp^3 content of the four DLC films drawn from G position are about 20% lower than those drawn from I(D)/I(G) ratio. A. Poukhovoi [A. Poukhovoi 2011] compared the calculation of sp^3 content in a:C-H films using Raman and FTIR. The results from "I(D)/I(G) ratio-sp^3 content" and FTIR matched very well with each other, however, the sp^3 content calculated from G position is always lower, 10-20% depending on the deposition parameters. So here the bonded sp^3 content gained from the I(D)/I(G) ratio is credible, in the range of 38-41% for different pure chemicals.

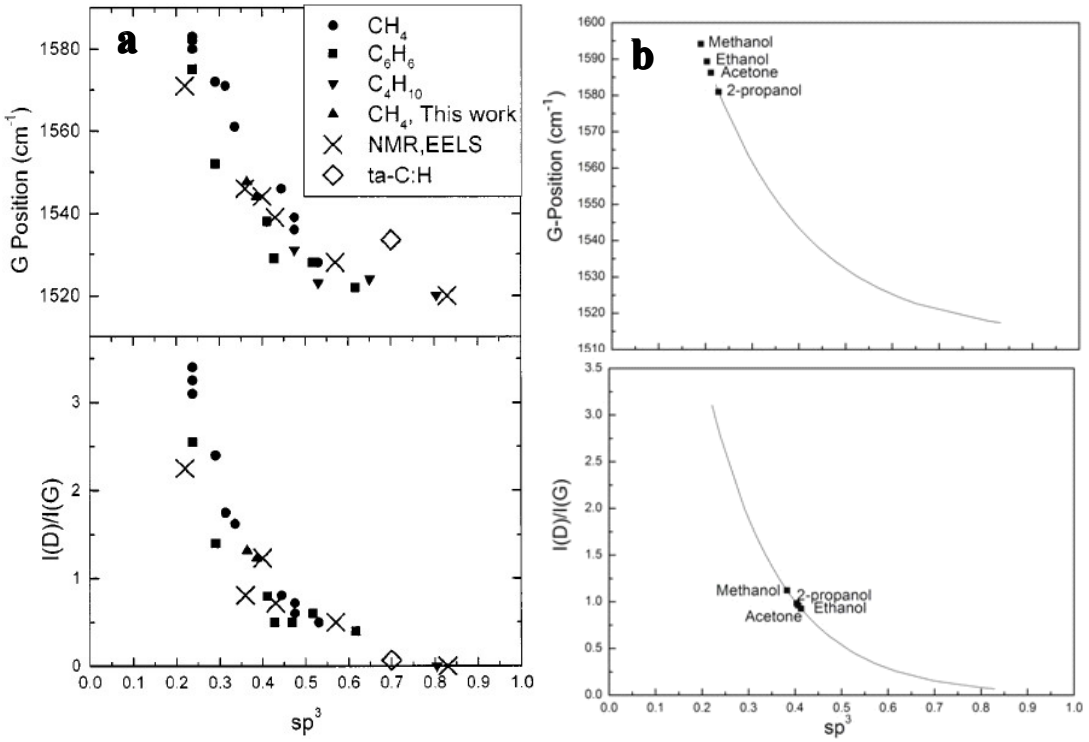

Fig. 6.4 Correlation between sp^3 content and parameters determined from Raman measurements of a:C-H films for 514 nm excitations (a: from A.C. Ferrari [A.C. Ferrari 2000]; b: fitting of the experimental data in Fig. 6.4a and the presentation of G peak position and I(D)/I(G) ratio of the DLC films deposited in this work on the exponential fitted curves).

In this work, deposition of DLC films was carried out in the organic liquid solutions. Because the organic molecules all contain hydrogen which may also take part in the formation of DLC films, the DLC films are presumed to be hydrogenated. On the one hand, whether the DLC films deposited is hydrogenated should be confirmed. On the other hand, the amount of hydrogen in the DLC films should be measured or calculated.

A typical signature of hydrogenated samples in visible Raman spectra is the increasing photoluminescence (PL) background for higher H content. This is due to the hydrogen saturation of nonradiative recombination centers [J. Robertson 1996; Rusli 1996; T. Heitz 1999]. The ratio between the slope *m* of the fitted linear background and the intensity of the G peak, *m/I(G)*, can be empirically used as a measure of the bonded *H* content [C. Casiraghi 2005]. The content of bonded hydrogen is calculated with the formula below.

$$H[at.\%] = 21.7 + 16.6 \log\{\frac{m}{I(G)}[\mu m]\} \tag{6.1}$$

Fig. 6.5 shows the results of hydrogen content calculation. The DLC films are all hydrogenated, with the bonded hydrogen in the range of 32-42%. This hydrogen content is from calculation using the classical formula, nevertheless it gives a general idea of hydrogen ratio in the DLC films deposited.

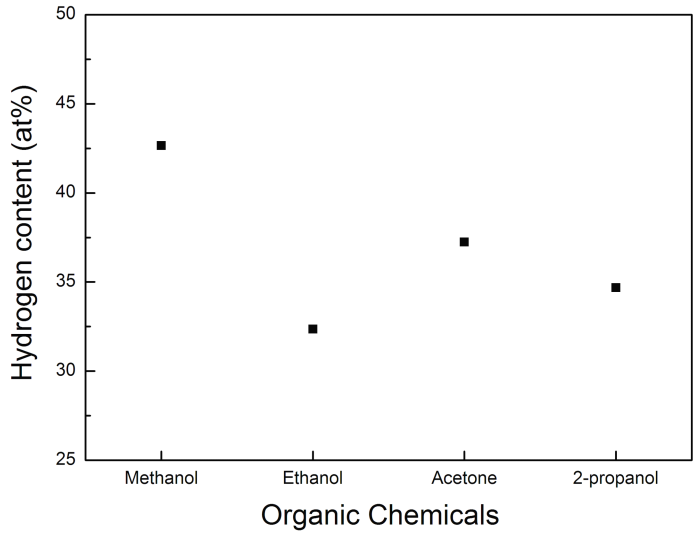

Fig. 6.5 Hydrogen content of the DLC films deposited using various analytically pure organic chemicals as electrolyte.

The a-C:H compounds can be described by the fully constrained non-crystalline network (FCN) model [J.C. Angus 1991]. The bonded sp^3 content gained from the I(D)/I(G) ratio and the corresponding calculated hydrogen content are laid in the FCN model, as shown in Fig. 6.6. Location of the data from electrolysis of four analytically pure organic chemicals as electrolyte are similar with the a-C:H from Angus. FCN is a classic model from vapor deposition. It is confirmed that DLC films of similar composition can be deposited by liquid phase deposition. Also the data are located in the ternary phase diagram, as shown in Fig. 6.7.

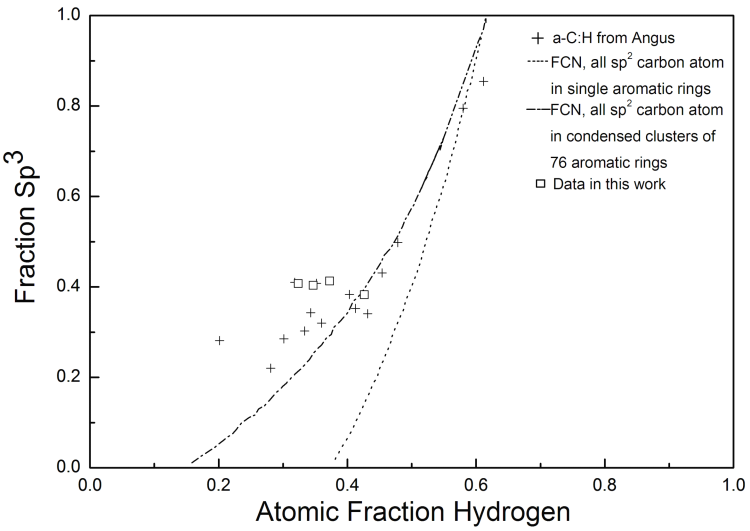

Fig. 6.6 Raman characterization of DLC films deposited using various analytically pure organic chemicals as electrolyte in the FCN model from Angus [J.C. Angus 1991].

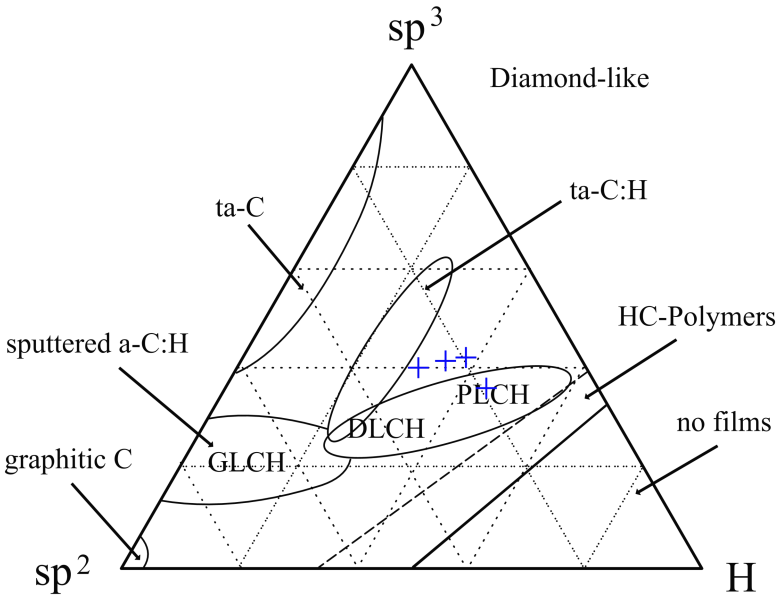

Fig. 6.7 Raman characterization of DLC films deposited using various analytically pure organic chemicals as electrolyte in the ternary phase diagram.

6.1.1.3 Morphology of DLC Films

The aim of characterizing thin film performances is capable to understand the relationship between the deposition parameters and film morphology. Microscopic methods such as SEM and AFM are particularly useful methods to investigate surface morphology in thin film technology.

Fig. 6.8 shows four typical SEM images of the DLC films deposited using four kinds of analytically pure organic chemicals as electrolyte under the same deposition parameters. Because no film was deposited from ethylene glycol or glycerol, there is lack of the other two SEM images from samples with reaction of ethylene glycol and glycerol.

The films are all continuously covering the substrates in the SEM observation. However, these four films appear different morphology. Thus, the electrolyte can obviously affect the performance of the DLC films deposited.

There are small and bright grains attached on the smooth surface of the films deposited from methanol. While the film deposited with electrolysis of ethanol has a relative rough surface, the films surface shown in Fig. 6.8c and Fig. 6.8d are continuous and compact. Acetone and 2-propanol are therefore favored for better film morphology.

The films from methanol and ethanol are quite thin because some pretreatment from the diamond paste polish can be seen. However the films deposited from the electrolysis of acetone and 2-propanol are thicker. This SEM observation is in agreement with the result of film growth rate measurement.

Although the films morphology was already shown by the above SEM images, the surface was further investigated by AFM which could present very high-resolution three-dimensional (3D) images and more quantitative information such as film roughness. Fig. 6.9 shows the corresponding AFM images of the DLC films deposited using various analytically pure methanol, ethanol, acetone and 2-propanol as electrolyte. The film roughness was analyzed with the help of software WSxM 3.1, the results of Root Mean Square (RMS) roughness are listed in Fig. 6.10.

With the comparison of the 3D AFM images and RMS roughness, the film deposited from methanol is the most smooth one, the films deposited using acetone and 2-propanol are becoming rough, and the film obtained from ethanol has the most rough surface. The roughness analysis is consistent to the SEM observation.

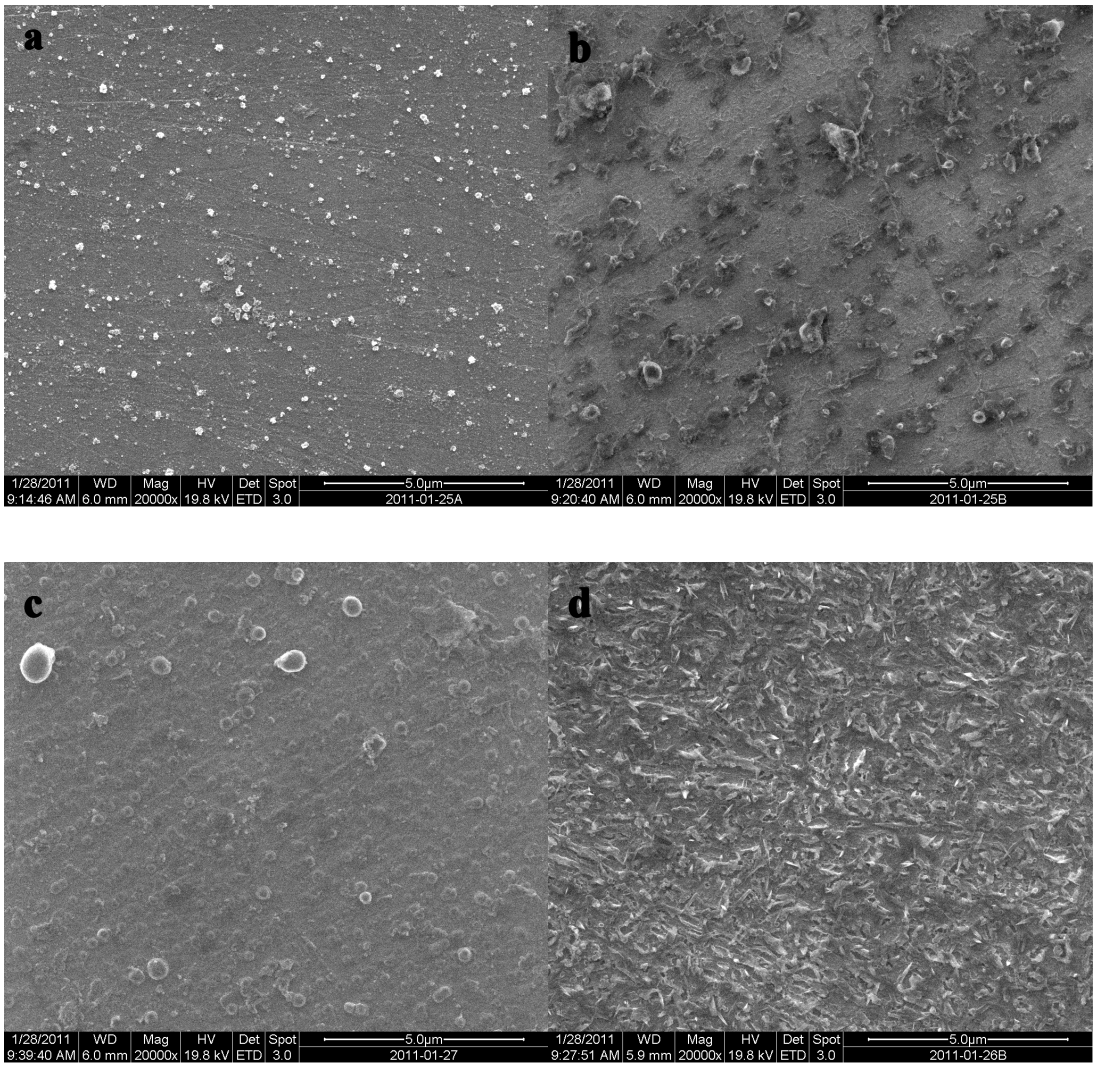

Fig. 6.8 Typical SEM images of the DLC films deposited using various analytically pure organic chemicals as electrolyte (a: methanol, b: ethanol, c: acetone, d: 2-propanol).

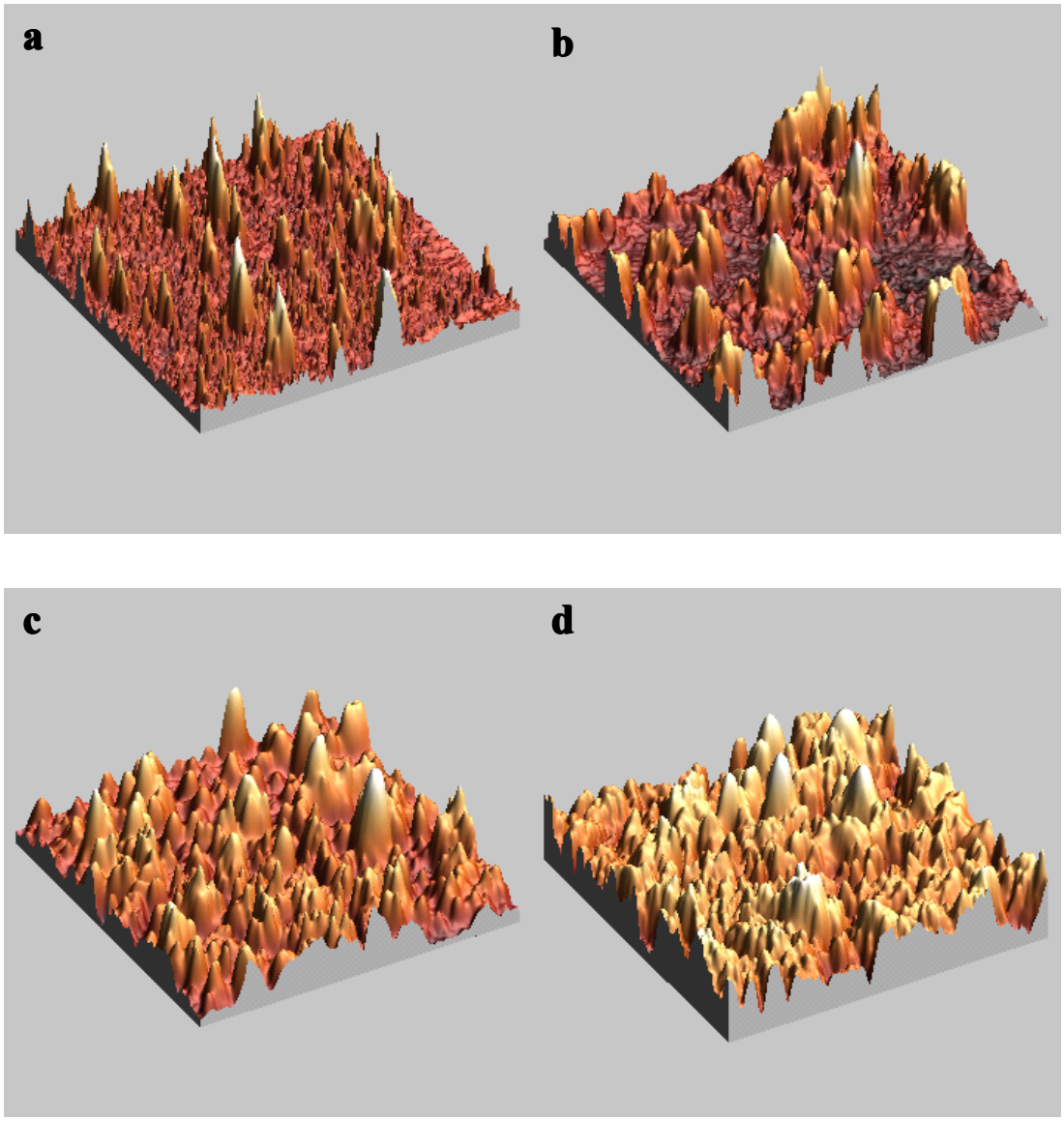

Fig. 6.9 Typical AFM images of the DLC films deposited using various analytically pure organic chemicals as electrolyte (a: methanol, b: ethanol, c: acetone, d: 2-propanol).

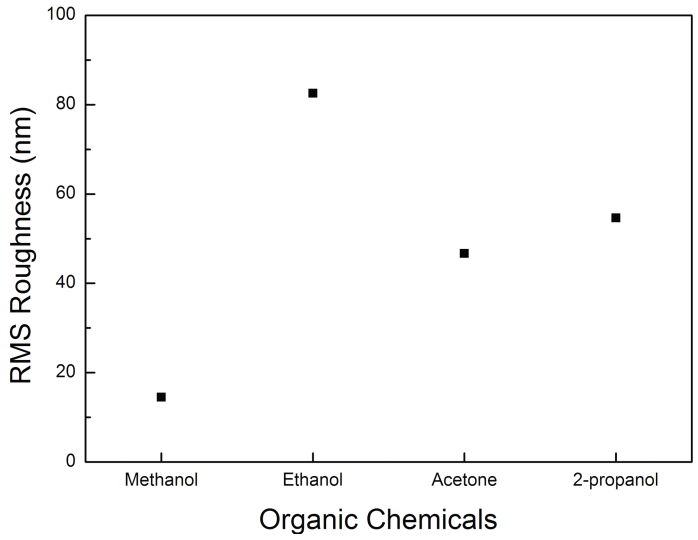

Fig. 6.10 RMS roughness of DLC films deposited using various analytically pure organic chemicals.

6.1.2 Mixed Organic Solutions

Pure organic solvent was used as electrolyte by most researchers to deposit DLC films by liquid electrochemical technique [Y. Namba 1992; H. Wang 1996; Z. Sun 2000; L.N. Huang 2006; R.S. Li 2009]. Nevertheless, some researchers tend to put additives into pure organic chemicals in order to avoid the disadvantages of pure chemicals and get ideal DLC films [T. Suzuki 1995; V.P. Novikov 1997].

Additive is another kind of chemical besides the carbon source added into the electrolyte in DLC films liquid electrochemical deposition. The additive plays the role of activator in the electrochemical reaction. Because the additive could directly change the composition and dielectric constant of electrolyte, it is possible to affect the deposition of DLC films using liquid electrochemical method.

Here deionized water was chosen as an additive because of several advantages. The purity of the solution affected the resistivity of the electrolyte. The resistivity of the solution can be slightly changed by adding deionized water. Deionized water has lower electrical resistivity than organic chemicals, and the films growth rate is increased which is reported before [Y.Y. He 2008; G.F. Zhang 2011]. The introduction of deionized water may bring more hydrogen into the electrolyte. And hydrogen may etch carbon and leave more diamond phase in the DLC films vapor deposition. The low cost of dionized water is another advantage.

Since DLC films of rough surface were deposited using analytically pure ethanol, deionized water was used as an additive to investigate its effects on the films deposition. In this section, deionized water was added into analytically pure ethanol,

and then the mixed ethanol/deionized water solutions were used as electrolyte to deposit DLC films on Si substrates at low temperature (60 ºC). The aim of this study is to investigate the influence of deionized water on the deposition of DLC films.

The amount of deionized water was in the volume ratio of 0% (analytically pure ethanol for comparison), 25%, 50% and 75%, respectively. The electric conductivity of the mixed ethanol/deionized water solution was measured by Metrohm 712 conductometer. The applied potential and deposition time were 1000 V (frequency 10 kHz, duty cycle 50%) and 2 h, respectively. The anode material, substrate and anode-substrate distance were graphite, silicon wafer and 6 mm, respectively. The experimental setup and deposition procedure were described in chapter 4.

After deposition, the film thickness and morphology were measured by the same facilities as above. The microstructure of the deposited DLC films was investigated by Raman and FTIR as well.

6.1.2.1 Films Deposition

After deposition, gray films can also be observed on the Si wafers and the films do not dissolve in organic chemicals, for instance ethanol and acetone. Since film growth rate is an important characterization in thin film technology, the samples were measured by profilometer for film thickness detection and then the corresponding film growth rate was calculated, as shown in Fig. 6.11.

The films growth rate can be distinctly changed with the addition of deionized water. Compared with analytically pure ethanol, the film growth rate firstly increased and then decreased with the addition of deionized water. The maximal growth rate is obtained when ethanol and deionized water are in the volume ratio of 1:1.

The better conductivity of the ethanol/deionized water solution might be the reason of higher growth rate when the volume ratio of deionized water is below 50%. The film growth rate was minimal when the ratio of deionized water was increased to 75%.

This result confirms that additive such as deionized water has influence on the film growth rate. And the influence is correlated with the ratio of deionized water in the mix solution. Adding appropriate amount of deioniezed water into analytically pure ethanol can increase the film growth rate, however, the film growth rate decreases if the deionized water is too much.

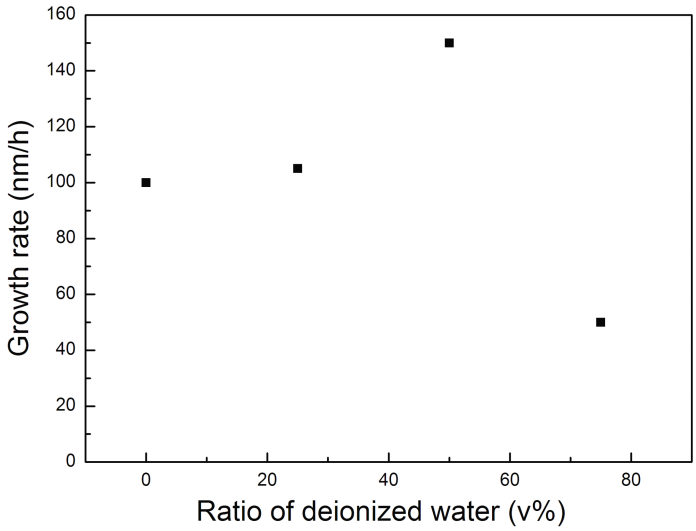

Fig. 6.11 Growth rate of the films deposited using analytically pure ethanol and various mixed ethanol/ deionized water solutions.

6.1.2.2 Morphology of DLC Films

The film performance was displayed to investigate the influence of adding deionized water on the resulting film morphology. The SEM images in Fig. 6.12 show the surface morphology of the films deposited from various mixed ethanol/ deionized water solutions. The film deposited using analytically pure ethanol has very rough surface, however, the films become smooth with the addition of deionized water.

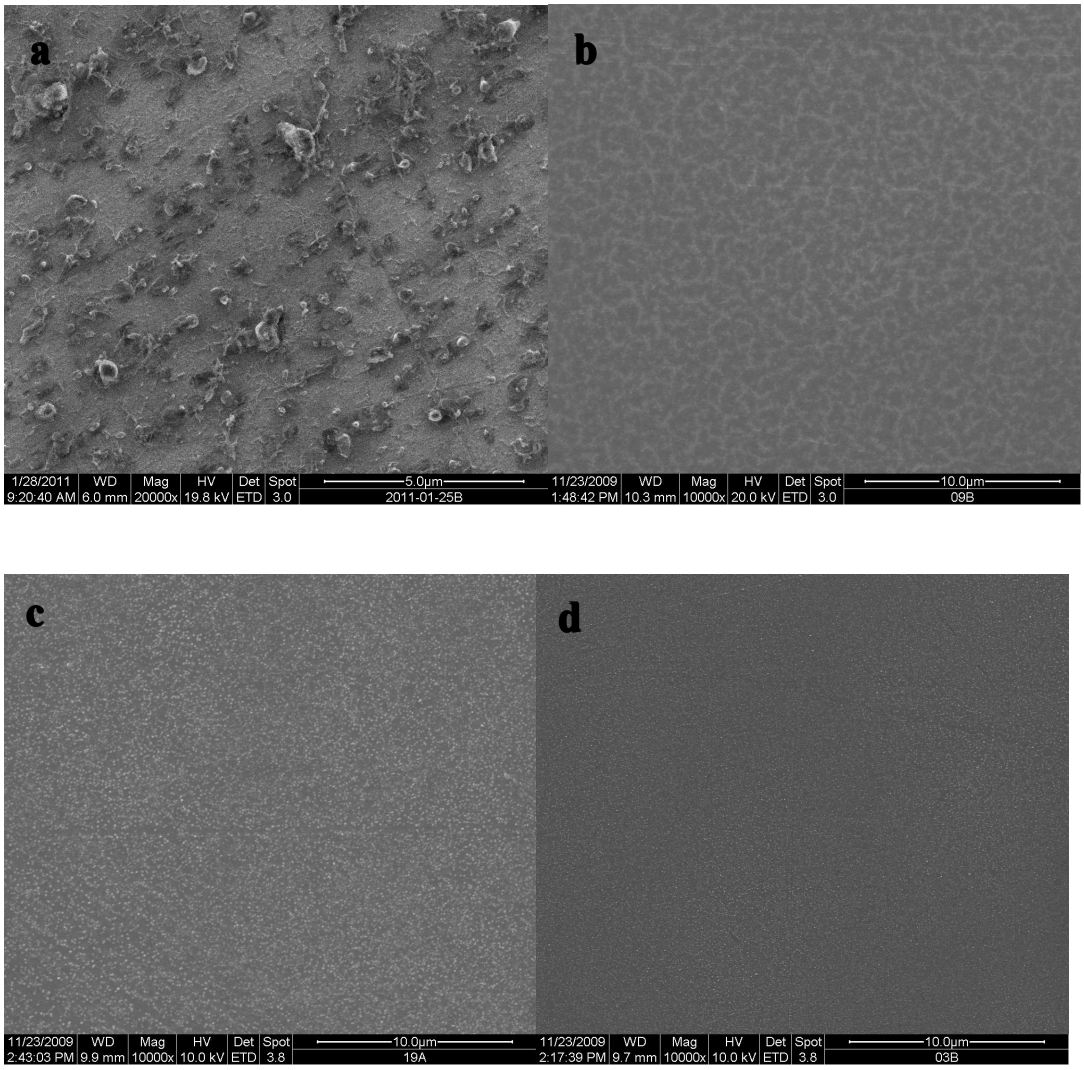

Fig. 6.12 Typical SEM images of the DLC films deposited using analytically pure ethanol and various mixed ethanol/ deionized water solutions as electrolyte (a: [CH_3CH_2OH] 100%, b: [CH_3CH_2OH] 75%/ [H_2O] 25% c: [CH_3CH_2OH] 50%/ [H_2O] 50%, d: [CH_3CH_2OH] 25%/ [H_2O] 75%).

6.1.2.3 Bond-structure and Chemical Composition of DLC Films

Raman spectroscopy is used to investigate the bond structure of the films deposited. Fig. 6.13 shows the Raman spectra with the electrolysis of ethanol/ deionized water solutions. It is confirmed that DLC films could be deposited from analytically pure ethanol and ethanol/ deionized water solutions. All of these four Raman spectra have two broad peaks which are related to D peak and G peak, respectively, indicating that some sp^2 amorphous carbon phases exist in the films [R.J. Nemanich 1988; D.S. Knight 1989; W.A. Yarbrough 1990].

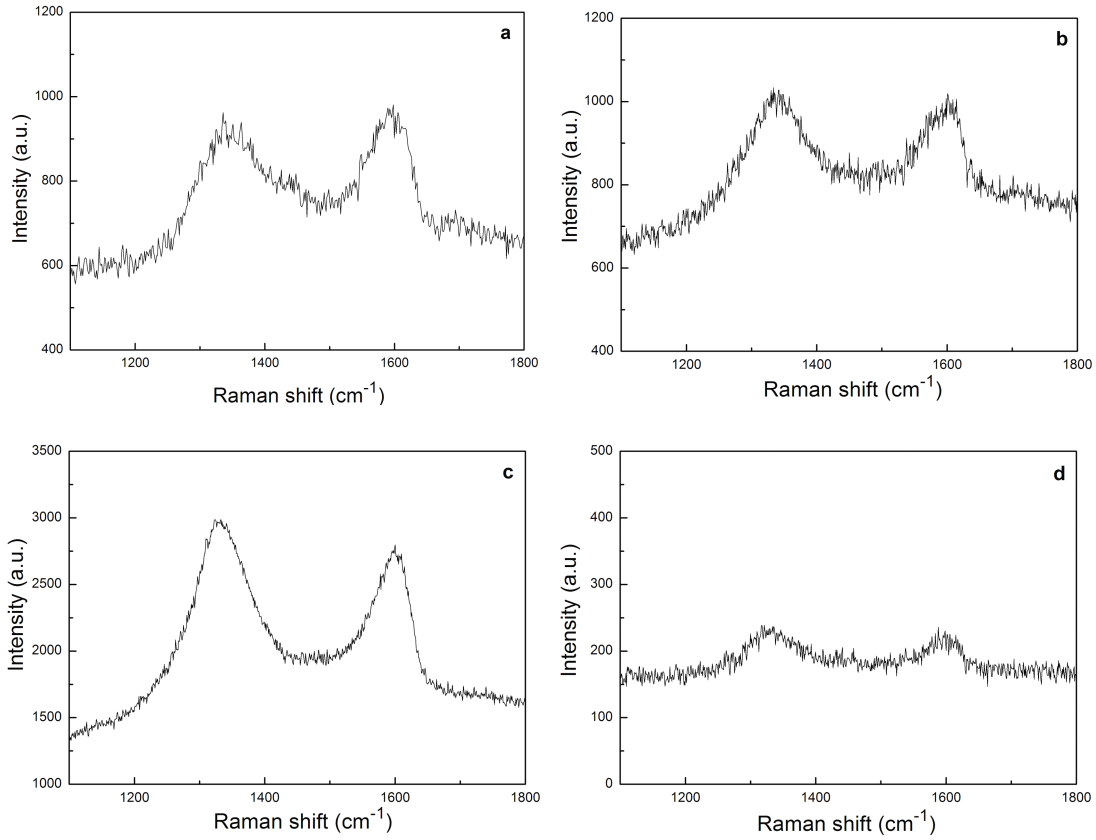

Fig. 6.13 Raman spectra of the films deposited using analytically pure ethanol and various mixed ethanol/ deionized water solutions as electrolyte (a: [CH_3CH_2OH] 100%, b: [CH_3CH_2OH] 75%/ [H_2O] 25% c: [CH_3CH_2OH] 50%/ [H_2O] 50%, d: [CH_3CH_2OH] 25%/ [H_2O] 75%).

For analysis, the region from 1150 cm^{-1} to 1800 cm^{-1} in all the Raman spectra was fitted very well with two Lorenz curves on a linear background. The trend of I(D)/I(G) ratio of DLC films and the G-position with various ratio of deionized water is shown in Fig. 6.14. The I(D)/I(G) ratio increased with the addition of deionized water compared with the electrolysis of analytically pure ethanol, approximately from 0.96 to 1.34. The G peak was up-shifted generally with the increase of deionized water. Since the I(D)/I(G) intensity ratio and the G peak position obtained with Raman measurements are correlated with the sp^3/sp^2 ratio. A lower intensity ration can be interpreted as corresponding to higher sp^3 content [C. Casiraghi 2005; G. Irmer 2005]. Thus, the sp^3 content decreased with addition of deizonized water. Analysis of Raman spectroscopy confirmed that adding deionized water will decrease the content of sp^3 carbon in the DLC films.

The G peak position and I(D)/I(G) ratio are placed on the "G peak position-sp^3 content" and "I(D)/I(G) ratio-sp^3 content" curves which were exponential fitted by A.C. Ferrari [A.C. Ferrari 2000]. As shown in Fig. 6.15, the sp^3 content drawn from G

position are about 19-20%, the sp^3 content drawn from I(D)/I(G) ratio is 35-40%. The sp^3 content calculated from G position is always lower than that drawn from I(D)/I(G) ratio. The bonded sp^3 content in the DLC films deposited from various solutions are suggested to be in agreement with the "I(D)/I(G) ratio-sp^3 content" curve.

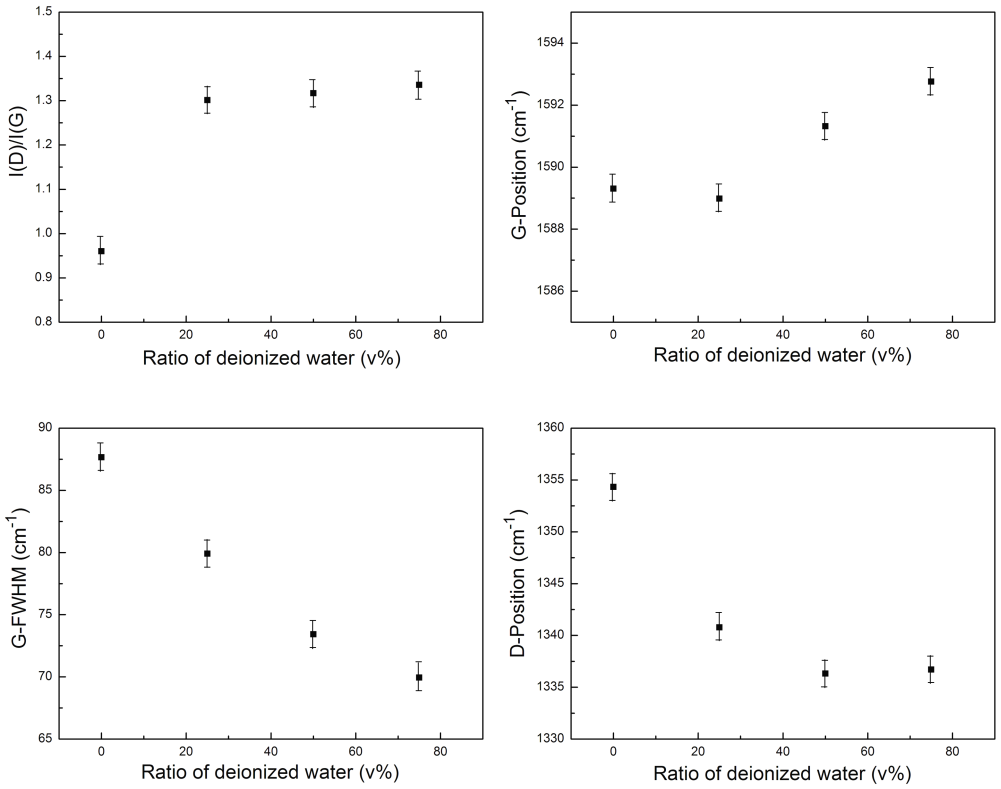

Fig. 6.14 Correlation between Raman fitting information and the DLC films deposited using analytically pure ethanol and various mixed ethanol/ deionized water solutions as electrolyte.

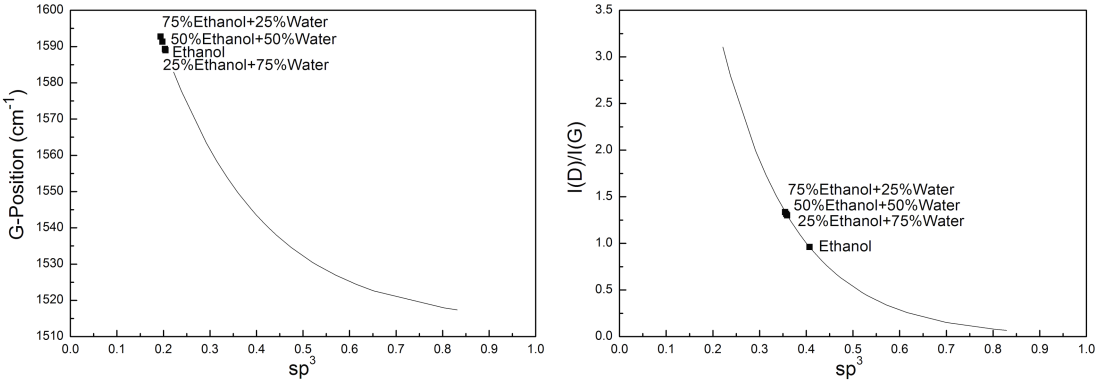

Fig. 6.15 Presentation of G peak position and I(D)/I(G) ratio on the exponential fitted curves from A.C. Ferrari [A.C. Ferrari 2000].

The content of bonded hydrogen is calculated by the formula from C. Casiraghi [C. Casiraghi 2005], using the slope *m* of the fitted linear background and the intensity of the G peak. Fig. 6.16 shows the results of hydrogen content calculation. The DLC films are all hydrogenated, the hydrogen content decreases with the increase of deionized water.

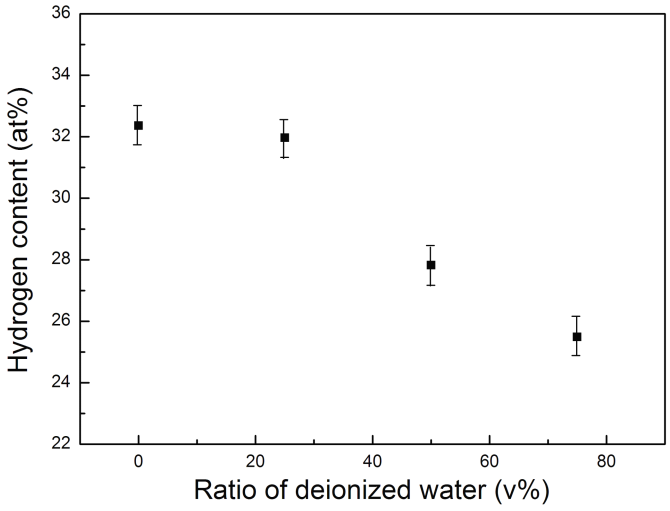

Fig. 6.16 Hydrogen content of the DLC films deposited using analytically pure ethanol and various mixed ethanol/ deionized water solutions as electrolyte.

The bonded sp^3 content gained from the I(D)/I(G) ratio and the corresponding calculated hydrogen content are laid in the FCN model, as shown in Fig. 6.17. Location of the data from electrolysis of analytically pure ethanol and various mixed ethanol/ deionized water solutions are similar with the a-C:H from Angus. Also the data are located in the ternary phase diagram, as shown in Fig. 6.18.

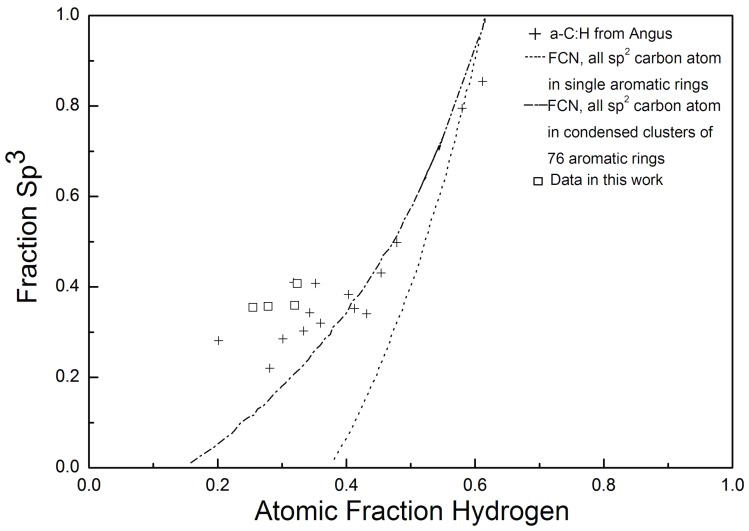

Fig. 6.17 Raman characterization of DLC films deposited using analytically pure ethanol and various mixed ethanol/ deionized water solutions as electrolyte in the FCN model from Angus [J.C. Angus 1991].

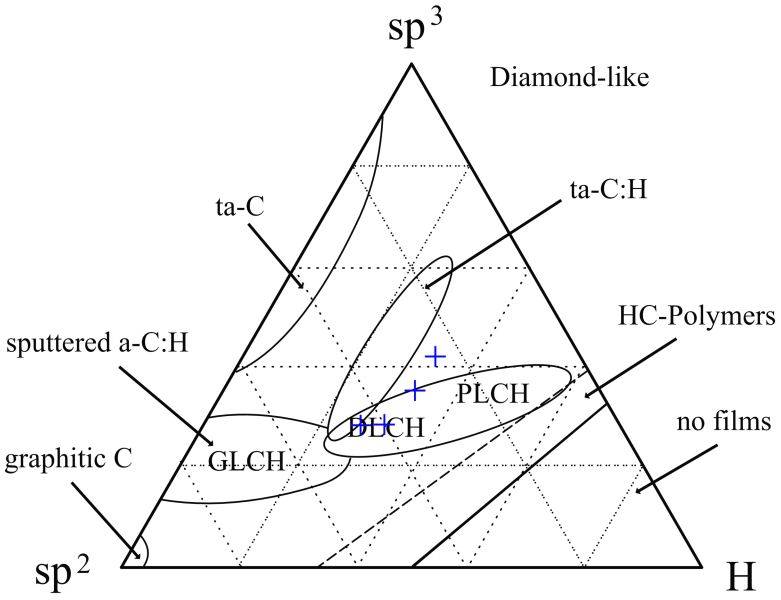

Fig. 6.18 Raman characterization of DLC films deposited using analytically pure ethanol and various mixed ethanol/ deionized water solutions as electrolyte in the ternary phase diagram.

Fig. 6.19 shows the absorption cures of the DLC films deposited using analytically pure ethanol and various mixed ethanol/ deionized water solutions as electrolyte. The C-H stretching vibrations are found between 2800 cm^{-1} and 3100 cm^{-1}, and C-H bending vibrations between 1300 cm^{-1} and 1500 cm^{-1} when analytically pure ethanol was used as electrolyte. The broad absorption band at approximately 1600 cm^{-1} refers to C=C double bonds. There are no characteristic absorption bands of H_2O around 1700 cm^{-1} and 3250 cm^{-1}, indicating that no water existed in the films [J. Ristein 1998; T. Heitz 1998].

The absorption band intensity decreases with the increase of deionized water. There are C-H bending vibrations and very weak C-H stretching vibrations when 25% deionized water was added into the electrolyte. The C-H bending vibrations and C-H stretching vibrations are both very weak when the deionized water was increased to 50% and 75%. This means that the carbon bonded hydrogen content decreased with the addition of deionized water. The observation of FTIR spectroscopy is in agreement with the hydrogen calculation by Raman spectroscopy in Fig. 6.16.

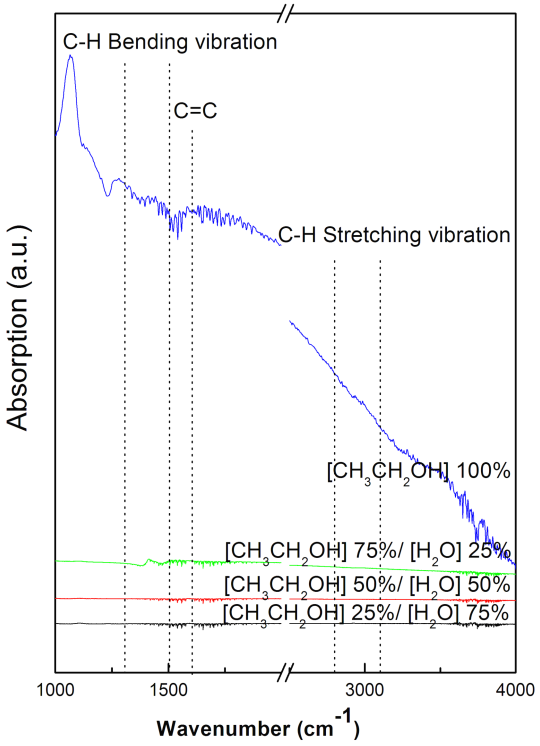

Fig. 6.19 FTIR spectra of the films deposited using analytically pure ethanol and various mixed ethanol/ deionized water solutions as electrolyte.

6.1.3 Discussions

6.1.3.1 Characterizations of Carbon Source

(1) Viscosity of Organic Chemicals

From the above characterizations of the resulting samples, it is concluded that no film was obtained using analytically pure ethylene glycol or glycerol as electrolyte in the same liquid phase deposition condition. Considering the description of DLC films formation process and the comparison of the electrolyte physical constants, high viscosity of ethylene glycol and glycerol is the critical reason of no film deposited. Some main physical constants of the organic chemicals used in this work are shown in Table. 6.1.

The growth process of DLC films using liquid electrochemical technique can be described as following: the organic molecules are polarized under the applied potential and the electropositive particles move to the Si substrate (cathode) in the electric field, and then these carbon-containing active particles react and form into DLC films attached on the surface of substrate. All the polarization, movement and film formation are carried out in liquid phase. The movement of polarized organic molecules is an important stage in the deposition process which could affect the DLC films formation. Compared with the vapor deposition methods which happen in low pressure vapor phase, the liquid active particles need more energy to overcome the collision of each other on their way towards the substrate surface.

And the migration rate of the molecules can obviously affect the DLC films growth rate. Because the carbon source of high viscosity decreases the fluid ability and hinder the migration of the molecules. It will take more time for the molecules to migrate from the liquid to the substrate surface and this will of course decrease the film growth rate or even prevent the film formation. The high viscosity causes another problem at the same time. The liquid stays on the substrate surface for too much time because of the poor fluidity. And this phenomenon slows down the new polarized organic molecules coming to react on the surface of substrate. The ethylene glycol and glycerol were almost immobile during the deposition process. However, bubbles and flow of the electrolyte can be observed by eyes when the low viscous organic chemical is used as electrolyte. These two factors lead to the decrease of film deposition rate, so no obvious deposit can be seen on the substrates by using carbon source with high viscosity.

Hence, viscosity of the electrolyte is considered to be an important factor affecting the film deposition by liquid electrochemical technique. Low viscosity is preferred in the selection of electrolyte used for DLC films liquid deposition. The organic chemicals of high viscosity, such as ethylene glycol and glycerol, are not appropriate electrolyte

for DLC films formation by liquid electrochemical technique. This is in agreement with the observation of other researchers [J.T. Jiu 2002; H.S. Zhu 2003].

In addition, a viscous solution will cause some difficulty in cleaning the substrates and experimental setup after deposition.

(2) Electrochemistry Constants of Electrolyte

As soon as the voltage is applied to the liquid deposition system, the molecules of the solution are polarized in the electric field and then react on the surface of substrate to form DLC films. The polarization ability of the molecules depends mainly on their properties and structures, which further affects the electro deposition process in the present reaction. Since liquid electrochemical technique was introduced to deposit DLC films, the influence of electrochemistry constants and molecular structure of the carbon source on the films deposition is investigated.

Some researchers suggested that the organic liquid with high dielectric constant is appropriate carbon source. Because their results showed that DLC films were deposited by the electrolysis of methanol and ethanol which both have high dielectric constants, while no obvious film was deposited from pure acetone and 2-propanol which have very low dielectric constants [J.T. Jiu 2002; H.S. Zhu 2003]. After then, many researchers follow this guide and focus deep investigation of DLC films liquid deposition using methanol. Using other organic chemicals as electrolyte in the deposition of DLC films by liquid electrochemical technique is neglected. However, typical DLC films were successfully deposited from methanol, ethanol, acetone and 2-propanol under the same experimental parameters in this work. And the films deposited from acetone and 2-propanol even appear to have higher growth rate and sp^3 carbon content. Although the dielectric constant of methanol is considered to be an important parameter to some extent, it is not the only crucial one. The selection of electrolyte for DLC films liquid deposition should not only be limited to methanol. Other organic chemicals such as acetone and 2-propanol may also be appropriate carbon source. There are other choices of electrolyte for DLC films liquid deposition, such as acetone and 2-propanol.

On the other hand, the results of using the same organic chemical as electrolyte might be different under different deposition parameters. With the comparison of our work and the publications, the parameters of the power supply (applied potential, pulse and frequency) and anode-substrate distance are different. And typical DLC films can be deposited from electrolysis of some unusual chemical by the adjustment of deposition parameters.

(3) Molecular Structure of Electrolyte

Because the CH_3 and CH_3^+ are the intermediate states for the deposition of diamond and DLC films in CVD methods. With the analysis of DLC films liquid deposition mechanism, it is suggested that the organic liquids with the methyl group bonding to the polar group are appropriate carbon sources [X.B. Yan 2004; W.L. He 2005]. Wang [H. Wang 1996] and Guo [D. Guo 2000] speculated that the CH_3 species also plays a

critical role in the electrolysis process of methanol, which is formed by the breaking of the covalent bond between the CH_3 and OH groups of methanol at a high enough voltage. They supposed that in the deposition of the carbon films the active CH_3 precursors had a higher concentration near the negative electrode surface, which would prefer the formation of more diamond-like carbon films.

In this work, typical DLC films were successfully deposited from methanol, ethanol, acetone and 2-propanol by liquid electrochemical technique. All these chemicals contain a methyl group in the molecule which can contribute to the process of DLC films formation.

Table 6.1 Physical constants of the organic chemicals used in this work.

NO	Organic chemicals	Boiling point(ºC)	Dielectric constant(ε)	Dipole moment(D)	Viscosity($mN \cdot s \cdot m^{-2}$)
1	Methanol	64.7	32.7^{25}	1.70	0.544^{25}
2	Ethanol	78.4	24.55^{25}	1.69	1.078^{25}
3	Acetone	56.5	20.70^{25}	2.88	0.337^{25}
4	2-Propanol	82.5	18.3^{25}	1.66	1.765^{30}
5	Ethylene glycol	197.4	38.66	2.20	21
6	Glycerol	290	42.5^{25}	2.56	945^{25}

6.1.3.2 Chemical Composition and the Component Ratio of C, H, and O of Electrolyte

Carbon phase films have already been prepared by conventional vapor deposition for many years, including PVD and CVD techniques. The ratio of elemental components of carbon (C), hydrogen (H) and oxygen (O) is an important factor in the growth of diamond. Thus the component ratio of C, H, and O has been the focus of attention in numerous experiments. Fig. 6.20 is a “C-H-O” diagram showing the C-H-O phase conditions for the growth of diamond films from Bachmann and co-workers [P.K. Bachmann 1991; P.K. Bachmann 1995], so called “Bachmann diagram”. This diagram has become a guide of diamond vapor deposition, diamond carbon deposits can only be obtained in the region close to C/O=1 values. For lower values, no deposition occurs whereas higher values lead to a degradation of the film quality.

Gottardi *et al.* [G. Gottardi 2008] introduced this diagram into deposition of hydrogenated amorphous carbon films by PECVD. They explored a non-conventional gas precursor, a mixture of methane and carbon dioxide with increasing percentage of CO_2, from 0 to 66%. According to the Bachmann diagram, the gas composition with lower CO_2 placed in the "non-diamond carbon region", the composition with 50% of CO_2 content tied in perfectly with the "diamond domain", the 66% of CO_2 fell in the "no growth region". Their results confirmed that the films growth rate decreased with the increase of [CO_2], until no growth at all for [CO_2]>50% which was already in the "no growth region". Thus, the C-H-O diagram is also helpful for the analysis of DLC films deposition by PECVD.

However, all these are about vapor techniques. Bachmann diagram has never been discussed in liquid electrochemical deposition of DLC films. Here the C-H-O phase diagram is introduced into the liquid phase method and attempted to discover the relationship between electrolyte composition and DLC films formation.

The analytically pure organic chemicals and mixed solutions have been used as electrolyte to prepare DLC films here, the positions of all the solutions are shown in the C-H-O diagram in Fig. 6.21. The deposition processes as well as morphology and microstructure of the resulting films were investigated.

On the one hand, six analytically pure organic chemicals were used to deposit DLC films by liquid electrochemical technique. Ethanol, acetone and 2-propanol are all in the "non-diamond carbon region", and DLC films were successfully prepared by electrolysis of these three organic chemicals, respectively. This is the same with the vapor deposition.

Methanol is at the "CO" line, the boundary of the "diamond domain". However, just DLC films were obtained from our work. While ethylene glycol and glycerol are also on the same boundary as methanol, but no films were deposited. The main reason is the high viscosity which is not appropriate for DLC films formation in liquid electrochemical deposition.

On the other hand, mixed organic solution was further introduced into liquid phase deposition as electrolyte. Deionized water was added into analytically pure ethanol to form mixed organic solution. Composition of the electrolyte was varied with the ratio of deionized water, so did the elemental component ratio of C, H, and O. With the increase of deionized water ratio, the positions of the mixed solutions start from the "non-diamond carbon region" and go through the "diamond domain", and then go into the "no growth region" in the Bachmann diagram. However, the Raman results confirmed that DLC films were successfully deposited from the electrolysis of these mixed chemicals. Thus, it is possible to prepare DLC films using electrolytes located in the "no growth region" for vapor deposition of diamond.

In addition, analysis of the resulting films confirmed that the morphology and microstructure of the DLC films deposited were affected by the electrolyte

composition even when the electrolytes are in the same area in the Bachmann diagram.

Liquid electrochemical deposition of DLC films is a complicated reaction which seems to be different from the vapor deposition process. The growth of DLC films can be affected by many factors. For example, the conductivity of the electrolyte is an important parameter in the electrochemical reaction. Although adding additive can change the composition of the solution, the conductivity of the electrolyte is changed at the same time. And this might affect the DLC films formation to some extent at the same time.

Since the Bachmann diagram came from the statistic of vapor deposition techniques, the results of liquid deposition do not exactly follow the component classification. Thus, it is necessary to develop DLC films deposition by liquid electrochemical technique, both experimentally and theoretically. A better understanding of the change of electrolyte composition and the correlation with the films properties needs to be developed.

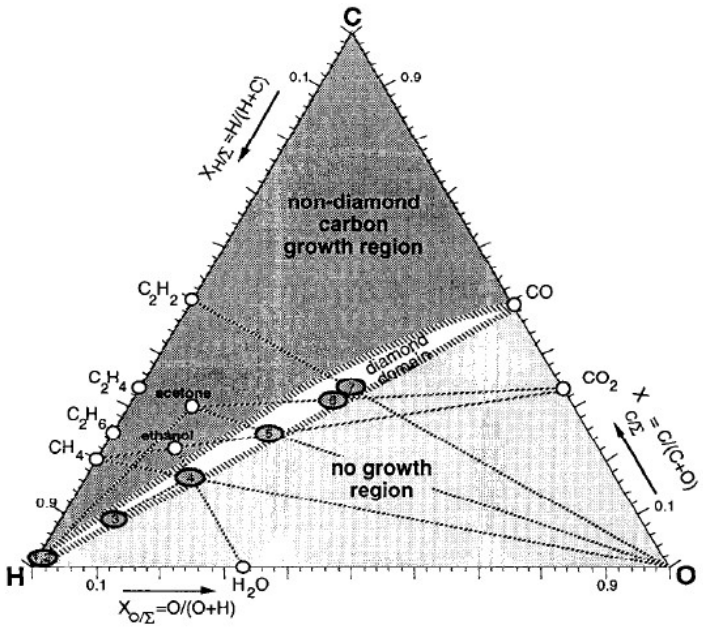

Fig. 6.20 The C-H-O phase diagram from Bachmann [P.K. Bachmann 1995].

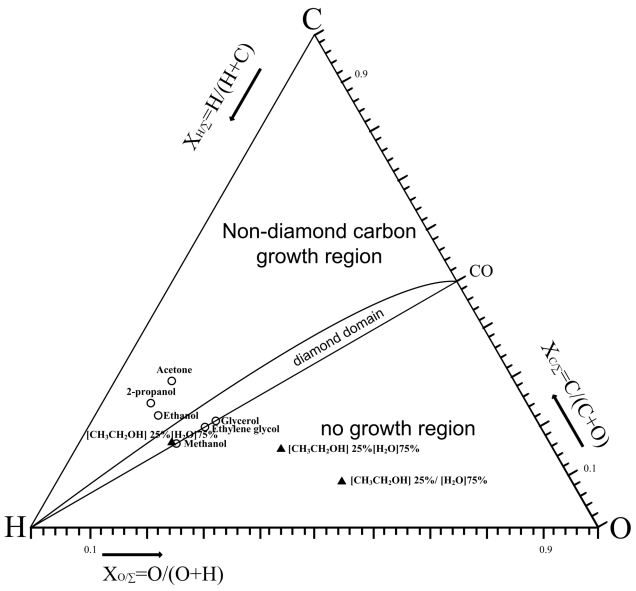

Fig. 6.21 Positions in the Bachmann diagram of the electrolytes used in this work.

6.1.3.3 Effects of Additives on Deposition of DLC Films by Liquid Electrochemical Technique

It is confirmed that adding deionized water into pure ethanol solution can affect the deposition of DLC films. This is an example of using additive in the DLC films liquid phase deposition. The advantages of using additive in the deposition of DLC films by liquid electrochemical technique are discussed here.

Firstly, adding additives can change the conductivity and composition of electrolyte. Normally, the electrolyte and additive have different electrical resistivity. The conductivity of the solution is changed with the addition of additive which has influence on the DLC films growth rate. The electric conductivity of the mixed ethanol/deionized water solutions are shown in Fig. 6.22. The conductivity increased with the addition of deionized water.

The component ratio of C, H, and O is obviously changed with the addition of additive. A mixture of organic solution can be designed so that the component ratio of C, H, and O in the solution would match the diamond growth conditions found in the Bachmann diagram.

Secondly, adding deionized water is a feasible method to decrease the viscosity of some chemicals, such as ethylene glycol and glycerol. It is possible to get better fluid ability which is favorable for DLC films formation in the liquid electrochemical deposition process.

Thirdly, using additive may decrease the cost of deposition. The additive such as deionized water is cheaper than organic chemicals. If DLC films of the same or even better properties can be deposited with the addition of deionized water, it is of course preferred by both scientific research and industry.

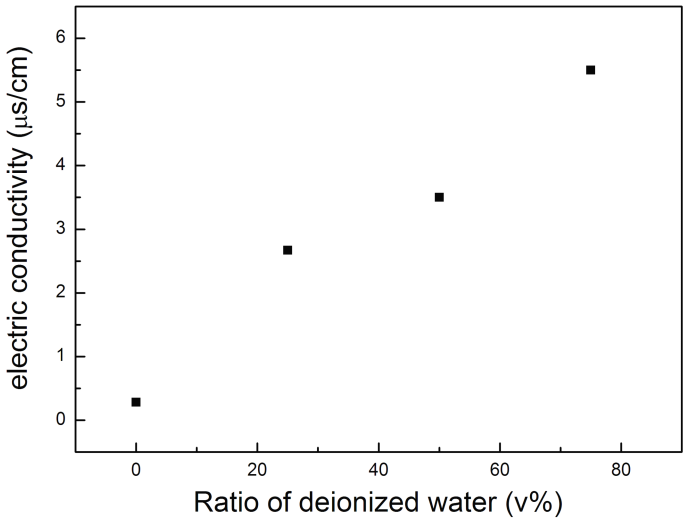

Fig. 6.22 The electric conductivity of each mixed ethanol/deionized water solution.

6.1.3.4 Effects of Hydrogen on the Deposition of DLC Films

In the vapor deposition of DLC films, the role of hydrogen is connected with the hydrogen ratio. On the one hand, hydrogen reacts with methane and the production is CH_3 which is an active role in the growth of DLC films. On the other hand, H atoms can etch both graphitic (sp^2) and diamond-like (sp^3) carbon, too much hydrogen will cause overmuch etching and decrease the films growth rate.

Adding deionized water as an additive in liquid phase deposition of DLC films can bring hydrogen and hydroxyl into the solution. The effects of the additional hydrogen and hydroxyl are complicated. It should be another topic in the deposition of DLC films using liquid electrochemical technique.

6.1.4 Conclusions

Analytically pure organic methanol, ethanol, acetone, 2-propanol, ethylene glycol and glycerol were used as electrolyte to deposit DLC films by liquid electrochemical technique, respectively.

The characterization suggested that hydrogenated DLC films were successfully deposited from methanol, ethanol, acetone and 2-propanol, respectively. The film deposited by electrolysis of methanol had the lowest growth rate and sp^3 content. The films deposited from ethanol had very rough surface although with the advantages of higher growth rate and sp^3 content. The DLC films deposited from acetone and 2-propanol had high growth rate, smooth surface and high sp^3 content. Thus, 2-propanl is widely used in the following work because acetone is more poisonous.

Because the film growth rate, morphology and microstructure were all correlated with the chemicals used, certain organic chemical should be selected as electrolyte depending on the requirements of the resulting DLC films.

No films were deposited from analytically pure ethylene glycol or glycerol mainly because of the high viscosity. Carbon sources with higher viscosities decrease their fluid ability and hinder the migration of the molecules. Low viscosity is preferred in the selecting of electrolyte used for DLC films liquid electrochemical deposition. The organic liquids with the methyl group bonding to the polar group are appropriate carbon sources.

Deionized water was used as an additive and added into analytically pure ethanol in the volume ratio of 25%, 50% and 75%, respectively. DLC films were deposited by liquid electrochemical technique using these ethanol/deionized water solutions.

Compared with the deposition of DLC films using analytically pure ethanol as electrolyte, the film growth first increased, and then decreased with the addition of deionized water. The maximal growth rate was obtained when ethanol and deionized water are in the volume ratio of 1:1. Compared with the DLC films deposited from analytically pure ethanol, the films surface became smooth with the increase of deionized water. The Raman results suggested that hydrogenated DLC films were deposited, the content of both sp^3 carbon and bonded hydrogen decreased with the increase of deioniezd water. Analysis of FTIR spectroscopy also suggested that the hydrogen content decreases with the addition of deionized water.

Deionized water which plays the part of additive can obviously affect the deposition of DLC films by liquid electrochemical technique, including the film morphology and microstructure. Although film growth rate can be increased with appropriate ratio of deionized water, the film structure is changed at the same time. This should be a guide of using deionized water as an additive to achieve ideal growth rate and films properties.

6.2 Geometrical Parameter

The term of "Anode-Substrate Distance" is the vertical distance between anode and substrate, and it is obviously a geometrical parameter in the DLC films liquid electrochemical deposition system. In our liquid deposition system, the distance between anode and substrate is designed adjustable, and can be continuously varied from 0 mm to 12 mm.

6.2.1 Comparison of Various Anode-Substrate Distances

Several distances from 4 mm to 10 mm have been reported in different deposition systems [Y. Namba 1992; J.T. Jiu 2002; X.B. Yan 2004; F.L. Shen 2005]. However, the analysis of anode-substrate distance is rare to see, e.g. the effects of various anode-substrate distances on the deposition of DLC films under the same other parameters. For this purpose various distances were adjusted in this section to investigate the effects of anode-substrate distance on the DLC films deposition in liquid electrochemical technique.

6.2.1.1 Experimental Details

The experimental setup and deposition procedure were described in chapter 4. The anode was made of graphite and silicon wafer was used as the substrate. Analytically pure 2-propanol and analytically pure methanol were chosen as the electrolyte, respectively. For each organic chemical, the distance between anode and substrate was set to 3 mm, 6 mm and 9 mm. The applied potential and the deposition time were 1000 V (frequency 10 kHz, duty cycle 50%) and 2 h, respectively.

After deposition, microstructure of the DLC films was investigated using a micro-Raman system Jobin Yvon with a laser source wavelength of 514.532 nm.

6.2.1.2 Results

Raman is a sensitive detection of carbon based materials, including diamond, graphite, carbon nanotubes and diamond-like carbon (DLC). Raman spectroscopy was therefore widely used for carbon films detection and film structure characterization [J. Robertson 1991; J. Robertson 1993; J. Robertson 2002].

Fig. 6.23 shows Raman spectra of the films deposited under various anode-substrate distances using analytically pure 2-propanol as electrolyte. As can be seen, no carbon signal is observed in the Raman spectrum of the sample deposited with the anode-substrate distance of 9 mm. This suggests that no carbon film was deposited at this distance. Typical Raman spectrum of DLC films is shown when the anode-substrate distance was set to 6 mm. Two broad peaks centered at 1350 cm^{-1} and 1590 cm^{-1} appear in the Raman spectrum, respectively. These two peaks are related to D band at 1355 cm^{-1} and G band at 1580 cm^{-1}, indicating that some sp^2 amorphous carbon phases exist in the film [R.J. Nemanich 1988; D.S. Knight 1989; W.A. Yarbrough 1990]. When the anode-substrate distance decreased to 3 mm, there are very weak peaks around 1360 cm^{-1} and 1580 cm^{-1} in the corresponding Raman spectrum.

The analysis of Raman spectra suggests that the anode-substrate distance has significant influence on the DLC films deposition in the electrolysis of 2-propanol. A middle distance such as 6 mm appears to be an optimal distance to get formation of DLC films during the adjustment of anode-substrate distance. Either increasing or decreasing the distance is not feasible to get DLC film under the same other parameters.

Liquid electrochemical deposition of DLC films is based on the electrolysis of organic solutions. Under the applied potential, the decomposition of organic molecules and deposition reaction of DLC films are carried out between the anode and substrate. The energy density between anode and substrate will be decreased when the distance is increased under the same applied potential. This causes the weak electric field and the organic molecules can not be easily polarized which will lead to low growth rate of DLC films during liquid electrochemical deposition. When the distance is longer than the maximum, it is impossible to get any film deposited. For example, it is too long to get film deposited when the anode-substrate distance is increased to 9 mm which has been confirmed by Raman analysis.

Under the same applied potential, decreasing the anode-substrate distance can increase the energy density, similar as increasing the applied potential. Some publications suggested that high applied potential could improve the formation of sp^3 carbon in the DLC films deposited by electrolysis of methanol because of the enhancement of electric field [H.S. Zhu 2003; X.B. Yan 2004]. However, short distance meanwhile leads to great heating effect and thus some difficulty in controlling the solution temperature. When the temperature comes to the boiling point, the organic solution between anode and substrate will boil and the violent boiling of the solution can disturb the polarized particles moving towards to the substrate to format DLC films. When the anode-substrate distance was set to 3 mm, the formation of a stream of bubbles could be distinctly seen by eyes as soon as the voltage was applied to the deposition reactor. The heating effect and boiling movement of the solution was much stronger than those of 6 mm and 9 mm. This is considered to be the main effect of decreasing the anode-substrate distance and therefore not good for film deposition.

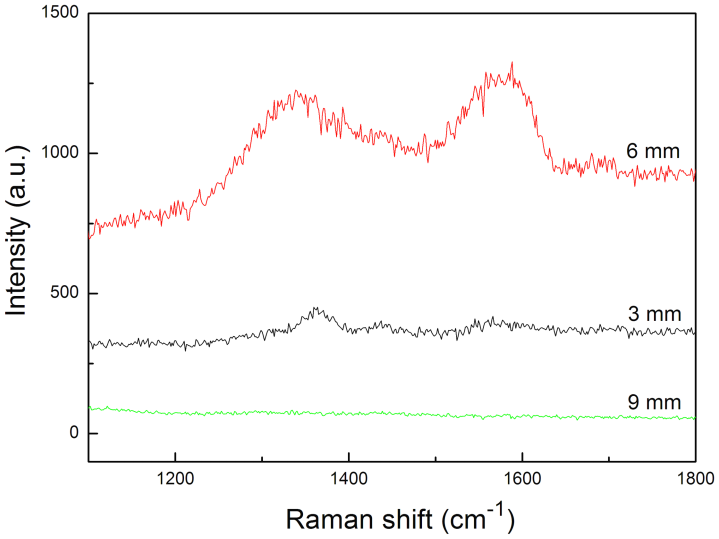

Fig. 6.23 Raman spectra of the films deposited using analytically pure 2-propanol as electrolyte under various anode-substrate distances.

Fig. 6.24 displays Raman spectra of the films deposited using analytically pure methanol as electrolyte. The Raman spectra under various anode-substrate distances in Fig. 6.24 show similar trend as the spectra in Fig. 6.23. This result confirms that there is a middle distance appropriate for the deposition of DLC films. The distance either longer or shorter than the optimal anode-substrate distances is not appropriate to get DLC films deposition. However, it has to be pointed out that it does not mean 6 mm is exactly the optimal anode-substrate distance, maybe better DLC films can be deposited at another value around 6 mm, of course between 3 mm and 9 mm.

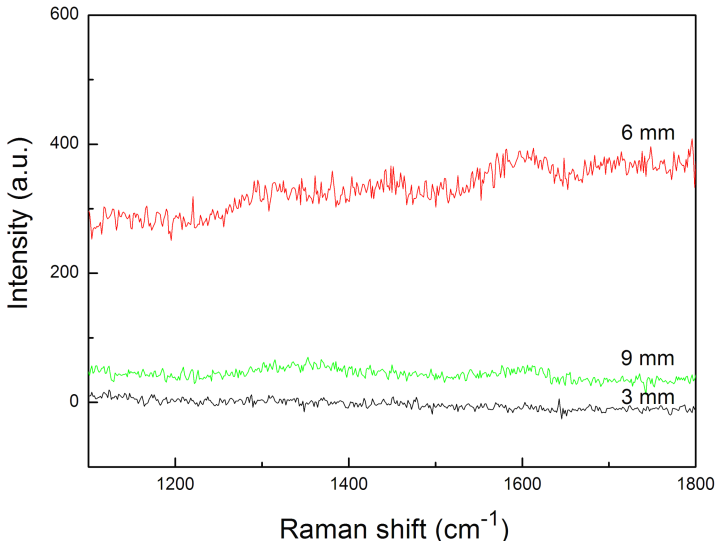

Fig. 6.24 Raman spectra of the films deposited using analytically pure methanol as electrolyte under various anode-substrate distances.

6.2.2 Comparison of Electrolytes

In the last section, we confirmed that the anode-substrate distance could affect the growth of DLC films in liquid electrochemical technique. An optimal anode-substrate distance exists around 6 mm for the electrolysis of both analytically pure 2-propanol and methanol, it is not appropriate to deposit DLC film under too long or too short anode-substrate distance. Then comes another question, are the optimal distances for other organic solutions all in this same range? Here methanol/deionized water solution is used to carry out the deposition process with the anode-substrate distance of 3 mm, 6 mm and 9 mm, respectively, for comparison.

The samples were measured by Raman after deposition. Fig. 6.25 shows the Raman spectra of the films deposited under various anode-substrate distances using methanol/deionized water solution as electrolyte.

In Fig. 6.25, no carbon films were deposited when the anode-substrate distance was set to 9 mm or 6 mm, however, typical DLC film was deposited with the distance of 3 mm. It seems that the optimal anode-substrate distance shifted to a smaller value than the electrolysis of 2-propanol and methanol. In conclusion, the optimal anode-substrate distance is correlated with the composition of electrolyte.

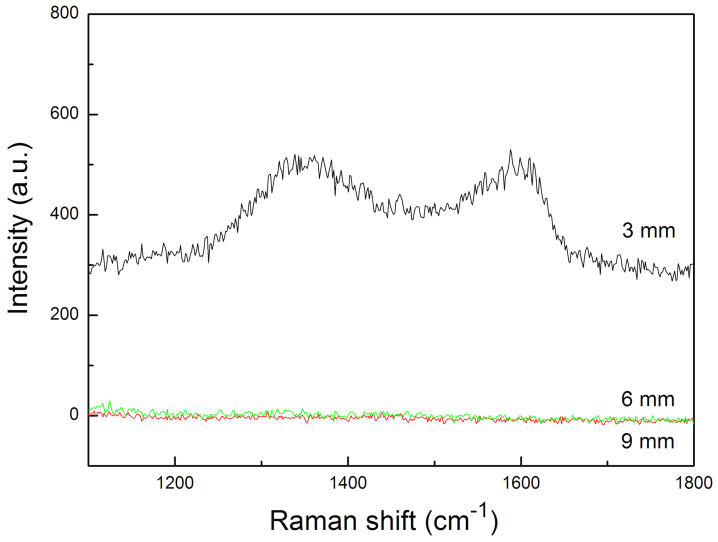

Fig. 6.25 Raman spectra of the films deposited using methanol/deionized water solution as electrolyte under various anode-substrate distances.

6.2.3 Discussions

Deposition of DLC films by liquid electrochemical technique is a complicated chemical and physical reaction with many parameters. Adjustment of anode-substrate distance can affect the energy density between the anode and substrate, but it is different from simply changing the applied potential under the same anode-substrate distance (investigated in section 6.3), because adjusting the anode-substrate distance will cause other changes. For example, decreasing the distance will lead to significant heating effect and the violent boiling of the solution can disturb the polarized particles moving towards to the substrate to format DLC films. Anyway, adjusting the anode-substrate distance is an approach for the films quality control.

6.2.4 Conclusions

Influence of the anode-substrate distance on the deposition of DLC films using liquid electrochemical technique has been investigated. The anode-substrate distance is an important geometrical parameter in the liquid electrochemical deposition system which can affect the formation of DLC films. There is an optimal distance during the adjustment of anode-substrate distance and it is appropriate to grow DLC films at this distance. The optimal anode-substrate distance is supposed to be the place to get the most energy from the applied potential and simultaneously the lowest influence of the solution movement. Neither longer nor shorter than the optimal distance is appropriate for the formation of DLC films.

The optimal distance is different with the composition of the organic solution. One optimal distance is not appropriate for all the other organic solutions which can be used in liquid electrochemical deposition of DLC films.

6.3 Electrical Parameter

Applied potential is the main electrical parameter in the deposition of DLC films using liquid electrochemical technique. It is exported from the power supply and applied to the deposition system. The energy required by the decomposition of organic molecules and the formation of DLC films can only be provided by the power supply during the deposition process. High applied potential of course means that more energy will be imported, however, it does not mean that high applied potential could definitely get DLC films formation or appropriate film structure. Different applied potentials were reported by the researchers. Some of them suggested that high applied potential could improve the formation of sp^3 carbon in the DLC films deposited by the electrolysis of methanol [J.T. Jiu 2002; H.S. Zhu 2003; X.B. Yan 2004]. Although some work has been done, little has been reported in detail about the influence of applied potential on the morphology and microstructure of DLC films using liquid electrochemical technique. Various applied potentials were used to prepare DLC films in this section, the film properties were investigated in order to discuss the influence of the applied potential.

6.3.1 Experimental Details

The experimental setup and deposition procedure were described in chapter 4. The applied potential was set to 1000 V, 800 V, 600 V and 400V (frequency 10 kHz, duty cycle 50%), respectively, and kept constant during each deposition process. Analytically pure 2-propanol was used as electrolyte, and the deposition process lasted for 2 h for each applied potential. The anode material, substrate and anode-substrate distance were graphite, silicon wafer and 6 mm, respectively.

After deposition, the film thickness and morphology were measured by the same facilities as above. The microstructure of the deposited DLC films was investigated by Raman and FTIR as well.

6.3.2 Results

6.3.2.1 Films Deposition

After deposition, the substrates were covered by gray films. Since the film growth rate is an important characterization in thin film technology, the film thickness was measured first and then the film growth rate was calculated with the deposition time; the results are displayed in Fig. 6.26. The film growth rates here vary with the applied potential. The film growth rate decreases with the increase of the reaction voltage.

The maximum and minimum of growth rate are obtained at 400 V and 1000 V, respectively.

The analysis of film growth rate confirms that the applied potential has influence on the film growth rate in liquid electrochemical deposition of DLC films. For example, growth rate of the films deposited by electrolysis of pure 2-propanol decreases with the increase of applied potential, in the range from 400 V to 1000 V.

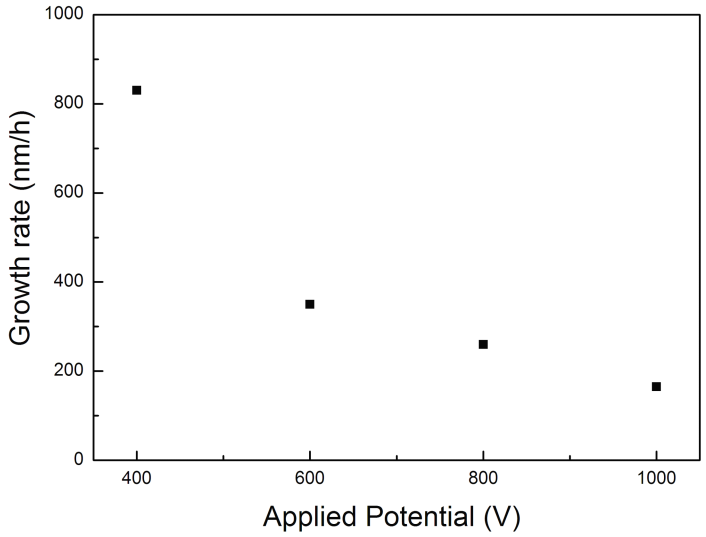

Fig. 6.26 Growth rate of the films deposited by electrolysis of analytically pure 2-propanol under various applied potentials.

6.3.2.2 Morphology of DLC Films

The film performance is needed here to exhibit the influence of applied potential on the film morphology. Since SEM and AFM are both practical methods to investigate the surface morphology in thin film technology. Fig. 6.27 shows the typical SEM images of the DLC films deposited under various applied potentials chosen in this work. The observation of the resulting samples suggests that all the samples were covered by films under the applied potential varied from 400 V to 1000 V using liquid electrochemical technique. However, the different morphology confirms that the applied potential can affect the film performance. Compared with the other three images, the film deposited under 1000 V is uniform and relative smooth. There are more and more rough areas on the film surface with the decrease of applied potential.

The film morphology was further investigated by AFM. 3D AFM images of the films are shown in Fig. 6.28, also comparison of the corresponding RMS roughness of the films is attached in Fig. 6.29. It is concluded that the film deposited under the applied

potential of 1000 V has the smoothest surface, and the roughness increases with low applied potentials. Both the AFM images and the RMS roughness results confirm that the resulting film becomes rough with the decrease of the applied potential in this work. The results of AFM measurement are coincident to the SEM observation.

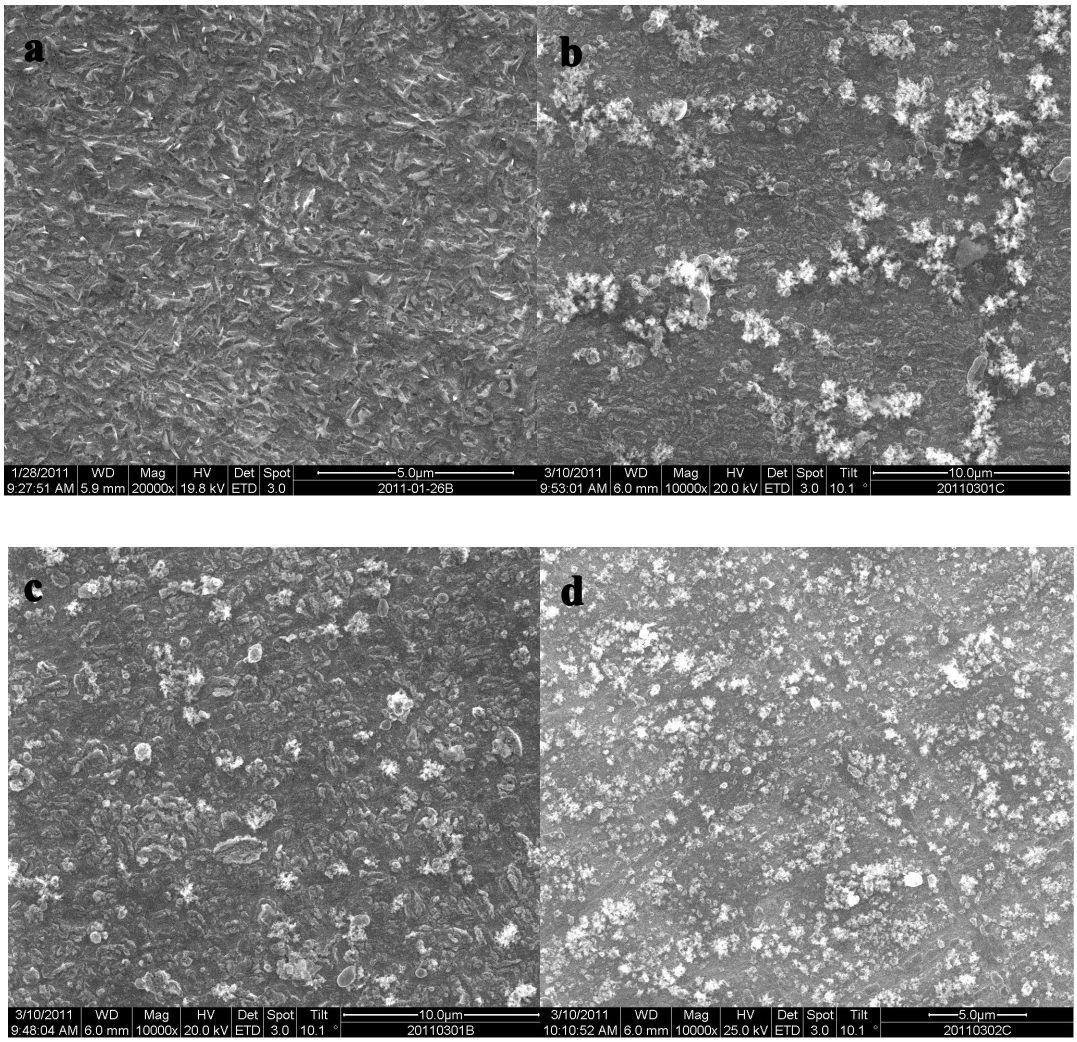

Fig. 6.27 Typical SEM images of the DLC films deposited by electrolysis of analytically pure 2-propanol under various applied potentials (a: 1000 V, b: 800 V, c: 600 V, d: 400 V).

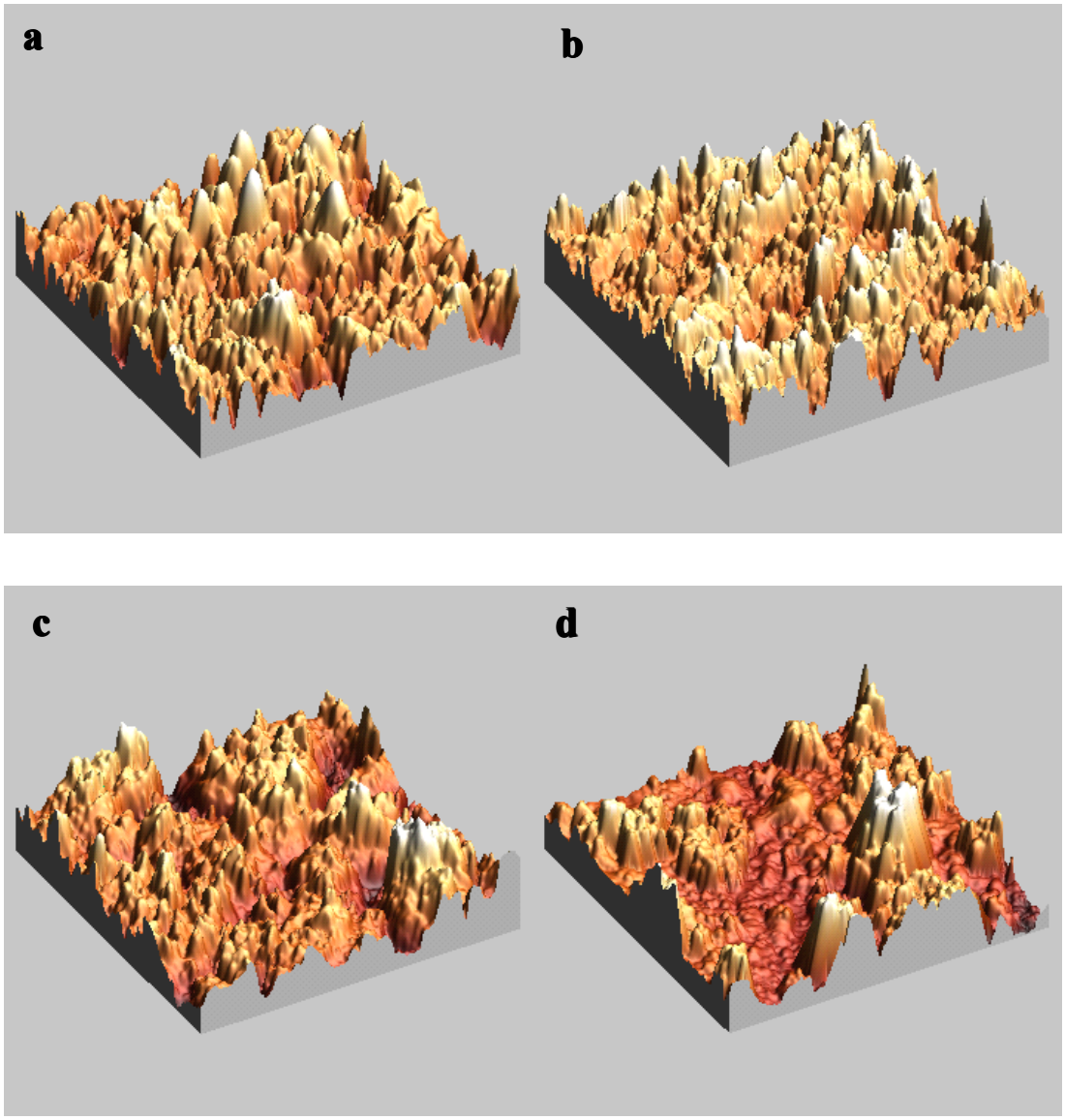

Fig. 6.28 Typical AFM images of the DLC films deposited by electrolysis of analytically pure 2-propanol under various applied potentials (a: 1000 V, b: 800 V, c: 600 V, d: 400 V).

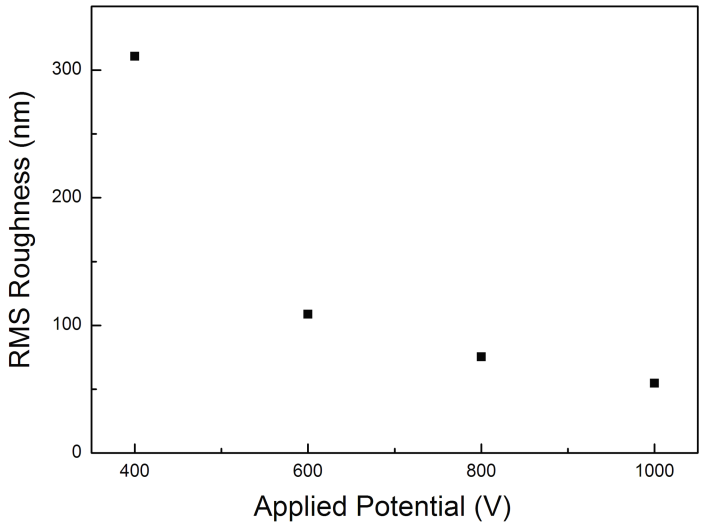

Fig. 6.29 Root Mean Square roughness of DLC films deposited by electrolysis of analytically pure 2-propanol under various applied potentials.

6.3.2.3 Bond-structure and Chemical Composition of DLC Films

Raman is a widely used non-destructive way to obtain the detailed bonding structure characterization of the DLC materials [J. Robertson 2002]. Raman spectroscopy was therefore employed to investigate influence of the deposition applied potential on the micro-structure of the resulting films.

Fig.6.30 shows Raman spectra of the films deposited under various applied potentials. It is confirmed that DLC films were successfully deposited by electrolysis of analytically pure 2-propanol under the applied potential in the range from 400 V to 1000 V. All the Raman spectra have two broad peaks which are corresponding to D peak and G peak, respectively. For example, there are two broad peaks centered at 1355 cm^{-1} and 1581 cm^{-1} appear in Fig. 6.30a. The two peaks are related to D peak at 1355 cm^{-1} and G peak at 1580 cm^{-1}, indicating that some sp^2 amorphous carbon phases exist in the film deposited by electrolysis of 2-propanol under the applied potential of 1000 V [R.J. Nemanich 1988; D.S. Knight 1989; W.A. Yarbrough 1990].

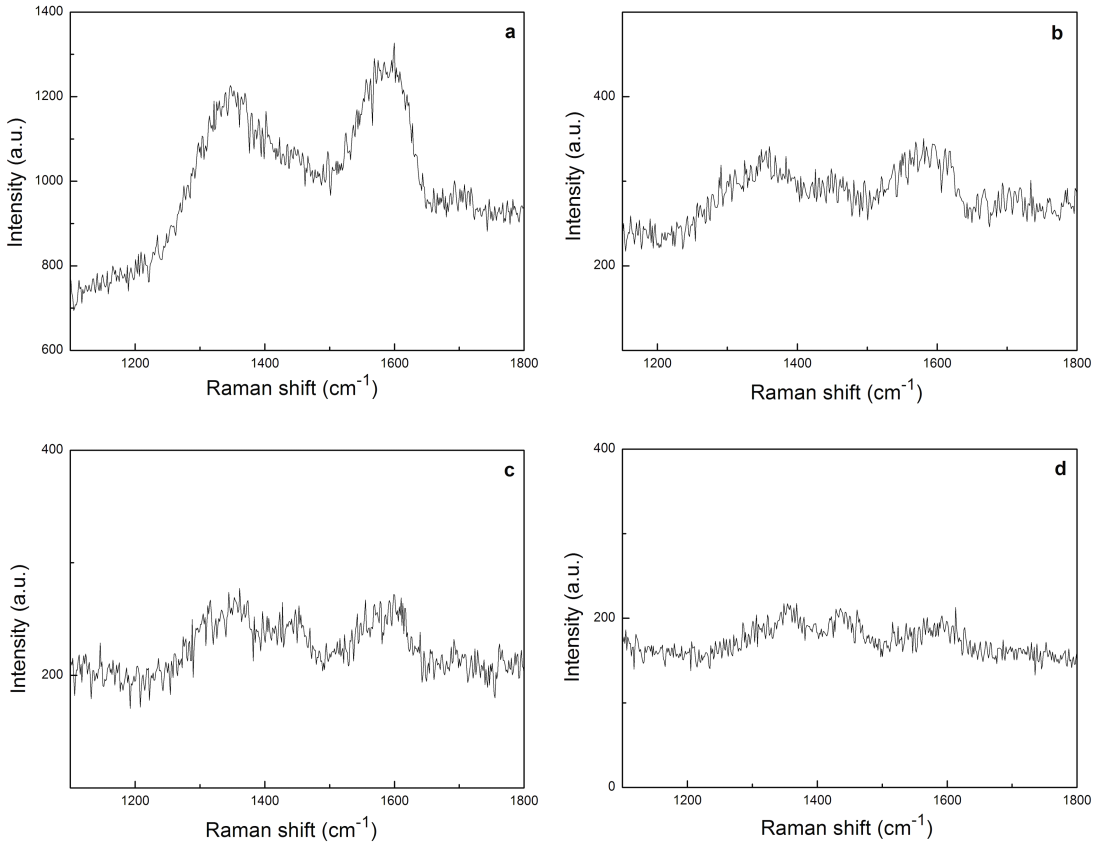

Fig. 6.30 Raman spectra of the DLC films deposited by electrolysis of analytically pure 2-propanol under various applied potentials (a: 1000 V, b: 800 V, c: 600 V, d: 400 V).

Although all the Raman spectra of the DLC films deposited were of quite similar form, the different center positions and intensities of D peak and G peak, considering the structures of the films may be different. For analysis, the region from 1150 cm^{-1} to 1800 cm^{-1} in all the Raman spectra were further Lorenz fitted on a linear background in order to determine the intensities, peak positions, and line widths of the individual Raman features. The relationship between the applied potential and Raman fitting information is displayed in Fig. 6.31.

The I(D)/I(G) ratio of each spectrum is approximately in the region of 0.98-1.26, and decreases with the increase of applied potential. The G peak position down shifted generally with the increase of applied potential. Since the I(D)/I(G) intensity ratio and the G peak position obtained with Raman measurements are correlated with the sp^3/sp^2 ratio, a lower intensity ration can be interpreted as corresponding to higher sp^3 content [C. Casiraghi 2005; G. Irmer 2005]. The DLC films deposited under 1000 V is therefore suggested to have the highest sp^3 content.

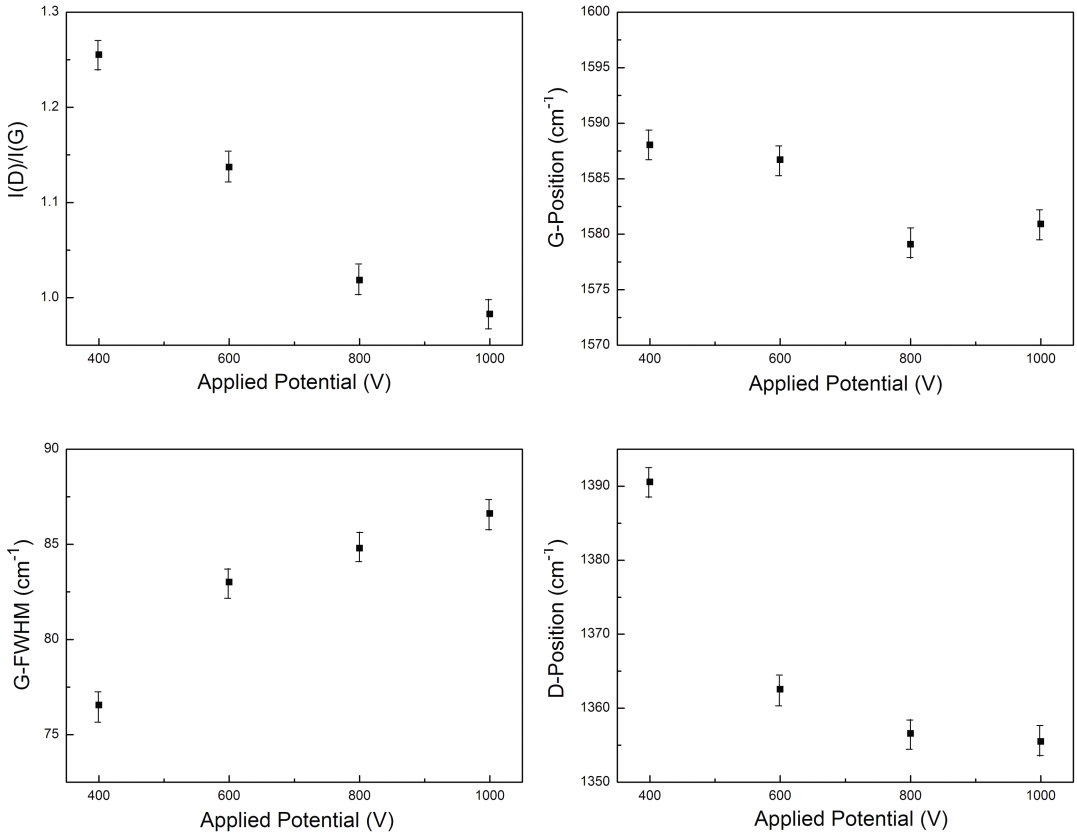

Fig. 6.31 Correlation between Raman fitting information and the DLC films deposition applied potential.

The G peak position and I(D)/I(G) ratio of the DLC films deposited under various applied potentials are placed on the "G peak position-sp^3 content" and "I(D)/I(G) ratio- sp^3 content" curves which were exponential fitted by A.C. Ferrari [A.C. Ferrari 2000]. As shown in Fig. 6.32, the sp^3 content drawn from G position are about 20-33%, the sp^3 content drawn from I(D)/I(G) ratio is 36-40%. However, the sp^3 content calculated from G position is always lower than that drawn from I(D)/I(G) ratio [A. Poukhovoi 2011]. The bonded sp^3 content in the DLC films deposited under different applied potentials are suggested to be in agreement with the "I(D)/I(G) ratio-sp^3 content" curve.

As a result, Raman spectroscopy analysis confirmed that hydrogenated DLC films were deposited by liquid electrochemical technique based on the electrolysis of analytically pure 2-propanol. In the range from 400 V to 1000 V, high applied potential is favorable for the formation of sp^3 carbon and bonded hydrogen in the DLC films.

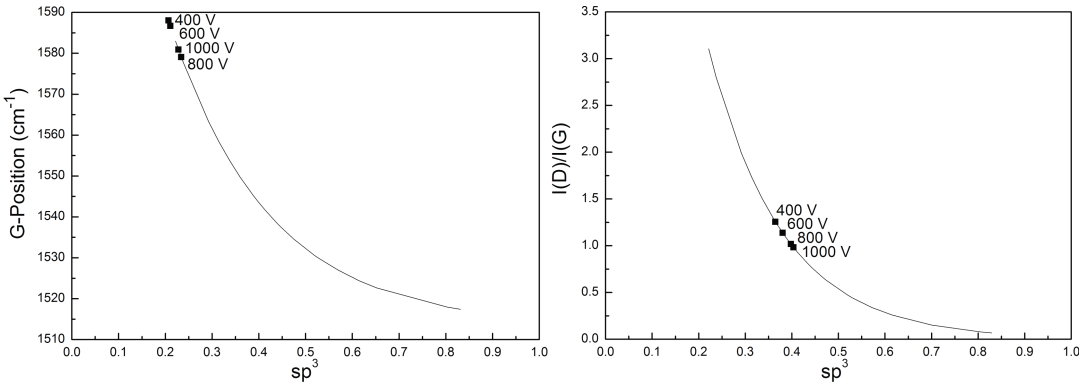

Fig. 6.32 Presentation of G peak position and I(D)/I(G) ratio on the exponential fitted curves from A.C. Ferrari [A.C. Ferrari 2000].

It has been confirmed that hydrogenated DLC films were deposited by electrolysis of analytically pure 2-propanol at the voltage of 1000 V in section 6.1. The influence of applied potential on the bonded hydrogen content is investigated.

A typical signature of hydrogenated samples in visible Raman spectra is the increasing photoluminescence (PL) background for higher H content. This is due to the hydrogen saturation of nonradiative recombination centers [J. Robertson 1996; Rusli 1996; T. Heitz 1999]. The content of bonded hydrogen is calculated by Formula 6.1.

Fig. 6.33 shows the results of hydrogen content calculation. The DLC films are all hydrogenated, with the bonded hydrogen in the range of 25-35%. The hydrogen content increased with the increase of the applied potential, the maximum of hydrogen content was obtained when the applied potential was set to 1000 V.

The bonded sp^3 content gained from the I(D)/I(G) ratio and the corresponding calculated hydrogen content are laid in the FCN model, as shown in Fig. 6.34. Location of the data from electrolysis of analytically pure ethanol and various mixed ethanol/ deionized water solutions are similar with the a-C:H from Angus [J.C. Angus 1991]. Also the data are located in the ternary phase diagram, as shown in Fig. 6.35.

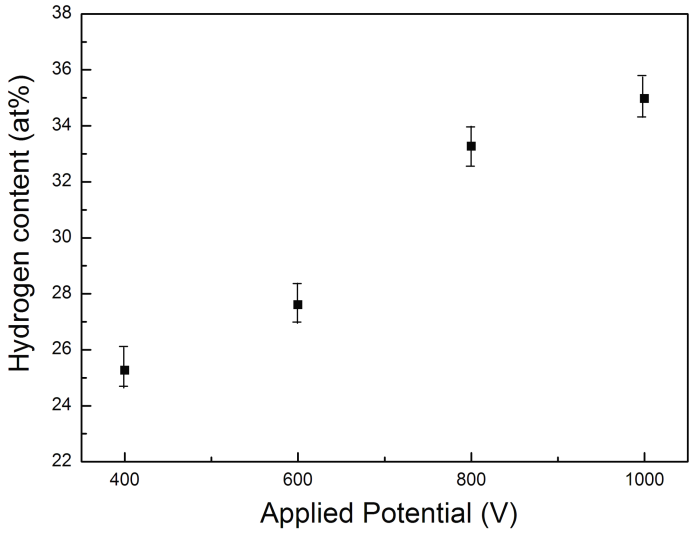

Fig. 6.33 Hydrogen content of the DLC films deposited under various applied potentials.

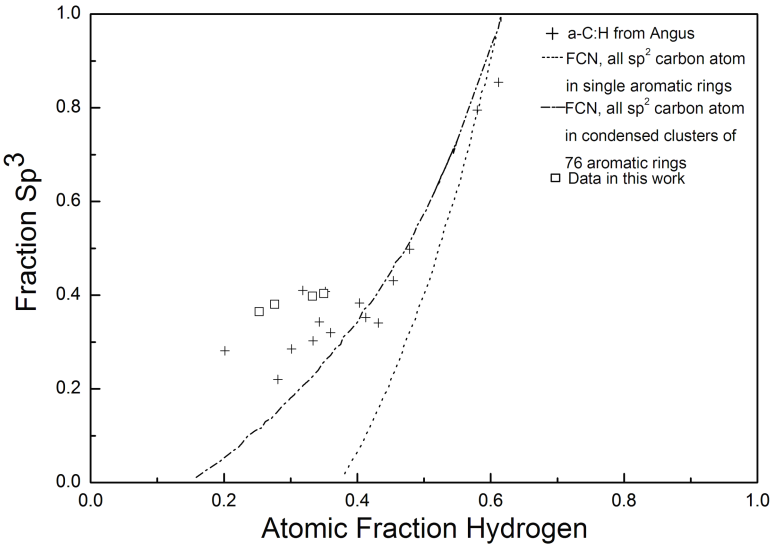

Fig. 6.34 Raman characterization of DLC films deposited under various applied potentials in the FCN model from Angus [J.C. Angus 1991].

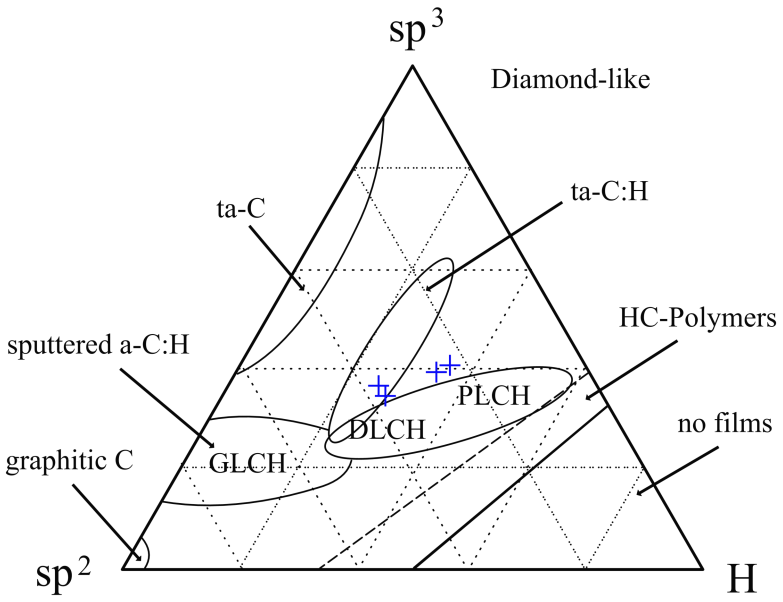

Fig. 6.35 Raman characterization of DLC films deposited under various applied potentials in the ternary phase diagram.

The DLC films were also investigated by FTIR to acquire information about structures and chemical compositions of a-C:H films. FTIR is based on the measurement of the wavelength and the intensity of mid-wave infrared light absorbed by a sample. The absorption bands in amorphous carbon are caused by CC- vibrations and CH-vibrations.

Fig. 6.36 shows the comparison of absorption cures of the DLC films deposited under various applied potentials. These spectra have a good resolution and a good signal-to-noise ratio. For all the curves, the C-H stretching vibrations are found between 2800 cm^{-1} and 3100 cm^{-1}, and a broad absorption band of C=C double bonds at approximately 1600 cm^{-1}. The C-H bending vibrations between 1300 cm^{-1} and 1500 cm^{-1} only appear when the applied potential was set to 1000 V. And the absorption band of C-H bending vibrations disappeared with the decrease of applied potential. This is to a certain extent in agreement with the hydrogen content calculation from Raman spectroscopy. There are especially no characteristic absorption bands of H_2O around 1700 cm^{-1} and 3250 cm^{-1}, indicating that no water existed in the films.

The C-H stretching vibration band is used for quantitative analysis, because it is more distinct than the C-H bending vibration band. The C-H stretching vibration band consists of vibrations of various CH_X configurations. In order to identify the parts of individual bonds, peak deconvolution was performed.

The C-H stretching vibration band was Gaussian fitted with the help of Origin 7.0. Fig. 6.37 shows an example of peak deconvolution of the C-H stretching vibration band and C-H bending vibration band. The following stretching vibrations were found in

all the samples: sp^3CH_2 (symmetric as well as asymmetric), sp^3CH, aromatic sp^2CH and olef sp^2CH. The asymmetric modes usually cause a bigger change of the dipole moment than the symmetric modes and they are more intense. The C-H bending vibrations of sp^3CH_3 sym and sp^2CH_2 olef were only found from the sample deposited from 1000 V.

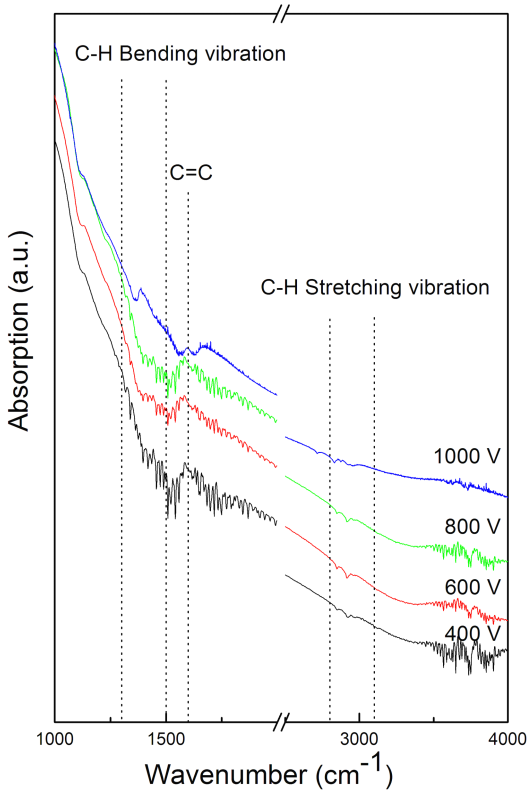

Fig. 6.36 FTIR spectra of the DLC films deposited under various applied potentials.

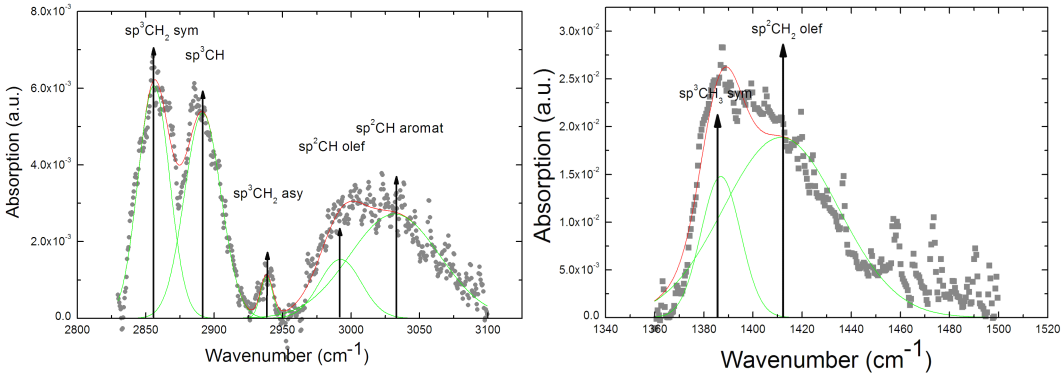

Fig. 6.37 Peak deconvolution by line fitting of the C-H stretching vibration band of the DLC films deposited under the applied potential of 1000 V.

Fig. 6.38 displays the peak positions of C-H stretching vibrations for all the films deposited from 400 V to 1000 V. Based on the overview of possible deconvolution of the C-H stretching vibration modes in a-C:H films, the positions of each peak in this work are constant [J. Ristein 1998].

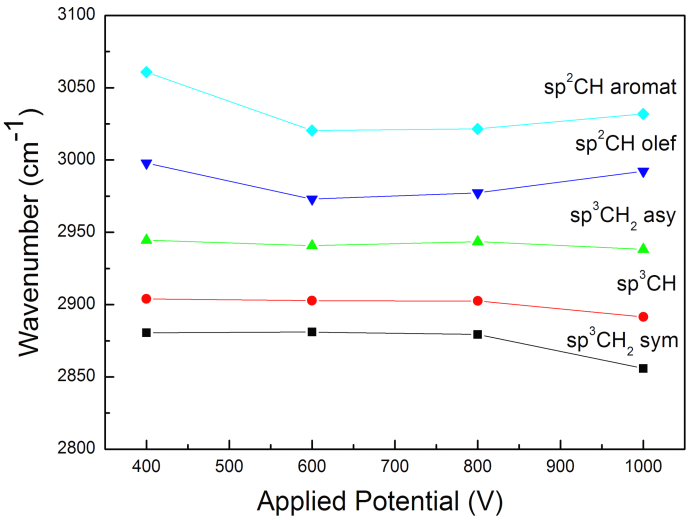

Fig. 6.38 Peak positions of C-H stretching vibrations.

6.3.3 Discussions

It has been confirmed that the film morphology and microstructure can be obviously affected by the applied potential. The applied potential can be easily set to deposit DLC films using liquid electrochemical technique, and adjusted during the deposition process. Adjusting the applied potential is therefore a convenient and feasible way to control DLC films formation and the properties.

6.3.4 Conclusions

DLC films were deposited on Si substrates by electrolysis of analytically pure 2-propanol under various deposition voltages. The deposition applied potential was set to 400 V, 600 V, 800 V and 1000 V, respectively.

The investigation of the resulting films denotes that hydrogenated DLC films were deposited by electrolysis of analytically pure 2-propanol under the applied potential in the region from 400 V to 1000 V. Adjusting applied potential could affect the film morphology and microstructure. The film growth rate and roughness both decreased

with the increase of applied potential. The analysis of Raman spectroscopy suggested that the increase of applied potential was favored for the formation of sp^3 carbon in DLC films. The hydrogen content also increased with the increase of applied potential, the maximum of hydrogen content was obtained when the applied potential was set to 1000 V.

References

A. Poukhovoi (2011). Abscheidung von amorphen wasserstoffhaltigen Kohlenstoffschichten mittels neuartiger hybrider RP-Plasma Quelle und deren spektroskopische Charakterisierung. Physics. Duisburg, University Duisburg Essen. **Doctor:** 142.

A.C. Ferrari, J. Robertson. "Interpretation of Raman spectra of disordered and amorphous carbon" Physical Review B **61**(2000): 14095-14107.

C. Casiraghi, A.C. Ferrari, J. Robertson. "Raman spectroscopy of hydrogenated amorphous carbons" Physical Review B **72**(2005): 085401-1-14.

D. Guo, K. Cai, L.T. Li, Y. Huang, Z.L. Gui, H.S. Zhu. "Electrodeposition of diamond-like amorphous carbon films on Si from N; N-dimethylformamide" Chemical Physics Letters **329**(2000): 346-350.

D.S. Knight, W.B. White. "Characterization of diamond films by Raman spectroscopy" Materials Research Society **4**(1989): 385-393.

F.L. Shen, D.J. Wen, H.W. Wan. "Influence of deposition condition on diamond-l ike carbon films by liquid deposition on the surface of Ti alloy" Journal of Functional Materials **36**(2005): 1278-1281.

G. Gottardi, N. Laidani, R. Bartali, V. Micheli, M. Anderle. "Plasma enhanced chemical vapor deposition of a-C:H films in CH_4-CO_2 plasma: Gas composition and substrate biasing effects on the film structure and growth process" Thin Solid Films **516**(2008): 3910-3918.

G. Irmer, A. Dorner-Reisel. "Micro-Raman studies on DLC coatings" Advanced Engineering Materials **7**(2005): 694-705.

G.F. Zhang, Y.Y. He, X.D. Hou, . "Influence of additive on diamond films synthesized using liquid phase electrochemical method" Materials Science Forum **687**(2011): 662-666.

H. Wang, M.R. Shen, Z.Y. Ning, C. Ye, C.B. Cao, H.Y. Dang, H.S. Zhu. "Deposition of diamond-like carbon films by electrolysis of methanol solution" Applied Physics Letters **69**(1996): 1074-1076.

H.S. Zhu, J.T. Jiu, Q. Fu, H. Wang, C.B. Cao. "Aroused problems in the deposition of diamond-like carbon films by using the liquid phase electrodeposition technique" Journal of Materials Science **38**(2003): 141-145.

J. Ristein, R. T. Stief, L. Ley. "A comparative analysis of a-C:H by infrared spectroscopy and mass selected thermal effusion" Journal of Applied Physics **84**(1998): 3836-3847.

J. Robertson. "Hard amorphous (Diamond-Like) carbons" Solid State Chemistry **21**(1991): 199-333.

J. Robertson. "Deposition mechanisms for promoting sp^3 bonding in diamond-like carbon" Diamond and Related Materials **2**(1993): 984-989.

J. Robertson. "Recombination and photoluminescence mechanism in hydrogenated amorphous carbon" Physical Review B **53**(1996): 16302-16305.

J. Robertson. "Diamond-like amorphous carbon" Materials Science and Engineering R **37**(2002): 129-281.

J.C. Angus. "Diamond and Diamond-like Phase" Diamond and Related Materials **1**(1991): 61-62.

J.T. Jiu, Q. Fu, H. Wang, H.S.Zhu. "Aroused problems in the deposition of diamond-like carbon films by using the liquid phase electrodeposition technique" Journal of Inorganic Materials **17**(2002): 571-578.

K. Cai, D. Guo, Y. Huang, H.S. Zhu. "Electrodeposition of diamond-like amorphous carbon films

on aluminum from acetonitrile " Applied Physics A **71**(2000): 227-228.

L.N. Huang, H.Q. Jiang, J.S. Zhang, Z.J. Zhang, P.Y. Zhang. "Synthesis of copper nanoparticles containing diamond-like carbon films by electrochemical method" Electrochemistry Communications(2006): 262-266.

P.K. Bachmann, D. Leers, H. Lydtin. "Towards a general concept of diamond chemical vapour deposition" Diamond and Related Materials **1**(1991): 1-12.

P.K. Bachmann, H.J. Hagemann, H. Lade, D. Leers, D.U. Wiechert, H. Wilson, D. Fournier, K. Plamann. "Thermal properties of C/H-, C/H/O-, C/H/N- and C/H/X-grown polycrystalline CVD diamond " Diamond and Related Materials **4**(1995): 820-826.

R.J. Nemanich, J.T. Glass, G. Lucovsky, R.E. Shroder. "Raman scattering characterization of carbon bonding in diamond and diamondlike thin films" Journal of Vacuum Science & Technology A: Vacuum, Surfaces, and Films **6**(1988): 1783-1787.

R.S. Li, M. Zhou, X. J. Pan, Z.X. Zhang, B.A. Lu, T. Wang, E.Q. Xie. "Simultaneous deposition of diamondlike carbon films on both surfaces of aluminum substrate by electrochemical technique" Journal of Applied Physics **105**(2009): 066107-1-3.

Rusli, J. Robertson, G.A.J. Amaratunga, . "Photoluminescence behavior of hydrogenated amorphous carbon" Jouranl of Applied Physics **80**(1996): 2998-3003.

T. Heitz, B. Dre´villon, C. Godet, J. E. Boure´e. "Quantitative study of C-H bonding in polymerlike amorphous carbon films using *in situ* infrared ellipsometry" Physical Review B **58**(1998): 13957-13973.

T. Heitz, C. Godet, J.E. Boure´e, B. Dre´villon. "Radiative and nonradiative recombination in polymerlike a-C:H films" Physical Review B **60**(1999): 6045-6052.

T. Suzuki, Y. Manita, T. Yamazaki, S. Wada, T. Noma. "Deposition of carbon films by electrolysis of a water-ethylene glycol solution" Journal of Materials Science **30**(1995): 2067-2069.

V.P. Novikov, V.P. Dymont. "Synthesis of diamondlike films by an electrochemical method at atmospheric pressure and low temperature" Applied Physics Letters **70**(1997): 200-202.

W.A. Yarbrough, R. Messier. "Current issues and problems in the chemical vapor deposition of diamond" Science **247**(1990): 688-696.

W.L. He, R. Yu, H. Wang, H. Yan. "Electrodeposition mechanism of hydrogen-free diamond-like carbon films from organic electrolytes" Carbon **43**(2005): 2000-2006.

X.B. Yan, T. Xu, G. Chen, H.W. Liu, S.R. Yang. "Effect of deposition voltage on the microstructure of electrochemically deposited hydrogenated amorphous carbon films" Carbon **42**(2004): 3103-3108.

X.B. Yan, T. Xu, S.R. Yang, H.W. Liu, Q.J. Xue. "Characterization of hydrogenated diamond-like carbon films electrochemically deposited on a silicon substrate" Journal of Physics D: Applied Physics **37**(2004): 2416-2424.

Y. Namba. "Attempt to grow diamond phase carbon films from an organic solution" Journal of Vacuum Science Technology A **10**(1992): 3368-3370.

Y.Y. He, G.F. Zhang, G.Q. Li, X.D. Hou, . "Deposition of amorphous diamond films on different substrates by electrolysis of methanol solution" Key Engineering Materials **373-374**(2008): 264-267.

Z. Sun, Y. Sun, X. Wang. "Investigation of phases in the carbon films deposited by electrolysis of ethanol liquid phase using Raman scattering" Chemical Physics Letters **318**(2000): 471-475.

7 Three-Dimensional (3D) Substrates and Superhigh Applied Potential Deposition of DLC Films by Liquid Electrochemical Technique

7.1 3D Substrates Deposition

DLC films have widespread applications in the fields of optical windows, magnetic storage disks, car parts, biomedical coatings and micro-electromechanical systems (MEM) because of their excellent physical and chemical properties, such as high mechanical hardness, low friction coefficient, wear-resistance and chemical inertness [A.A. Voevodin 1997; Y. Lifshitz 1999; J. Robertson 2002; N. Paik 2005; H.B. Guo 2008]. Considering the request of industrial applications, it is necessary to investigate a method which could deposit DLC films on three-dimensional (3D) substrates. Besides the conventional vapor deposition methods, liquid electrochemical technique owns the possibility to carry out DLC films deposition on complex substrates due to the advantage of electrochemistry reaction. However, the reported liquid phase deposition of DLC films mainly concentrates on planar substrates, made of silicon, metal or conductive glass [V.P. Novikov 1997; H. Kiyota 1999; K. Cai 1999; Z. Sun 1999; Z. Sun 2000; D. Guo 2001]. The latest work showed that DLC films were deposited on both sides of an aluminum substrate based on the electrolysis of N,N-dimethylformamide solution [R.S. Li 2009]. Publication about 3D deposition of DLC films by liquid electrochemical technique is rare to see. The aim of this section is to deposit DLC films on 3D stainless steel substrates using liquid phase deposition.

7.1.1 Experimental Details

The 3D substrates were carried into execution with the simultaneously aligned horizontal and vertical stainless steel substrates. The schematic diagram of our deposition system with 3D substrate is displayed in Fig. 7.1. Compared with several deposition systems reported before [Y. Namba 1992; H. Wang 1996; H.Q. Jiang 2004; R.S. Li 2009], the one used in our work owns the advantage of simultaneous import of horizontally and vertically aligned substrates. Thus, the 3D deposition of DLC films could be therefore carried out by liquid electrochemical technique.

The anode electrode was made of graphite, and the distance between anode and horizontal substrate was fixed at 6 mm. The horizontally aligned substrate was a stainless steel wafer with the dimensions of 13×12×0.5 mm^3. While the vertically aligned stainless steel rods in the diameter of 3 mm were mounted around the graphite

anode with a distance of 24.5 mm to the graphite electrode. The tip of each vertical substrate was immersed 30 mm below the surface of the organic solution. In order to investigate the film structure along the vertically aligned substrate, six points with the same distance of 5 mm between each other are chosen, No.1 to No.6 are orderly from the surface of organic solution to inside. No.1 to No.4 were located above the horizontally aligned substrate, No.5 and No.6 were below.

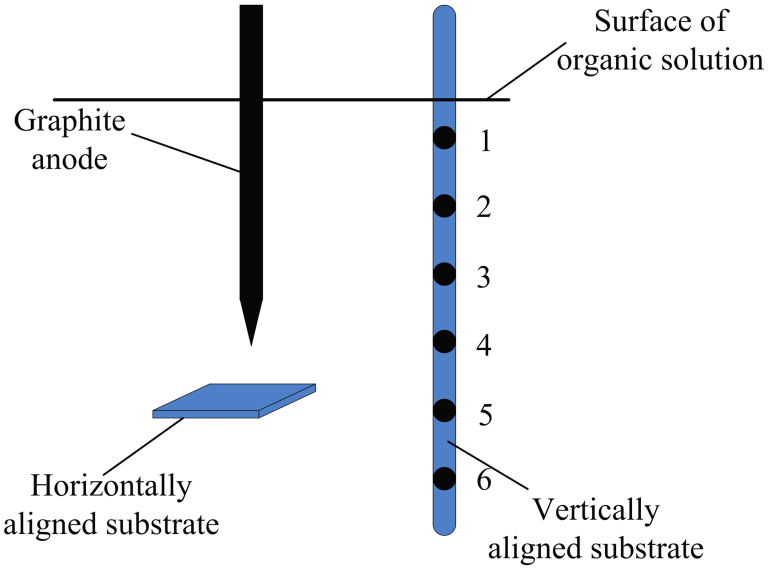

Fig. 7.1 Schematic diagram of the 3D substrate in the liquid electrochemical deposition system.

The experimental setup and deposition procedure were described in chapter 4. The electrolyte, applied potential and the deposition time were analytically pure 2-propanol, 1000 V (frequency 10 kHz, duty cycle 50%) and 2 h, respectively.

The surface morphology of the films deposited was measured by scanning electron microscopy (SEM) using Quanta 400 FEG. Also the cross sections of the films deposited on the horizontally aligned stainless steel substrates were taken to measure the film thickness. The microstructure of the DLC films was investigated using a micro-Raman system Jobin Yvon with a laser source wavelength of 514.532 nm.

7.1.2 Results

7.1.2.1 Horizontally Aligned Substrate

Films were deposited on the horizontally aligned stainless steel substrate from analytically pure 2-propanol under the applied potential of 1000 V in two hours. The films deposited appeared grey in color. The horizontally aligned stainless steel substrate was covered with grey film after deposition. The film growth rate was calculated with the help of SEM film cross sections measurement and deposition time, approximately 650 nm/ h. Fig. 7.2 shows a typical SEM image (a) of the films deposited on the horizontally aligned stainless steel substrates and the corresponding Raman spectrum (b). The film deposited on the horizontally aligned substrate is continuous and smooth. It consists of small and compact ball-like grains in the diameter of about 300 nm.

Raman spectroscopy is one of the most widely used techniques to investigate the state of carbon in detail, because of its sensitivity to changes in translation symmetry. Diamond has a single Raman-active first-order phonon mode, which appears as a single sharp line at 1332 cm^{-1}. Graphite also has only one high-frequency first-order Raman line at 1580 cm^{-1} seen in the spectra of single crystals which refer to the G peak. For the disorder or fine graphite crystallites with small particle size, another peak appears at lower wave numbers around 1355 cm^{-1}, referred to the D peak [A.C. Ferrari 2000].

The films covering the horizontally aligned substrate have quite similar Raman spectra. The typical Raman spectrum in Fig. 7.2b confirms that DLC films were obtained, with two broad peaks around 1335 cm^{-1} and 1595 cm^{-1}. These two peaks are related to D peak at 1355 cm^{-1} and G peak at 1580 cm^{-1}, respectively, indicating that some sp^2 amorphous carbon phases exist in the films deposited [R.J. Nemanich 1988; D.S. Knight 1989; W.A. Yarbrough 1990]. The Raman spectrum is further Lorenz fitted, and the I(D)/I(G) ratio is 1.13. As will be shown later, the sp^3 content can be estimated from this ratio.

The analysis of SEM and Raman measurement suggest that the whole film deposited on the horizontally aligned substrate owned uniform morphology and microstructure.

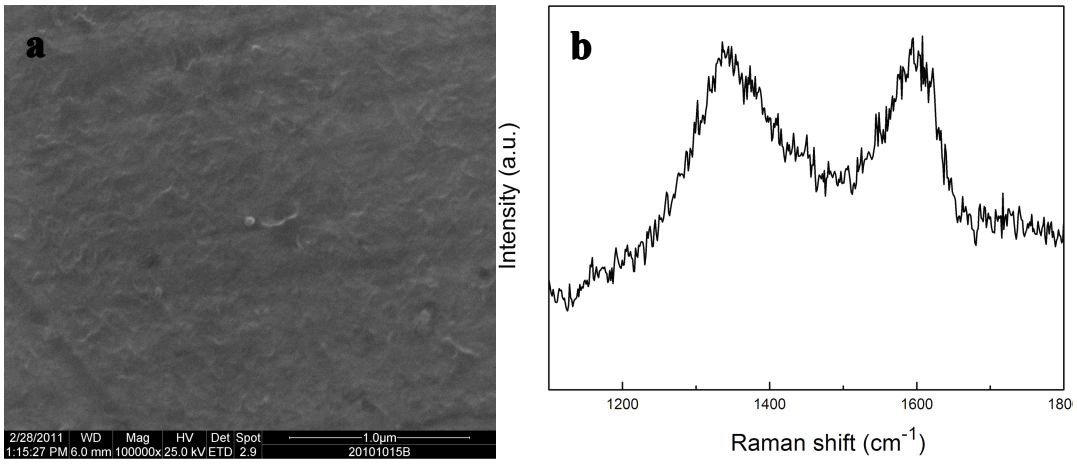

Fig. 7.2 SEM image (a) and Raman spectrum (b) of DLC films deposited on the horizontally aligned substrate.

7.1.2.2 Vertically Aligned Substrate

After deposition, films could also be observed on part of vertically aligned stainless steel substrate which was located inside the organic solution. Also the structure of the films at each point was investigated by Raman. The Raman results confirmed that typical DLC films were deposited on the vertically aligned substrates in the liquid electrochemical deposition system.

On the one hand, uniform DLC films were deposited at the same depth inside the organic solution because the same spectra were obtained at the same cross section on the vertically aligned substrate. On the other hand, Raman spectra appear different with the position along the vertically aligned substrates.

Typical Raman spectra at each chosen position on the vertically aligned stainless steel substrates are displayed in Fig. 7.3. The Raman spectra of the films deposited on the vertically aligned substrates appear different with its depth inside the organic solution. The intensity decreases when the positions go inside the solution. When the position goes below the horizontally aligned substrate, the DLC signal is becoming weak, even no significant carbon signal could be found at No. 6. Nevertheless, the Raman spectra (No.1-No.5) have two broad peaks which are corresponding to D peak and G peak, respectively.

Although all the Raman spectra have two peaks, the different center positions and intensities of D peak and G peak, considering the film structures may be different. For analysis, the region from 1150 cm^{-1} to 1800 cm^{-1} in all the Raman spectra were carefully Lorenz fitted on a linear background in order to determine the intensities, peak positions, and line widths of the individual Raman features. The relationship

between the positions and Raman fitting information is displayed in Fig. 7.4. The intensity of the Raman peaks suggests that at position 1 the films of the most thickness are obtained, this has to be investigated in more detail.

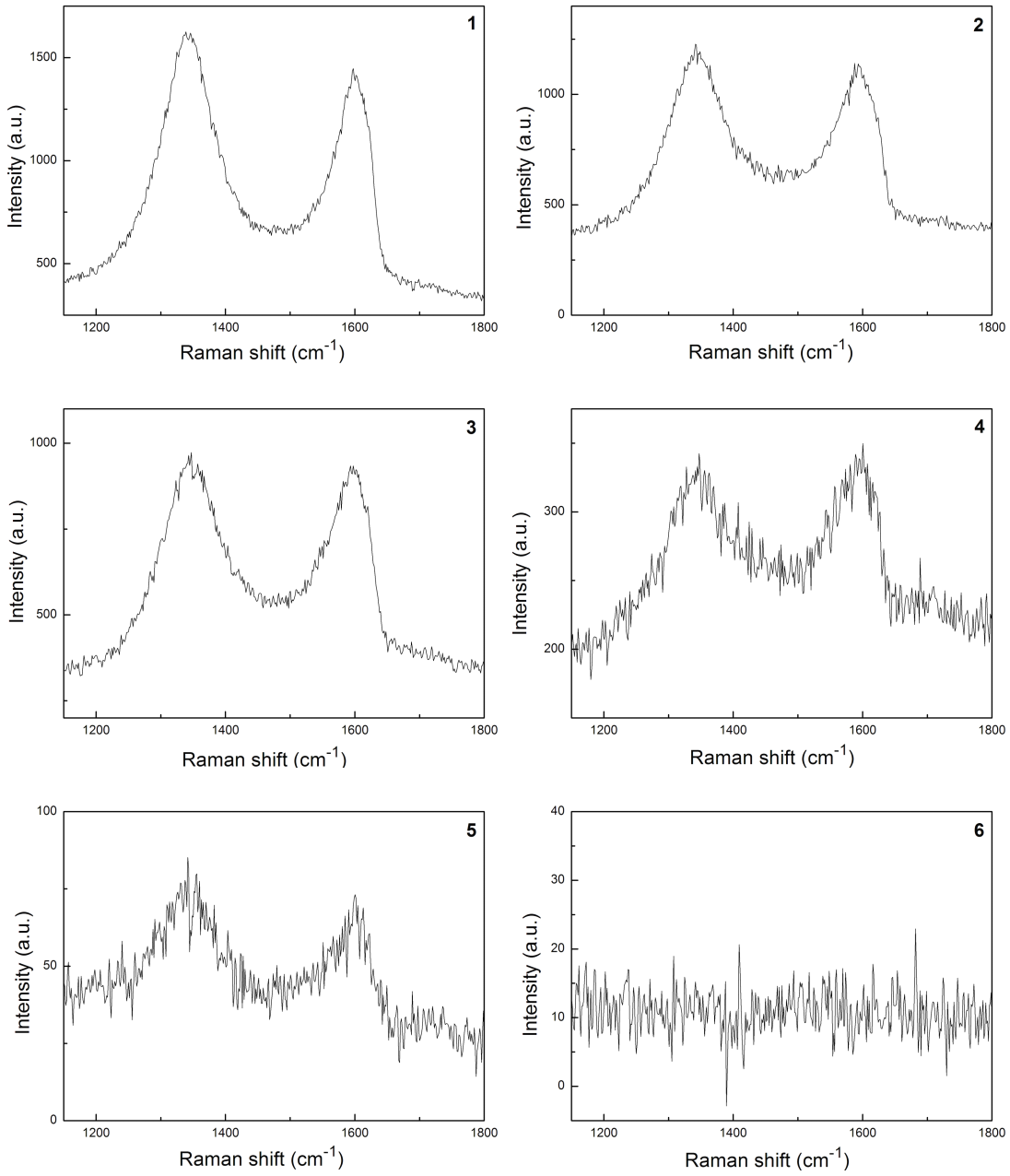

Fig. 7.3 Raman spectra of DLC films deposited on different positions of the vertically aligned substrate, the numbers are corresponding to the points in Fig. 7.1 on the vertically aligned substrate.

The I(D)/I(G) ratio of each the spectrum is approximately in the region of 0.98-1.16. The I(D)/I(G) intensity ratio and the G band position obtained with Raman measurements are correlated with the sp^3/sp^2 ratio. In general, a lower intensity ration can be interpreted as corresponding to higher sp^3 content [C. Casiraghi 2005; G. Irmer 2005].

The I(D)/I(G) ratio first decreases and then increases, the G-position down shifts first and then up shifts, both of which have the minimum at No.4. It seems that No.4 is a critical position which is the lowest chosen point above the horizontally aligned substrate. The I(D)/I(G) intensity ratio and the G peak position obtained from Raman measurements are correlated with the sp^3/sp^2 ratio.

The error bars for I(D)/I(G) in Fig. 7.4 correspond to σ/I(D), and σ is given by $\sigma = \sqrt{\frac{\sum_{i=1}^{N}(x_{im} - x_{ic})^2}{N}}$, where x_{im} is the measured Raman intensity on a linear background, x_{ic} is the Raman intensity after fitting on a linear background.

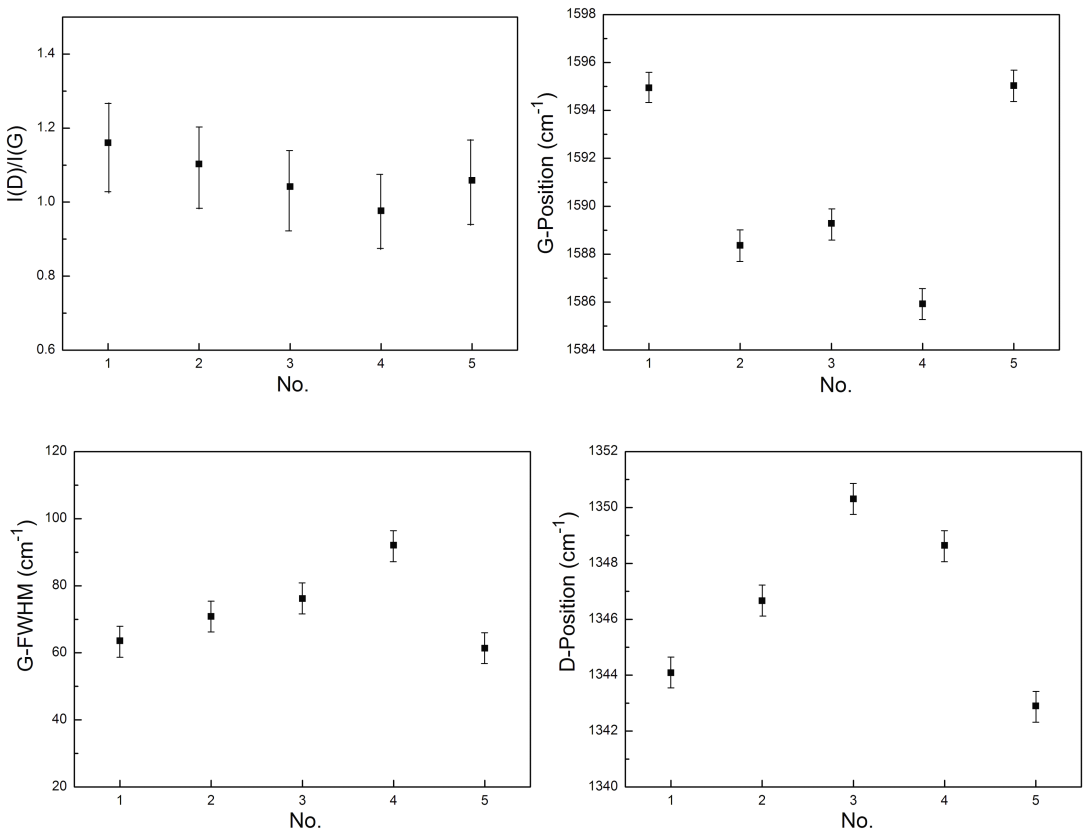

Fig. 7.4 Correlation between Raman fitting information and the DLC films deposited on different positions of the vertically aligned substrate.

To give a quantitative analysis of the sp^3 content in the DLC films, the parameters determined from Raman measurements of a:C-H films for λ=514 excitations can be introduced as a reference. Fig. 7.5a shows the correlation between G position and sp^3 content, I(D)/I(G) ratio and sp^3 content, respectively, from A.C. Ferrari [A.C. Ferrari 2000], the experimental data are exponential fitted and presented in Fig. 7.5b. The G peak position and I(D)/I(G) ratio of the DLC films at various positions are placed on the "G peak position-sp^3 content" and "I(D)/I(G) ratio-sp^3 content" curves.

The corresponding sp^3 content in each DLC film deposited can be derived. As shown in Fig. 7.5b, all the sp^3 content of the four DLC films drawn from G position are about 20% lower than those drawn from I(D)/I(G) ratio. A. Poukhovoi [A. Poukhovoi 2011] compared the calculation of sp^3 content in a:C-H films using Raman and FTIR. The results from "I(D)/I(G) ratio-sp^3 content" and FTIR matched very well with each other, however, the sp^3 content calculated from G position is always lower, 10-20% depending on the deposition parameters. So here the bonded sp^3 content gained from the I(D)/I(G) ratio is credible, in the range of 37-40%. Fig. 7.6 shows the sp^3 content at each position. The sp^3 content first decreases and then increases, with the maximum at No. 4. Thus, structure of the films deposited on the vertically aligned substrate is not uniform, changing with the location.

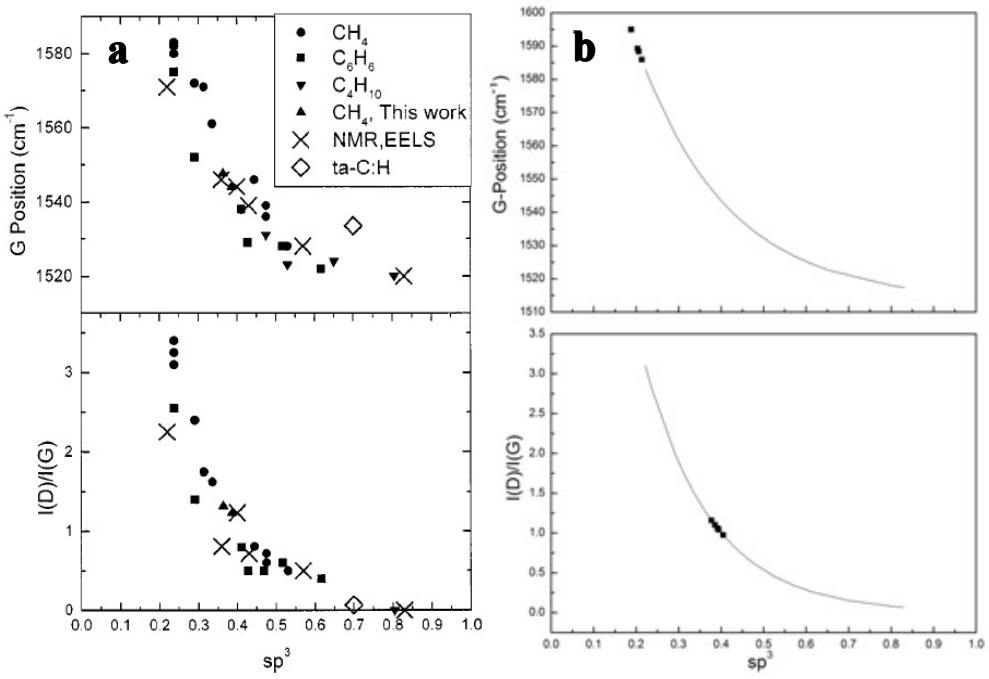

Fig. 7.5 Correlation between sp^3 content and parameters determined from Raman measurements of a:C-H films for 514 excitations (a: from A.C. Ferrari [A.C. Ferrari 2000]; b: fitting of the experimental data in Fig. 5a and the presentation of G peak position and I(D)/I(G) ratio of the DLC films deposited in this work on the exponential fitted curves).

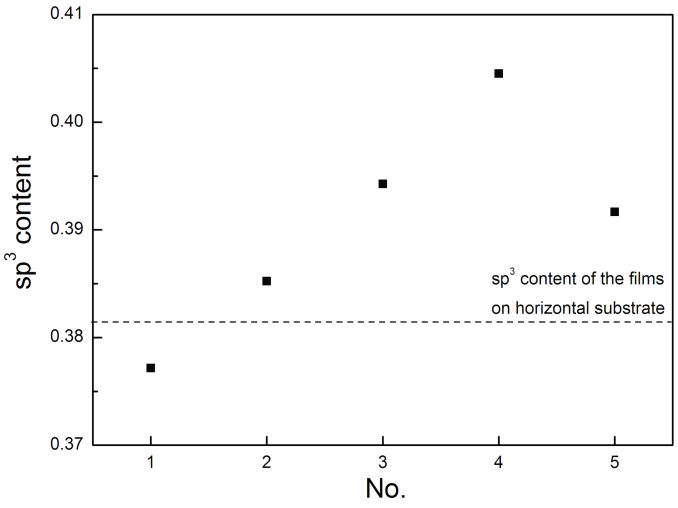

Fig. 7.6 Correlation between the calculated sp^3 content and the DLC films deposited on different places of vertically aligned substrate, with the comparison of the calculated sp^3 content of the DLC films deposited on the horizontal substrate.

7.1.3 Discussions

The simultaneous import of horizontally and vertically aligned substrates into liquid electrochemical deposition system is a simple model of 3D substrates. Thus it is possible to deposit DLC films on 3D or other complex conductive substrates by liquid electrochemical technique. This is favored for the industrial applications of DLC films and the liquid deposition technique.

Raman analysis suggested that the film deposited on the horizontally aligned substrate owned uniform microstructure. However, the films deposited on the vertically aligned substrates appeared slight difference in microstructure, depending on the position inside the organic solution. To achieve uniform DLC films on 3D substrates, other parameters should be investigated.

7.1.4 Conclusions

DLC films were simultaneously deposited on horizontally and vertically aligned stainless steel substrates by electrolysis of analytically pure 2-propanol at low temperature (60ºC). It is confirmed that liquid electrochemical technique is feasible to carry out DLC films deposition on 3D conductive substrates.

7.2 Superhigh Applied Potential Deposition of DLC Films by Liquid Electrochemical Technique

Liquid electrochemical deposition of DLC films was first published by Namba [Y. Namba 1992]. The applied potential is an important electrical parameter in liquid electrochemical method and has influence on the DLC films structure and morphology [T. Suzuki 1995; H. Wang 1996; K. Cai 1999; M.C. Tosin 1999; W.L. He 2005]. The results suggested that high applied potential could improve the formation of sp^3 carbon in the DLC films deposited by electrolysis of methanol [H.S. Zhu 2003; X.B. Yan 2004]. However, the reported applied potentials are mostly below 2000 V, the investigation of superhigh voltage deposition is rare to see. In this section, superhigh applied potential is introduced into the liquid electrochemical deposition system to provide energy for DLC films growth. On the one hand, the aim of this work is to test the possibility of DLC films deposition by liquid electrochemical technique under the superhigh applied potential which has never been attempted. On the other hand, the influence of increasing applied potential on the deposition of DLC films is investigated, both the deposition process and resulting films.

7.2.1 Experimental Details

The experimental setup and deposition procedure were described in chapter 4. The anode material, substrate and anode-substrate distance were graphite, silicon wafer ($13\times12\times0.5mm^3$) and 6 mm, respectively. The applied potential was set to 5 kV, 10 kV, 15 kV and 20 kV, respectively. The frequency was 50 Hz and each plus lasted for 0.18 ns.

After deposition, microstructure of the resulting samples was investigated using a micro-Raman system Jobin Yvon with a laser source wavelength of 514.532 nm.

7.2.2 Results

7.2.2.1 Current and Voltage

Current and voltage are both critical parameters in any electrochemical reaction. The applied potential was kept constant during each deposition process. The voltage and current were measured and recorded. Fig. 7.7 shows the relationship between the logarithm of current and various applied potentials. The current in the circuit was measured at the beginning of the experiment because the current will change with the

time. The current is proportional to the applied potential. The logarithm of current increased linear with the applied potential increased from 5 kV to 20 kV.

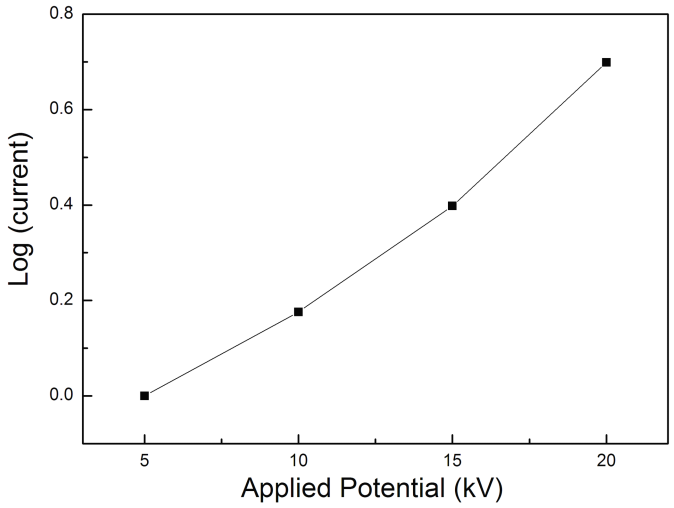

Fig. 7.7 The relationship between the logarithm of current and the applied potential.

7.2.2.2 Raman Analysis

Raman spectroscopy is a widely used and non-destructive way in the classification and characterization of carbon phase materials, and also available for the DLC films bonding structure investigation [J. Robertson 1986; J. Robertson 1991; J. Robertson 2002]. Raman was therefore used to measure the resulting samples. When the applied potential was set to 5 kV, 10 kV and 15 kV, the Si substrates were all not covered by continuous films, however, some islands were observed with the help of microscope attached to the Raman facility. These islands were measured by Raman spectroscope, comparison of the Raman spectra is displayed in Fig. 7.8.

When the applied potential was 5 kV, two sharp peaks around 1350 cm^{-1} and 1572 cm^{-1} appear in the Raman spectrum, respectively. These two peaks are related to D peak at 1355 cm^{-1} and G peak at 1580 cm^{-1}, indicating that some sp^2 amorphous carbon phases exist in the film [R.J. Nemanich 1988; D.S. Knight 1989; W.A. Yarbrough 1990]. The Raman was further Lorenz fitted, and the I(D)/I(G) ratio is 0.54. While compared with the DLC films deposited under the applied potential of 1000 V, the I(D)/I(G) ratio is 0.95. The I(D)/I(G) intensity ratio and the G band position obtained with Raman measurements are correlated with the sp^3/sp^2 ratio. In general, a lower intensity ration can be interpreted as corresponding to higher sp^3 content [G. Irmer 2005]. Thus the DLC structure deposited by the applied potential of 5 kV has more sp^3 carbon.

Several peaks at 1337 cm^{-1}, 1456 cm^{-1} and 1600 cm^{-1} appear in the Raman spectra of the deposited island when the applied potential was 10 kV. The peak at 1337 cm^{-1} is D peak and 1600 cm^{-1} is G peak. There are three peaks in the Raman spectrum when the applied potential was set to 15 kV. The peaks centered at 1360 cm^{-1}, 1440 cm^{-1} and 1585 cm^{-1}. The peak at 1360 cm^{-1} is D peak and 1585 cm^{-1} is G peak. When the applied potential was fixed to 10 kV and 15 kV, there was another peak besides D and G peak. The peaks around 1440 cm^{-1} and 1470 cm^{-1} which may be assigned to the symmetrical deformation frequency of C-CH with sp^2 hybridized C-C bonding [Y.F. Lu 1999] or a sp^3-bonded diamond precursor phase [Y.F. Lu 2000].

However, no islands could be found on the Si substrate when the applied potential was 20 kV. Nevertheless, the sample was measured by Raman. The result suggests that no obvious carbon structure was deposited on the substrate, as shown in Fig. 7.8 for comparison.

Over all, the peaks become weak with the increase of the applied potential. This means that lower applied potential such as 5 kV is favorable for carbon films formation.

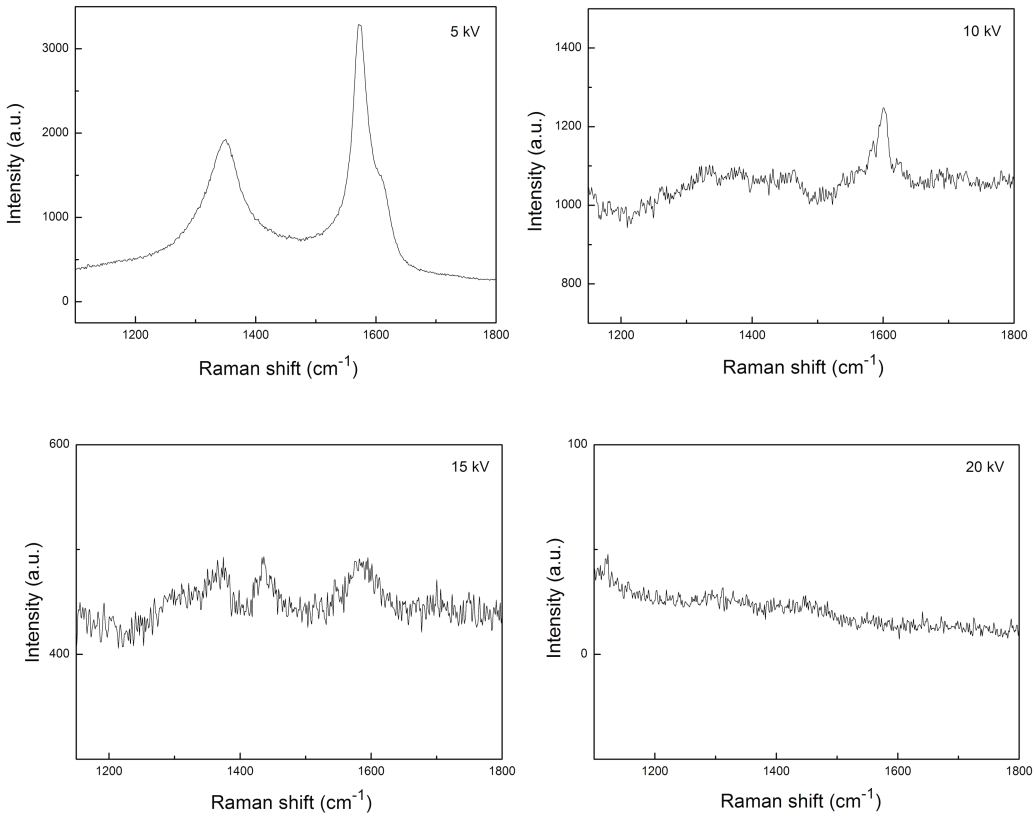

Fig. 7.8 Raman spectra of the films deposited under various applied potentials.

For the samples deposited under 5 kV, 10 kV and 15 kV, the places without islands deposition were also measured by Raman, it has been confirmed that no carbon film is deposited there. A typical Raman spectroscopy is displayed in Fig. 7.9. This means that there is no continuous DLC film covering the whole substrate, only DLC structure islands were obtained by these superhigh applied potential depositions.

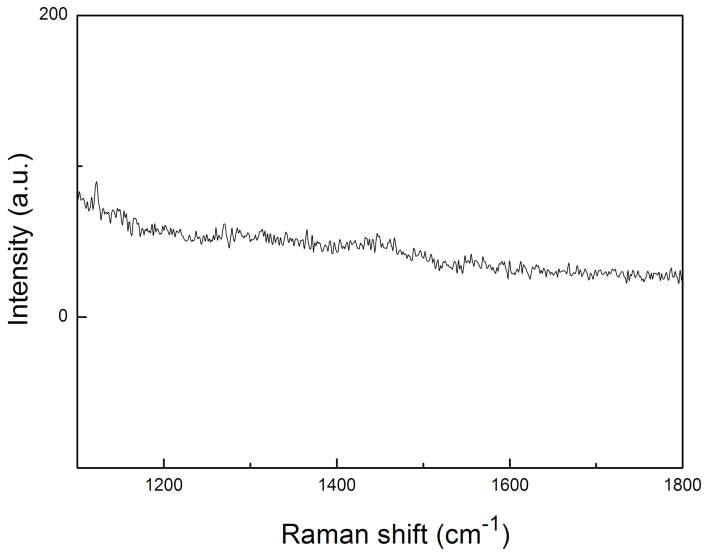

Fig. 7.9 A typical Raman spectrum of the places on the Si substrates without any deposited islands.

7.2.3 Discussions

The generator can only deliver pulses which last for 500 ns each one in this work, so the effective deposition time during the 2 h is only 0.18 s (500 ns $\times 50 \times 10^{-9} \times 60$ s/min $\times 60$ min/h $\times 2$ h). It was really a very short deposition time although very high voltage was applied to the deposition system. That is the reason why the DLC structure was only obtained on some islands, not a continuous DLC films covering the whole substrate.

Compared with the low voltage deposition of DLC films described in section 7.1, continuous film with the thickness of 330 nm was successfully deposited under the applied potential of 1000 V (frequency 10 kHz, duty cycle 50%). All the other parameters are the same as the superhigh applied potential deposition: the electrolyte and deposition time were analytically pure 2-propanol and 2 h, the anode material, substrate and anode-substrate distance were graphite, silicon wafer and 6 mm, respectively. The effective deposition time under the low applied potential lasted for 1 h, it was as long as 20000 times of the effective time under the superhigh applied

potential. Although more energy can be introduced into the liquid electrochemical deposition system, deposition time is a key parameter which can obviously affect the film formation. If there is enough time, more islands of DLC structure can be deposited and the islands can join together to form a continuous film. So it is believed that continuous DLC films can be deposited under superhigh applied potential if the deposition time is long enough.

Although DLC films can be deposited by liquid electrochemical technique under superhigh applied potential, its disadvantages can not be ignored. For example, superhigh applied potential deposition of course requires more safety precautions and more costly than low voltage deposition. Anyway, lower applied potential is preferred if DLC films of similar properties can be obtained, especially in the industrial application.

7.2.4 Conclusions

DLC films can be deposited on Si substrate by liquid electrochemical technique under superhigh applied potential. Applied potential has influence on the deposition of DLC films by liquid electrochemical technique. In this work, DLC film of the most sp^3 carbon was deposited when the applied potential was set to 5 kV. However, it was not a continuous DLC film because the deposition time was too short. The films structure changed with the increase of applied potential. There was no DLC structure deposited when the applied potential was increased to 20 kV.

References

A. Poukhovoi (2011). Abscheidung von amorphen wasserstoffhaltigen Kohlenstoffschichten mittels neuartiger hybrider RP-Plasma Quelle und deren spektroskopische Charakterisierung. Physics. Duisburg, University Duisburg Essen. **Doctor:** 142.

A.A. Voevodin, M.S. Donley, J.S. Zabinski. "Pulsed laser deposition of diamond-like carbon wear protective coatings: a review" Surface and Coatings Technology **92**(1997): 42-49.

A.C. Ferrari, J. Robertson. "Interpretation of Raman spectra of disordered and amorphous carbon" Physical Review B **61**(2000): 14095-14107.

C. Casiraghi, A.C. Ferrari, J. Robertson. "Raman spectroscopy of hydrogenated amorphous carbons" Physical Review B **72**(2005): 085401-1-14.

D. Guo, K. Cai, L.T. Li, Y. Huang, Z.L. Gui, H.S. Zhu. "Evaluation of diamond-like carbon films electrodeposited on an Al substrate from the liquid phase with pulse-modulated power" Carbon **39**(2001): 1395-1398.

D.S. Knight, W.B. White. "Characterization of diamond films by Raman spectroscopy" Materials Research Society **4**(1989): 385-393.

G. Irmer, A. Dorner-Reisel. "Micro-Raman studies on DLC coatings" Advanced Engineering Materials **7**(2005): 694-705.

H. Kiyota, H. Araki, H. Kobayashi, T. Shiga, K. Kitaguchi, M. Iida, H. Wang, T. Miyo, T. Takida, T. Kurosu, K. Inoue, I. Saito, M. Nishitani-Gamo, I. Sakaguchi, T. Ando, . "Electron field emission from diamond-like carbon films deposited by electrolysis of methanol liquid" Applied Physics Letters **75**(1999): 2331-2333.

H. Wang, M.R. Shen, Z.Y. Ning, C. Ye, C.B. Cao, H.Y. Dang, H.S. Zhu. "Deposition of diamond-like carbon films by electrolysis of methanol solution" Applied Physics Letters **69**(1996): 1074-1076.

H.B. Guo, Y. Qi, X.D. Li. "Predicting the hydrogen pressure to achieve ultralow friction at diamond and diamondlike carbon surfaces from first principles" Applied Physics Letters **92**(2008): 241921-2419213

H.Q. Jiang, Z.J. Zhang, T. Xu, W.M. Liu. "Research progress on the preparation of diamond-like carbon film by the liquid phase electrodeposition technique" Surface Technology **33**(2004): 4-6.

H.S. Zhu, J.T. Jiu, Q. Fu, H. Wang, C.B. Cao. "Aroused problems in the deposition of diamond-like carbon films by using the liquid phase electrodeposition technique" Journal of Materials Science **38**(2003): 141-145.

J. Robertson. "Amorphous carbon" Advances in Physics **35**(1986): 317-374.

J. Robertson. "Hard amorphous (Diamond-Like) carbons" Solid State Chemistry **21**(1991): 199-333.

J. Robertson. "Diamond-like amorphous carbon" Materials Science and Engineering R **37**(2002): 129-281.

K. Cai, C.B. Cao, H.S. Zhu. "Deposition of diamond-like carbon films on aluminum in the liquid phase by an electrochemical method" Carbon **37**(1999): 1860-1862.

K. Cai , C.B. Cao, J.T. Jiu, Q. Fu , H. Wang, H.S. Zhu. "DLC films deposited on conductive glass in DMF solution" Chinese Journal of Applied Chemistry **16**(1999): 80-82.

M.C. Tosin, A.C. Peterlevitz, G.I. Surdutovich, V. Baranauskas. "Deposition of diamond and diamond-like carbon nuclei by electrolysis of alcohol solutions" Applied Surface Science

144-145(1999): 260-264.

N. Paik. "Field emission characteristics of Diamond-like Carbon (DLC) films prepared using a Magnetron Sputter-type Negative Ion Source (MSNIS)" Diamond and Related Materials **14**(2005): 1556-1561.

R.J. Nemanich, J.T. Glass, G. Lucovsky, R.E. Shroder. "Raman scattering characterization of carbon bonding in diamond and diamondlike thin films" Journal of Vacuum Science & Technology A: Vacuum, Surfaces, and Films **6**(1988): 1783-1787.

R.S. Li, M. Zhou, X. J. Pan, Z.X. Zhang, B.A. Lu, T. Wang, E.Q. Xie. "Simultaneous deposition of diamondlike carbon films on both surfaces of aluminum substrate by electrochemical technique" Journal of Applied Physics **105**(2009): 066107-1-3.

T. Suzuki, Y. Manita, T. Yamazaki, S. Wada, T. Noma. "Deposition of carbon films by electrolysis of a water-ethylene glycol solution" Journal of Materials Science **30**(1995): 2067-2069.

V.P. Novikov, V.P. Dymont. "Synthesis of diamondlike films by an electrochemical method at atmospheric pressure and low temperature" Applied Physics Letters **70**(1997): 200-202.

W.A. Yarbrough, R. Messier. "Current issues and problems in the chemical vapor deposition of diamond" Science **247**(1990): 688-696.

W.L. He, R. Yu, H. Wang, H. Yan. "Electrodeposition mechanism of hydrogen-free diamond-like carbon films from organic electrolytes" Carbon **43**(2005): 2000-2006.

X.B. Yan, T. Xu, G. Chen, H.W. Liu, S.R. Yang. "Effect of deposition voltage on the microstructure of electrochemically deposited hydrogenated amorphous carbon films" Carbon **42**(2004): 3103-3108.

Y. Lifshitz. "Diamond-like carbon-present status " Diamond and Related Materials **8**(1999): 1659-1676.

Y. Namba. "Attempt to grow diamond phase carbon films from an organic solution" Journal of Vacuum Science Technology A **10**(1992): 3368-3370.

Y.F. Lu, S.M. Huang, C.H.A. Huan, X.F. Luo. "Amorphous hydrogenated carbon synthesized by pulsed laser deposition from cyclohexane" Applied Physics A **68**(1999): 647-651.

Y.F. Lu, S.M. Huang, Z. Sun. "Raman spectroscopy of phenylcarbyne polymer films under pulsed green laser irradiation" Jouranl of Applied Physics **87**(2000): 945-951.

Z. Sun, X. Wang, Y. Sun. "Diamond film growth on the carbon films from electrolysis of ethanol" Materials Science and Engineering B **65**(1999): 194-198.

Z. Sun, Y. Sun, X. Wang. "Investigation of phases in the carbon films deposited by electrolysis of ethanol liquid phase using Raman scattering" Chemical Physics Letters **318**(2000): 471-475.

8 Further Attempts and Outlook

8.1 Liquid Plasma and DLC Films Liquid Electrochemical Deposition

8.1.1 Plasma

Plasma is a quasineutral gas of charged and neutral particles which exhibits collective behavior. Plasma is different from gas because plasma contains charged particles. The charges can easily move and thus cause local concentration of positive or negative charge. The difference of electric concentration can generate electric field, and then current and magnetic fields [F.F. Chen 1974]. Plasma can conduct electricity is because of the movement and collision of the charged particles.

Plasma is used widely in many fields of research, technology and industry, including thin film technology. For example, DLC films can be deposited by plasma-enhanced chemical vapor deposition (PECVD) [J. Robertson 2002].

8.1.2 Liquid Plasma

Plasma in and in-contact with liquid has received a lot of interest because of their considerable environmental and medical applications, such as in water treatment [B.R. Locke 2006], a plasma scalpel for surgery [K.R. Stalder 2005] and electrical discharge machining [E.C. Jameson 2001].

There are many related research articles published within recent years on methods and processes for plasma formation in and in contact with liquids [P. Bruggeman 2009]. Plasma formation on non-thermal atmospheric or high pressure discharges in and in contact with liquids is always discussed in three main types, as shown in Fig. 8.1.

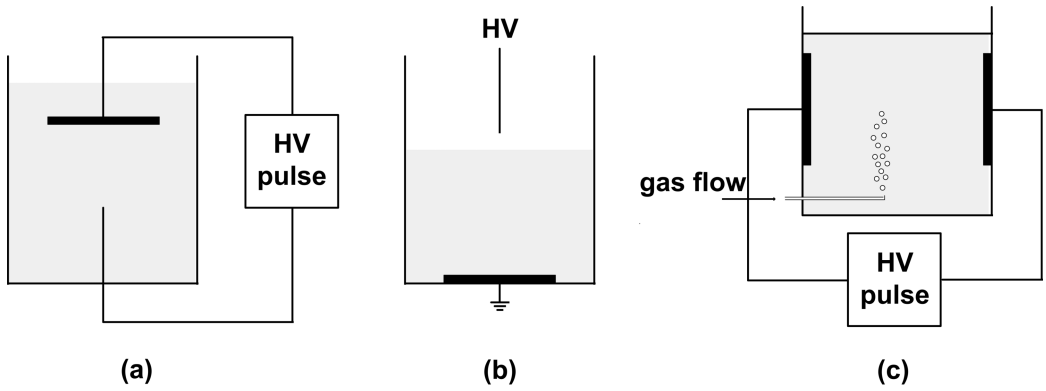

Fig. 8.1 Typical electrode configurations for the three different types of discharges in and in contact with liquids (a: Direct liquid phase discharges; b: Discharges in the gas phase with liquid electrode; c: Discharges in bubbles in liquids).

8.1.3 Investigation of Liquid Plasma Generation during DLC Films Liquid Electrochemical Deposition

Plasma has been generated in organic liquids or pure water with the help of microwave (MW) or radio-frequency waves (RF). And these techniques have been applied to the field of carbon materials deposition, such as deposition of diamond, diamond-like carbon, and silicon carbide to a substrate by irradiating microwave (MW) or radio-frequency waves (RF) in liquid [S. Nomura 2006; H. Toyota 2008].

Liquid electrochemical deposition of DLC films utilizes the reactions between the electrode and substrate which are both immerged into the organic solution. There is discharge between the electrode and substrate when the reaction is running which is the basic of plasma generation. However, the plasma generation in this field has never been investigated. With here the investigation of plasma generation during the process of DLC films deposition by liquid electrochemical technique is reported.

8.1.3.1 Experimental Details

In our deposition system, a graphite anode was used as the anode electrode and p-type (100) silicon substrates with the dimensions of $13\times12\times0.5mm^3$ were mounted on the negative electrode. The distance between anode and substrate was fixed at 6 mm. The distance between the needle tips of graphite anode and fiber was 2 mm. Prior to the deposition, the substrates were polished by 0.1 μm diamond paste and then ultrasonically cleaned in 2-propanol and deionized water for 10 min, respectively, and then dried with pure nitrogen. The applied potential and the electrolyte were 1000 V

(frequency 4.2 kHz, duty cycle 50%) and methanol/deionized water solution in the volume ratio of 1:1 and 5 h, respectively.

The Optical Emission Spectroscopy (OES) for liquid plasma detection was introduced in our liquid electrochemical deposition system. The spectra in this work were obtained by a Jobin Yvon HR 460 spectrometer which was coupled through an optical fiber. The fiber was inserted into the deposition experimental setup with the protection of a quartz tube, as shown in Fig. 8.2.

The data acquisition system included a current probe, a voltage probe, an oscillograph and a computer. Testec High Voltage Probe TT-HVP 15HF was used to measure the voltage during deposition process, while P6022 Current Probe was used to measure the current at the same time. The real time voltage and current were simultaneously recorded by the TDS 2012 two-channel digital storage oscilloscope. The dependence of voltage and current on time was recorded by the computer.

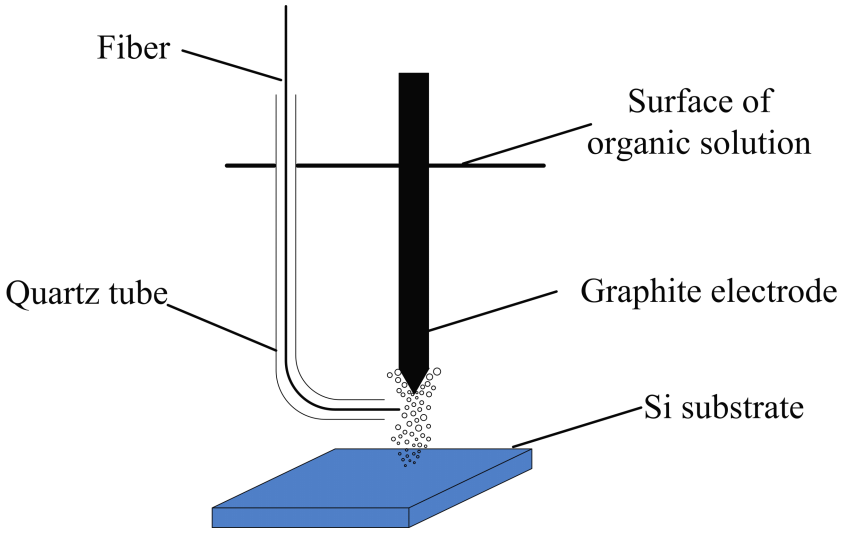

Fig. 8.2 Schematic diagram of the construction of liquid electrochemical deposition system with liquid plasma detection facility in this work.

8.1.3.2 Results and Discussions

As soon as the voltage was applied to the deposition reactor, formation of a stream of bubbles could be distinctly seen by eyes. The bubbles formed at the tip of the electrode and near substrate, and a surrounding vapor layer may be formed near the tip of electrode and substrate. The existence of cavitation bubbles in the liquid is necessary for generating in-liquid plasma because the plasma is apparently generated inside bubbles or around the bubble boundary in the liquid. However, these bubbles

were not pre-bubbles like in other in-liquid plasma generation system reported before [S. Nomura 2006; H. Toyota 2008].

To analysis the discharge during the process of liquid electrochemical deposition of DLC films, the waveforms of the discharge current and voltage should be investigated. The current and voltage waveforms were measured simultaneously with the deposition process. Fig. 8.3a is a overview of the current and voltage waveforms, both of the waveforms appear similar in the nearby circle. The current suddenly goes down when the voltage breaks through, and this repeats in the next circle. This is quite similar with the waveforms of current and voltage when there is oxygen plasma generation [V. Puech 2008].

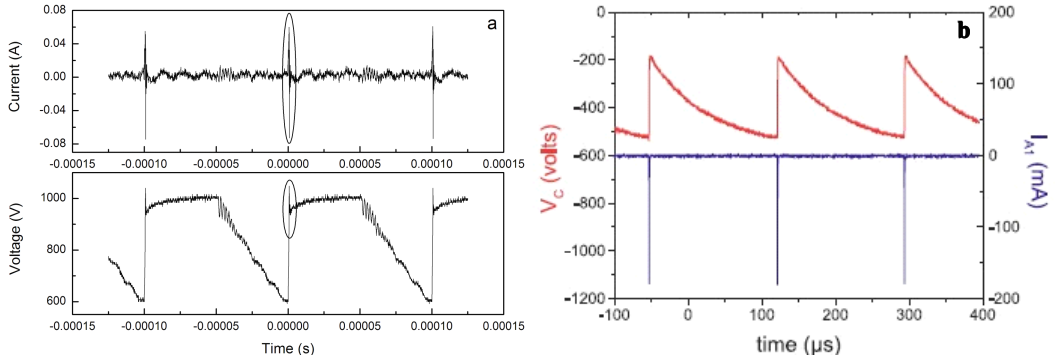

Fig. 8.3 Waveforms of the discharge current and voltage in this work and with oxygen plasma generation (b) [V. Puech 2008].

Consequently, the generation of in-liquid plasma is sufficiently expected in the process of liquid deposition of DLC films. The OES was used to examine the plasmas. The aim of our first detection was to catch any plasma signal, unfortunately, no plasma discharge was obtained at this moment. Nevertheless, it is a beginning in this research field. It only suggests no signals under this group of experimental parameters, not all the other deposition conditions.

Possibilities of this unsuccessful detection of liquid plasma during the process of liquid electrochemical deposition of DLC films are discussed as below.

(1) The optical fiber used was only for detecting luminous plasma. The known research work suggests that the discharges in and in contact with liquids generate intense UV radiation, shock waves and actives (OH, atomic oxygen, hydrogen peroxide, etc). Therefore, the detection facility for examining other plasma singles should be built in the further work.

(2) Water conductivity plays an important role in the generation of the corona discharge, this point is discussed in the formal publications.

On the one hand, at a low water conductivity ($\sigma < 10$ μS cm^{-1}) there is only a very narrow gap in the applied voltage to generate a stable discharge without sparking. On the other hand, at high water conductivity ($\sigma < 400$ μS cm^{-1}) streamers became short and the efficiency of radical production decreases [P. Bruggeman 2009]. The results from Sato et al [M. Sato 1996] using a pulse power supply with storage condenser, production of OH and O radicals was found to be more efficient at water conductivity in the range below 100 μS cm^{-1}, without any minimum reported.

However, the solution conductivity is below 1 μS cm^{-1} in our work which is obviously much lower than the conductivities reported before. It is therefore a blank area needs a lot of work to be filled in.

(3) The liquid molecular structure can have a significant effect on streamer propagation [P. Bruggeman 2009].

In our liquid deposition using organic chemicals (pure or water solution) as electrolyte, the possible excited particles are hydroxyl radicals (OH) and hydrogen atoms (H).

The ratio of the elemental components of carbon (C), hydrogen (H) and oxygen (O) is an important factor in the growth of diamonds. The component ratio of carbon, hydrogen, and oxygen has been the focus of attention in numerous experiments, and Bachmann diagram shows the conditions for the growth of diamond [P.K. Bachmann 1991].

So there is supposed to be a balance of both molecular structure and elemental components between the plasma generation and carbon films deposition.

(4) Parameters of applied potential are also very important, including the discharge and the pulse time. For example, the microsecond and nanosecond pulse time have different influence on the formation and movement of bubbles, and therefore affect the in liquid plasma.

There are of course some other reasons beyond our consideration. As a conclusion, the determination of liquid plasma in the process of DLC films liquid deposition is a completely new research field. The ideal aim of this work is to set up a model to describe the relationship between the deposition of DLC films and liquid plasma signal. A systematic connection between discharge current and voltage and structures and properties of DLC films may be included in this model to develop a better understanding for the deposition mechanism of liquid electrochemical technique. It is distinct that many questions and issues should to be resolved before the model is made.

8.2 Large Area Deposition of DLC Films by Liquid Electrochemical Technique

DLC films have been successfully deposited on Si substrate with the size of 13 mm × 12 mm × 0.5 mm in the former part of this dissertation. Additionally, a Si wafer with the size of 30 mm × 30 mm × 0.5 mm and a stainless steel substrate in the diameter of 32 mm were attempted as substrates, respectively. Fig. 8.4 shows the photos of substrates, Fig. 8.4a is silicon wafer and Fig. 8.4b is stainless steel substrate. The anode was made of graphite and the anode-substrate distance was 6 mm. The applied potential was set to 1000 V (frequency 10 kHz, duty cycle 50%). Analytically pure 2-propanol was used as electrolyte, and the deposition lasted for 2 h.

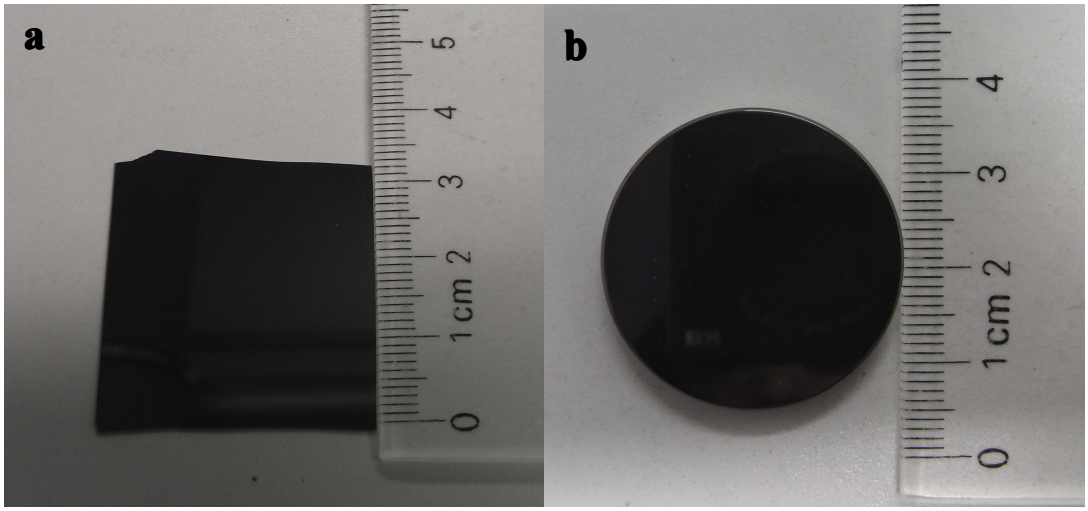

Fig. 8.4 Two photos of the substrates for single anode deposition (a: Si; b: stainless steel).

However, this deposition is achieved with single graphite anode which is a rod in diameter of 6 mm with a cone-shaped tip. To show that DLC films can be deposited on even larger substrate with a combination of anodes, a scalable multiple-anode device has been developed. The schematic diagrams of single anode and multiple-anode liquid electrochemical deposition systems are compared in Fig. 8.5. Fig. 8.6 shows the photos of the multiple-anode deposition facility (a) and the Si substrate used (b).

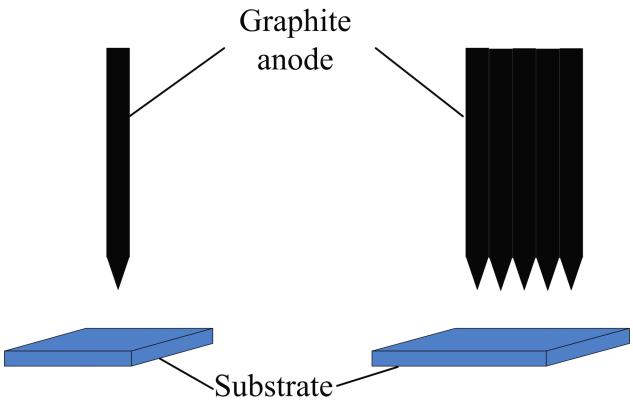

Fig. 8.5 Schematic diagrams of single anode and multiple-anodes liquid electrochemical deposition systems.

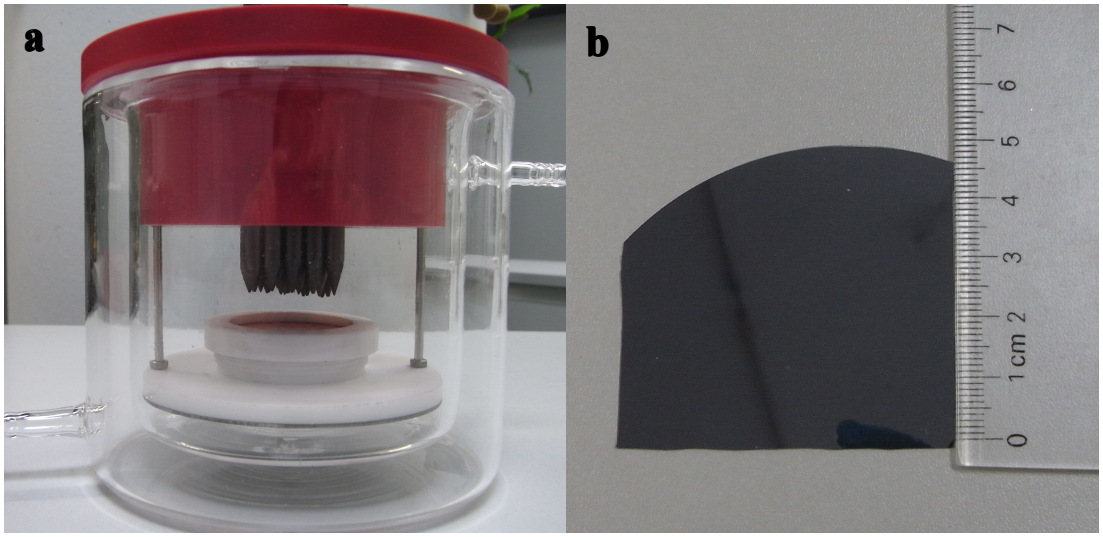

Fig. 8.6 Photos of the multiple-anode deposition facility and the Si substrate used

8.3 Mechanical Properties of DLC Films Deposited by Liquid Electrochemical Technique

Since typical DLC films have been deposited by liquid electrochemical technique, they have been characterized with respect to film morphology and microstructure. For technical applications additionally tribological properties of these DLC films should be measured, such as friction coefficient and nanohardness, and compared with the

typical DLC films deposited by vapor techniques. Optical applications are not possible because the substrate must be electrical conductor.

8.3.1 Friction Coefficient

Friction coefficient of the film deposited on the stainless steel was measured by a Wazau TRM 1000 tribometer. The force was 50 N, and the rate was 20 rotations per minute. The friction coefficient was around 0.085 (humidity was 54%, temperature 21.5°C), and no damage was observed with naked eyes after 200 rotations. This friction coefficient is in the usual range of amorphous hydrogenated carbon films. The humidity is pointed out because a strong dependence of friction coefficient on the relative humidity was found by K. Enke [K. Enke 1989].

The friction coefficient measurement shows that DLC films deposited by liquid electrochemical technique has low friction coefficient.

8.3.2 Nanohardness

Nanohardness of several DLC films deposited in this work was measured. The result and deposition parameters are shown in Table 8.1. Both of the films were deposited on Si substrates for 2 h, using graphite anode with an anode-substrate distance of 6 mm. It is suggested that hardness of the DLC films deposited by liquid electrochemical technique is in the range of a: C-H soft [P. Koidl 1990].

Table 8.1 Nanohardness measurement of two films deposited in this work.

No.	Nanohardness (Gpa)	Deposition Parameters
1	4.2	Pure 2-propanol, 1000 V
2	1.9	Acetone/deionized water(2:1), 900 V

In conclusion, the DLC films deposited by liquid electrochemical technique appear to possess similar friction coefficient and nanohardness with the films prepared by vapor deposition. Liquid electrochemical deposition is therefore an effective technique to prepare DLC films. In thin film technology, the films properties can be adjusted by the deposition parameters. So DLC films of various properties to match the requirements of application can be prepared by liquid phase deposition in the further work.

References

B.R. Locke, M. Sato, P. Sunka, M.R. Hoffmann, J.-S. Chang, . "Electrohydraulic discharge and nonthermal plasma for water treatment" Industrial and Engineering Chemistry Research **45**(2006): 882-905.

E.C. Jameson. "Electrical Discharge Machining". Michigan, Society of Manufacturing(2001).

F.F. Chen. "Introduction to plasma physics and controlled fusion, Volume 1: Plasma Physics". New York, Plenum Press(1974).

H. Toyota, S. Nomura, Y. Takahashi, S. Mukasa. "Submerged synthesis of diamond in liquid alcohol plasma" Diamond and Related Materials **17**(2008): 1902-1904.

J. Robertson. "Diamond-like amorphous carbon" Materials Science and Engineering R **37**(2002): 129-281.

K. Enke. "Amorphous hydrogenated carbon (a-C:H) for optical, electrical and mechanical applications" Materials Science Forum **52-53**(1989): 559-576.

K.R. Stalder, D.F. McMillen, J. Woloszko. "Electrosurgical plasmas" Journal of Physics D: Applied Physics **38**(2005): 1728-1738.

M. Sato, T. Ohgiyama, J.S. Clements. "Formation of chemical species and their effects on microorganisms using a pulsed high-voltage discharge in water" IEEE Transactions on Industry Applications **32**(1996): 106-112.

P. Bruggeman, C. Leys. "Non-thermal plasmas in and in contact with liquids" Jouranl of Physics D: Applied Physics **42**(2009): 1-27.

P. Koidl, Ch. Wild, B. Dischler, J. Wanger, M. Ramsteiner, . "Plasma deposition, properties and structure of amorphous hydrogenated carbon films" Materials Science Forum **52-53**(1990): 41-70.

P.K. Bachmann, D. Leers, H. Lydtin. "Towards a general concept of diamond chemical vapour deposition" Diamond and Related Materials **1**(1991): 1-12.

S. Nomura, H. Toyot, S. Mukasa, H. Yamashita, T. Maehara, M. Kuramoto. "Microwave plasma in hydrocarbon liquids" Applied Physics Letters **88**(2006): 211503-1-3.

V. Puech. "Microplasmas: physics and application to the production of singlet oxygen $O_2(a^1\Delta g)$" The European Physical Journal Applied Physics **42**(2008): 17-23.

9 Conclusions

9.1 Conclusions (in English)

Diamond-like carbon films (DLC) are metastable form of amorphous carbon with significant sp^3 bonding, with or without hydrogen. DLC films have been deposited by various vapor methods, especially with plasma technique. On the other hand, DLC films can be deposited by liquid electrochemical technique which is based on the electrolysis of organic solutions. Effects of experimental facilities and deposition parameters, and the application of liquid electrochemical deposition of DLC films were investigated in this work.

Effects of experimental facilities on the deposition of DLC films mainly concentrate on the reactor and anode design. The materials of reactor and anode both have significant influence on DLC films composition, morphology and microstructure. Glass reactor, glass reactor with PTFE-coating inside and glass reactor with quartz-coating inside could introduce Ca or non-metallic impurities into the DLC films prepared by liquid electrochemical deposition. Using quartz reactor could successfully avoid the impurities from other reactor materials. Anodes made of graphite and Pt show good stability against organic solution and will not bring any impurity to the DLC films deposited. Cu and stainless steel anodes are easily eroded and therefore bring impurities into the deposits. Reactor made of quartz and anode made of graphite should be used to prepare undoped-DLC films by liquid electrochemical technique.

Deposition of DLC films by liquid electrochemical technique is a complicated process with physical and chemical reaction. The deposition parameters are classified into chemical parameters, geometrical parameters and electrical parameters, and then the effects of these parameters on the deposition of DLC films are investigated.

The electrolyte made of organic chemicals is a critical chemical parameter in DLC films liquid deposition. DLC films were successfully deposited from analytically pure methanol, ethanol, acetone and 2-propanol, respectively. The film deposited by electrolysis of methanol had the lowest growth rate and sp^3 content. Using ethanol made the film very rough although owned the advantages of higher growth rate and sp^3 content. The DLC films deposited from both acetone and 2-propanol had high growth rate, smooth surface and high sp^3 content. It is confirmed that the film growth rate, morphology and microstructure were correlated with the chemicals. Certain organic chemical should be selected as electrolyte depending on the requirements of resulting DLC films. Thus, 2-propanl was widely used in the following work because acetone is more poisonous. On the other hand, organic chemicals of high viscosities, such as ethylene glycol and glycerol are not appropriate for DLC films formation, because high viscosity can decrease the fluid ability and hinders the migration of the molecules.

Since DLC films of rough surface were deposited using analytically pure ethanol, deionized water was used as an additive to investigate its effects on the films deposition. The characterizations suggested that DLC films could be deposited from various ethanol/deionized water solutions. The films surface became smooth with the increase of deionized water. The Raman results suggested that hydrogenated DLC films were deposited, the content of both sp^3 carbon and bonded hydrogen decreased with the increase of deioniezd water. Analysis of FTIR spectroscopy also suggested that the hydrogen content decreased with the addition of deionized water. Deionized water which plays the part of additive can obviously affect the deposition of DLC films by liquid electrochemical technique, including the film morphology and microstructure. Although film growth rate can be increased with appropriate ratio of deionized water, the film structure is changed at the same time. This should be a guide of using deionized water as an additive to achieve ideal growth rate and films properties.

The anode-substrate distance is an important geometrical parameter in the liquid electrochemical deposition system which can affect the formation of DLC films. There is an optimal distance during the adjustment of anode-substrate distance and it is appropriate to grow DLC films at this distance. Neither longer nor shorter than the optimal distance is favored for the growth of DLC films. The optimal anode-substrate distance is supposed to be the place to get the most energy from the applied potential and simultaneously the lowest influence of the solution movement. The optimal distance is strongly correlated with the composition of the organic solution.

The applied potential belongs to electrical parameters in liquid phase deposition of DLC films. The investigation of resulting films denotes that hydrogenated DLC films were deposited by electrolysis of analytically pure 2-propanol under the applied potential in the range of 400 V to 1000 V. Adjusting applied potential could affect the film morphology and microstructure. The film growth rate and roughness both decreased with the increase of applied potential. The analysis of Raman spectroscopy suggested that the increase of applied potential was favored for the formation of sp^3 carbon in the DLC films. The hydrogen content also increased with the increase of applied potential, the maximum of hydrogen content was obtained when the applied potential was 1000 V.

DLC films were simultaneously deposited on horizontally and vertically aligned stainless steel substrates by electrolyzing analytically pure 2-propanol. Thus, liquid electrochemical technique is feasible to carry out DLC films deposition on “3D” or complex conductive substrates.

Superhigh applied potential in the range of 5 kV to 20 kV were introduced to DLC films liquid phase deposition. DLC film of the most sp^3 carbon was deposited when the applied potential was set to 5 kV. It is believed that DLC films can be deposited under superhigh applied potential by liquid electrochemical technique. The film structure changed with the increase of applied potential, no films were deposited when the applied potential was set to 20 kV.

Liquid plasma is supposed to exist in the process of DLC films liquid phase deposition, although many questions and issues should be resolved. In order to understand the mechanisms of liquid phase deposition, the possibility that DLC films can be deposited by plasma in liquid should be considered. Therefore, the aim of liquid plasma determination is to set up a model to describe the relationship between the deposition of DLC films and liquid plasma signal. A systematic connection between discharge current and voltage and the structures and properties of DLC films should be included in this model to develop a better understanding of the DLC films liquid phase deposition mechanism.

Friction coefficient and nanohardness of the typical films deposited in this work were measured. The results suggest that mechanical properties of DLC films deposited by liquid electrochemical are in the usual range of DLC films. Thus the DLC films deposited by liquid technique have the possibility for application with further investigation. Liquid electrochemical deposition is therefore an effective technique to prepare DLC films besides vapor techniques.

9.2 Conclusions (in Chinese)

类金刚石薄膜(DLC)是指含有 sp^3 键的无定形石墨结构，可含氢或者不含氢。DLC 薄膜可以通过物理气相沉积和化学气相沉积等方法制备。而本论文采用液相电化学方法，电解有机溶液沉积 DLC 薄膜。主要研究实验装置和参数对 DLC 薄膜形貌和结构的影响，以及液相法制备 DLC 薄膜的潜在应用。

研究实验装置对 DLC 薄膜沉积的影响主要集中在反应容器和阳极材料的选择方面。实验结果表明，反应容器和阳极的组成材料能够影响 DLC 薄膜的成分，形貌和结构。使用玻璃容器和内壁带有 PTFE 涂层或石英涂层的玻璃容器会造成薄膜中含有钙或其它非金属杂质，使用石英容器能够有效地避免这些杂质。由石墨或铂制成的阳极在有机溶液中表现出良好的稳定性，不会给沉积的薄膜带来任何杂质。铜电极和不锈钢电极在反应过程中极易被腐蚀，造成沉积物含有杂质。因此，之后在研究其他实验参数对液相沉积 DLC 薄膜的影响时，均采用石英容器和石墨电极以避免实验装置带来杂质。

液相电化学沉积 DLC 薄膜是一个包括化学变化和物理变化的复杂过程，为了研究实验条件对薄膜沉积的影响，本论文把其实验参数简化并分为化学参数，几何参数和电参数等三类进行研究。

由有机溶液组成的电解液是液相电沉积 DLC 薄膜过程中关键的化学参数。实验结果表明，利用分析纯的甲醇，乙醇，丙酮和异丙醇做电解液，均可获得 DLC 薄膜。电解甲醇的薄膜生长速率和 sp^3 碳含量都最低。电解乙醇虽然薄膜生长速率和 sp^3 碳含量都增加，但是薄膜表面非常粗糙。电解丙酮和异丙醇获得的 DLC 薄膜，具有较高的生长速率和 sp^3 碳含量，而且薄膜表面光滑。由此可见，薄膜的生长速率，表面形貌和结构受到电解液种类的显著影响。因此可以通过选择不同种类的电解液来实现薄膜质量的控制。由于异丙醇相比丙酮的毒性较低，在后续研究中广泛采用异丙醇作为电解液来沉积 DLC 薄膜。在相同实验条件下电解粘度过高的有机溶液，例如乙二醇和丙三醇，均未能获得薄膜。这是因为过高的粘度阻碍了溶液中活性粒子的运动，不利于 DLC 薄膜的形成。

由于电解纯乙醇可以获得 DLC 薄膜，在乙醇中加入去离子水作为添加剂来研究去离子水对薄膜沉积的影响。检测结果表明电解乙醇/去离子水混合溶液做可以获得 DLC 薄膜。与电解纯乙醇获得的薄膜相比，加入去离子水后，薄膜的生长速率先升高后降低。当混合溶液中乙醇和去离子水体积比为 1:1 时，生长速率达到最大值。并且随去离子水含量增加，薄膜表面粗糙度减小，改善了利用纯乙醇获得的薄膜表面粗糙的现象。拉曼光谱分析表明，DLC 薄膜中 sp^3 碳和氢含量都随电解液中去离子水含量增加而降低。FTIR 光谱分析表明，薄膜中氢含量随去离子水增加而降低。去离子水作为一种添加剂，能够显著影响液相电化学沉积 DLC 薄膜的生长速率，薄膜形貌以及结构。虽然加入适量的去离子水能够提高薄膜的生长速率，但是会同时影响薄膜的结构。通过调整去离子水的比例，可以获得理想的生长速率和薄膜性能。

阳极和阴极之间的距离是液相电化学沉积 DLC 薄膜系统中的一个几何参数。研究表明两极间距能够影响 DLC 薄膜的形成。在两极间距的调节过程中，发现存在一个有利于获得 DLC 薄膜的临界值。该临界值应该是能获得的能量最大并且

受到溶液流动影响最小的位置，最有利于薄膜沉积。两极间距大于或者小于这个临界值，都不利于获得薄膜。另外，两极间距的临界值与做电解液的有机溶液成分密切相关，同一个临界值不适用于所有溶液。

电压是电化学沉积DLC薄膜实验中的电参数。电解分析纯的异丙醇在400V-1000V电压范围内均获得DLC薄膜。调节沉积电压能够显著影响薄膜的形貌和结构，薄膜的生长速率和粗糙度都随电压升高而降低。拉曼光谱的分析结果表明，电压升高有利于提高DLC薄膜中sp^3碳的含量。氢含量亦随沉积电压升高而增加，当电压为1000 V时达到最大值。

电解异丙醇在水平和竖直的不锈钢基底上同时沉积获得了 DLC 薄膜，这证明采用液相电化学方法可以在三维复杂基底上沉积类金刚石薄膜。

在液相电化学沉积 DLC 薄膜系统中引入 5 kV-20 kV 的超高电压。拉曼光谱分析显示，当沉积电压为 5 kV 时，获得的 DLC 薄膜中含有最多的 sp^3 碳。这表明在超高电压下，可以利用液相电化学方法沉积 DLC 薄膜。并且电压变化会影响薄膜结构，sp^3 碳含量随电压升高而降低，当电压为 20 kV 时没有获得 DLC 薄膜。

本论文尝试在液相电化学沉积 DLC 薄膜过程中检测液相等离子体。目的是探求液相电化学沉积 DLC 薄膜的成膜机理，即 DLC 薄膜是否由液相等离子体作用而形成的。试图表征 DLC 薄膜沉积和液相等离子体信号之间的关系，建立联系电压电流与薄膜结构性能的模型，然而要建立这个模型还有很多需要解决的问题。

另外，我们检测了薄膜的机械性能。结果表明，液相沉积的 DLC 薄膜的摩擦系数和纳米硬度均在常规 DLC 薄膜的性能范围内。因此，可以预测液相法制备的 DLC 薄膜有广阔的应用前景，液相电化学技术也成为除气相法以外的沉积 DLC 薄膜的一种有效方法。

9.3 Conclusions (in German)

Diamond-like Carbon (DLC)-Schichten sind eine metastabile Form von amorphem Kohlenstoff mit einem hohen Anteil an sp^3-Bindungen, sowohl mit als auch ohne Wasserstoff. Üblicherweise werden sie durch plasmagestützte Verfahren erzeugt. DLC-Schichten können aber auch durch eine elektrochemische Technik aus der flüssigen Phase abgeschieden werden, welche auf der Elektrolyse organischer Lösungen basiert. In dieser Arbeit sind die Auswirkung von Versuchsanlagen und Beschichtungsparametern bei der Anwendung von elektrochemischer Abscheidung von DLC-Schichten aus der flüssigen Phase untersucht worden.

Die Auswirkungen der Versuchsanlagen auf die Erstellung der DLC-Schichten konzentrieren sich hauptsächlich auf den Reaktor und den Anodenaufbau. Das Reaktor- und Anodenmaterial haben einen großen Einfluss auf Zusammensetzung, Morphologie und Mikrostruktur der DLC-Schichten. Glasreaktoren – sowohl unbeschichtet, als auch mit PTFE- und Quarzbeschichtung – erzeugen Ca-Verunreinigungen und nichtmetallische Verunreinigungen in den DLC-Schichten. Durch den Einsatz eines Quarzreaktors konnten die Verunreinigungen durch Reaktormaterialien erfolgreich vermieden werden. Anoden aus Graphit und Platin zeigen eine hohe Stabilität gegenüber organischer Lösung und verursachen keine Verunreinigungen in den erstellten DLC-Schichten. Edelstahl- und Cu-Anoden hingegen erodieren leicht, so dass durch diese Verunreinigungen erzeugt werden. Daher sollten Reaktoren aus Quarz und Anoden aus Graphit benutzt werden um undotierte DLC-Schichten mittels elektrochemischen Verfahrens aus der flüssigen Phase zu erstellen.

Die Beschichtungsparameter lassen sich in chemische, geometrische und elektrische Parameter unterteilen. Die Auswirkungen dieser Parameter auf die Abscheidung der DLC-Schichten sind untersucht worden.

Die organische Eletrolytlösung ist ein entscheidender Parameter bei der Abscheidung von DLC-Schichten aus der flüssigen Phase. DLC-Schichten sind aus analysenreinem Methanol, Ethanol, Aceton und 2-Propanol erfolgreich abgeschieden worden. Die Schichten, die durch die Elektrolyse von Methanol hergestellt worden sind, hatten die niedrigste Wachstumsrate und den geringsten sp^3-Gehalt. Bei der Verwendung von Ethanol wurden die Schichten sehr rau, wenngleich Schichtwachstum und sp^3-Gehalt höher waren. Die DLC-Schichten, die sowohl mit Aceton als auch mit 2-Propanol abgeschieden wurden, wiesen hohe Schichtwachstumsrate, glatte Oberflächen und hohen sp^3-Gehalt auf. Es wurde bestätigt, dass Schichtwachstum, Morphologie und Mikrostruktur mit den verwendeten Chemikalien korrelieren. Bestimmte organische Chemikalien sollten als Elektrolyt in Abhängigkeit von den Anforderungen der zu erstellenden DLC-Schichten ausgewählt werden. Organische Chemikalien mit hoher Viskosität wie Ethylenglycol und Glycerol sind nicht geeignet für die Bildung von DLC-Schichten, da hohe Viskosität die Fließeigenschaften vermindert und die Oberflächendiffusion der Moleküle verhindert.

DLC-Schichten konnten auch aus Lösungen von Ethanol und entionisiertem Wasser abgeschieden werden. Die Schichten wurden bei steigendem Wassergehalt glatter. Die Raman-Messungen lassen darauf schließen, dass bei steigendem Gehalt von entionisiertem Wasser sowohl der Anteil an sp^3 hybridisierten Kohlenstoff als auch an gebundenem Wasserstoff abgenommen hat. Aus der Analyse mittels FTIR-Spektroskopie geht ebenso hervor, dass durch die Zugabe von entionisiertem Wasser der Wasserstoffgehalt abnimmt. Entionisiertes Wasser kann als Beimengung offensichtlich die Abscheidung von DLC-Schichten aus der flüssigen Phase beeinflussen, was die Schichtmorphologie und die Mikrostruktur beinhaltet. Die Abscheidungsrate kann einerseits durch einen geeigneten Anteil an entionisiertem Wasser erhöht werden, andererseits wirkt sich dies auch auf die Schichtstruktur aus. Dies ist bei der Verwendung von entionisiertem Wasser als Zusatz zu beachten um bestmögliche Beschichtungsrate und Schichteigenschaften zu erreichen.

Der Abstand zwischen Anode und Substrat ist ein wichtiger geometrischer Parameter bei der elektrochemischen Abscheidung aus der flüssigen Phase auf die Bildung von DLC-Schichten. Es ist ein optimaler Abstand zwischen Anode und Substrat gefunden worden, welcher für die Erstellung von DLC-Schichten geeignet ist. Sowohl eine Vergrößerung als auch eine Verkleinerung des Abstands wirken sich negativ auf das Schichtwachstum der DLC-Schichten aus. Der optimale Anoden-Substrat-Abstand ist der Ort, an dem die größte Energie vom angelegten Potential und gleichzeitig der kleinste Einfluss auf die Bewegung der Lösung erreicht wird. Dieser Abstand ist stark von der Zusammensetzung der organischen Lösung abhängig.

Das angelegte Potential gehört zu den elektrischen Parametern in der Abscheidung von DLC-Schichten aus der flüssigen Phase. Die Untersuchung der sich ergebenden Schichten deutet an, dass hydrierte DLC-Schichten durch Elektrolyse von analysereinem 2-Propanol unter einem angelegten Potential im Bereich von 400 V bis 1000 V abgeschieden worden sind. Durch Variation des angelegten Potentials werden die Morphologie und die Mikrostruktur der Schichten beeinflusst. Die Beschichtungsrate und die Rauhigkeit nahmen mit einer Erhöhung des angelegten Potentials ab. Aus der Analyse der Raman-Spektroskopie folgt, dass eine Erhöhung des angelegten Potentials sich positiv auf die Bildung von sp^3-Kohlenstoff in den DLC-Schichten auswirkt. Das Maximum des Wasserstoffgehalts wurde bei einem angelegten Potential von 1000 V erreicht.

DLC-Schichten wurde gleichzeitig auf horizontal und vertikal ausgerichteten Edelstahlsubstraten durch die Elektrolyse von analysereinem 2-Propanol abgeschieden. Demnach ist das Verfahren der elektrochemischen Abscheidung aus der flüssigen Phase geeignet, um DLC-Schichten auf leitende "3D"- oder komplex geformte Substrate aufzubringen.

Die Verwendung des Hochspannungsbereich zwischen 5 kV bis 20 kV ist in die Abscheidung von DLC-Schichten aus der flüssigen Phase eingeführt worden. Die Schichtstruktur wurde mit einer Erhöhung des angelegten Potentials beeinflusst. DLC-Schichten mit dem meisten sp^3-Kohlenstoff wurden bei einem Potential von 5

kV abgeschieden. Es lässt sich daraus schließen, dass DLC-Schichten durch elektrochemisches Verfahren aus der flüssigen Phase unter Hochspannung abgeschieden werden können.

Zur Klärung des Mechanismus der Abscheidung sollte auch die Möglichkeit betrachtet werden, dass DLC-Schichten mittels eines Plasmas in der Flüssigkeit abgeschieden werden. Dazu muss eine Vielzahl an Fragen und Aspekten geklärt werden. Das Ziel bei der Untersuchung von flüssigen Plasmen sollte dann sein, ein Modell zu erstellen, welches den Zusammenhang zwischen der Abscheidung von DLC-Schichten und den Eigenschaften des flüssigen Plasmas beschreibt. Eine systematische Abhängigkeit zwischen Entladungsstrom und -Spannung, Struktur und Eigenschaften der DLC-Schichten sollte in einem solchen Modell einbezogen werden, um ein besseres Verständnis über die Mechanismen bei der Abscheidung von DLC-Schichten aus der flüssigen Phase zu erhalten.

Es sind Reibungskoeffizienten und Nanohärte von typischen Schichten, die in dieser Arbeit erstellt wurden, gemessen worden. Die Ergebnisse zeigen, dass die mechanischen Eigenschaften der DLC-Schichten, die elektrochemisch aus der flüssigen Phase abgeschieden worden sind, denen von gewöhnlichen DLC-Schichten entsprechen. Daher sind aus der flüssigen Phase abgeschiedene DLC-Schichten viel versprechend für weitere Anwendungen und sollten weiter untersucht werden. Demnach stellt die elektrochemische Abscheidung aus der flüssigen Phase neben der Gasphasenabscheidung eine effektive Technik zur Herstellung von DLC-Schichten dar.

Acknowledgements

This work was carried out in thin film technology group which belongs to Faculty of Physics in University Duisburg-Essen.

I would first like to express my acknowledgement to my supervisor, Prof. Dr. Volker Buck, for his providing me the opportunity to work in thin film group, for his guidance in this dissertation, and for his kindly help during my time here.

I would like to acknowledge China Scholarship Council (CSC) because I worked in the frame of CSC scholarship for three years.

I would like to thank Prof. Dr. Guifeng Zhang (Dalian University of Technology, China) and Prof. Dr. Dieter Mergel (University Duisburg-Essen) for their help during my work.

I would like to thank Mrs. Heidi Pärschke for her help, and I would to thank Mr. Klaus Pärschke, Mr. Heinz Loffeld and Mr. Peter Walter for their technical assistance.

I would like to express thanks to Dipl.-Phys.Ing. Martin Jerman (University Duisburg-Essen) and PD Dr. Sabine Seisel (Ruhr University Bochum) for their technical assistance in the deposition of PTFE-coating and quartz coating.

I would like to thank PD Dr. Telgheder Uschi and Techn. Angest. Ullrich Claudia (Faculty of Chemistry, University Duisburg-Essen) for their help on the examination of liquid composition.

I would like to thank Dr. Klaus Kerpen, Dr. Andriy Kuklya, Dipl. Svetlana R. Gasanova and Mr. Robert Marks (Faculty of Chemistry, University Duisburg-Essen) for their help on the superhigh applied potential deposition.

I would like to thank Dipl.-Ing. Smail Boukercha (Faculty of Chemistry, University Duisburg-Essen) for his help in SEM measurements.

I would like to thank Dr. Verena Ney (Faculty of Physics, University Duisburg-Essen) for her help in XRD measurements.

I would like to thank Mrs. Hanna Bukowska (Faculty of Physics, University Duisburg-Essen) for her help in AFM measurements.

I would like to thank Dr. Schulz-von der Gathen (Ruhr-University Bochum) for his help in liquid plasma investigation.

I would like to thank Mr. Ingo Erdmann and Mrs. Ying Ren (Bergische University Wuppertal) for their help in films friction coefficient measurement.

I would like to thank Dr. Martin Fenker (fem Research Institute Precious Metals & Metals Chemistry) for the help of film hardness measurement.

I would like to thank Sebastain Schipporeit for his translation of the conclusion into German.

I am very grateful to all the colleagues in thin film technology group, Dr. Nicolas Wöhrl, Dr. Alexei Poukhovoi, Monika Timpner, Berrin Kuezuen, Himani Jain, Victoria Khlopyanova, Matthias Haase, Markus Neubert, Oleksiy Filipov, Patryk Hallek, Rishi Sharma, Reinhard Remfort, Stefan Huber, for their kindly help, cooperation and friendship all the time.

I appreciate the help from Shuangli Ye, Yan Yin, Huinan Yang, Yuansen Chen, Xudong Cui and Quanchao Dong.

I want to thank all the people helped me during my time in Germany.

I express my special appreciation to my parents and husband for their encouragement, support and selfless love in these years.